JPRS-CST-86-048

19 NOVEMBER 1986

China Report

SCIENCE AND TECHNOLOGY

FBIS FOREIGN BROADCAST INFORMATION SERVICE

NOTE

JPRS publications contain information primarily from foreign newspapers, periodicals and books, but also from news agency transmissions and broadcasts. Materials from foreign-language sources are translated; those from English-language sources are transcribed or reprinted, with the original phrasing and other characteristics retained.

Headlines, editorial reports, and material enclosed in brackets [] are supplied by JPRS. Processing indicators such as [Text] or [Excerpt] in the first line of each item, or following the last line of a brief, indicate how the original information was processed. Where no processing indicator is given, the information was summarized or extracted.

Unfamiliar names rendered phonetically or transliterated are enclosed in parentheses. Words or names preceded by a question mark and enclosed in parentheses were not clear in the original but have been supplied as appropriate in context. Other unattributed parenthetical notes within the body of an item originate with the source. Times within items are as given by source.

The contents of this publication in no way represent the policies, views or attitudes of the U.S. Government.

PROCUREMENT OF PUBLICATIONS

JPRS publications may be ordered from the National Technical Information Service, Springfield, Virginia 22161. In ordering, it is recommended that the JPRS number, title, date and author, if applicable, of publication be cited.

Current JPRS publications are announced in Government Reports Announcements issued semi-monthly by the National Technical Information Service, and are listed in the Monthly Catalog of U.S. Government Publications issued by the Superintendent of Documents, U.S. Government Printing Office, Washington, D.C. 20402.

Correspondence pertaining to matters other than procurement may be addressed to Joint Publications Research Service, 1000 North Glebe Road, Arlington, Virginia 22201.

JPRS-CST-86-048

19 NOVEMBER 1986

CHINA REPORT

SCIENCE AND TECHNOLOGY

CONTENTS

PEOPLE'S REPUBLIC OF CHINA

ABSTRACTS

/7310

NATIONAL DEVELOPMENTS

IMPLEMENTATION OF TECHNICAL CONTRACTING SYSTEM DISCUSSED

Beijing KEYAN GUANLI [SCIENCE RESEARCH MANAGEMENT] in Chinese No 3, 1986 pp 28-32

[Article by Chen Changhui [7115 2490 1741] of the Science and Technology Bureau, Ministry of Aerospace Industry: "On Problems Associated with the Implementation of Economic Responsibility System for Technical Programs at Research Institutes"]

[Text] The reform of the funding system to research institutes is an important measure in the reform of the S&T system. In order to adapt to this reform, research institutes must implement various technical economic responsibility system centered around contracting based on scientific management methods. The following is a discussion of several problems associated with the implementation of this technical economic responsibility system by research institutes.

I. Necessity of Implementing Technical Economic Responsibility System

In the past, the Chinese government paid for all research expenses. There are serious drawbacks associated with the distribution of research money since everyone is getting funded from the same pool of funds.

1. There is no economic pressure at research institutes. The assignments are handed down from above and the funding also comes from above. The accomplishments are also reported to superior organizations. Thus, technology is detached from economics and scientific research is separated from production. This affects the wide application of research accomplishments.

2. There is a lack of scientific basis and rigorous proof in the distribution of funds. Most of the time, the money is split based on historic levels. Thus, the research assignments are not in sync with fund distribution. Projects with higher allocations often spend the extra money on other items. Projects with insufficient funding cannot keep with the schedule.

3. Research funding is managed out of phase with spending. The technical personnel only spend and do not manage. Whatever is spent is getting reimbursed. Research funding is not rigorously controlled. However,

research expenses and materials consumed are somewhat flexible in nature. Waste will occur if the technical staff does not consider the economics.

In order to overcome these problems, the funding system must be changed. Externally, we must implement a technical contract system. Internally, we must have a technical economic responsibility system.

This reform was implemented in several experimental sites for a few years. The experience shows that the management of research funding is improved and some research money is saved. The research people have a stronger sense of responsibility and the efficiency of research is improved. For instance, after implementing the responsibility system for the development of a certain product in our ministry, the research staff followed a strict budget to save expenses. In addition, the organization was managed based on system engineering principles. The result is that the development time is reduced by two thirds as compared to that of a similar project prior to the implementation of the responsibility system. The cost is saved by one half as well. The implementation of this system also encourages the research institutes to be oriented toward the economy and the society. It will break them away from department ownership and locality ownership, and will alter the various dependencies under the present structure. It will promote the linkage between research and production to allow technical accomplishments to be rapidly applied to manufacturing so that they can be converted to profits and social benefits. In the mean time, new sources for research funding are created. For example, a certain research institute in our ministry had a pure annual profit of approximately 2,000,000 yuan in 1983 and 1984. Due to the implementation of the reform, the 1985 profit is expected to be over 5,000,000 yuan. The institute created a research and development fund and a collective welfare fund from the profit. The government has reduced its support by 15 percent.

II. Methods for Implementing a Technical Economic Responsibility System

To implement a technical economic responsibility system and external contract system, we must bring economic and management concepts into the domain of scientific research to directly link research assignments with expenses. The technical and economic responsibilities of the research unit must be clearly identified so that responsibility, power and benefit are combined.

The ministry issues the research assignments to the institutes. The ministry signs a primary contract with the lead organization which then signs various lateral subcontracts with other collaborating units (or subcontractors of various systems). The contract must specify the tasks, accomplishments, schedules, costs and bonuses. Under the premise that the completion of all contracts within the ministry must be ensured, the institute can sign lateral contracts with outside organizations to face the economy and the society. Within the institute, all contracting responsibilities are assigned to various levels and individuals. The following is a discussion on the methods employed to implement the economic responsibility system in the institute.

1. General Contract Method

Different contracting methods should be applied to different research laboratories and shops. The situation is introduced in the following:

a. Major laboratories and machine shops, because of their ability to undertake research and production assignments of specific directives and to accept external contracted work, have their own incomes. They should be treated as independent accounting units, responsible for their own profits. The contracts should primarily contain targets specifying the research and production items as well as incomes. The research funding is determined by subtracting a specific proportion of the contracted amount for a risk fund and for management fee. At the end of the year, or upon completion of the project, a portion is set aside as bonuses based on the status of the assignment and on the net income. There are two ways to set the bonuses. One is to assign different percentages to net incomes derived from contracted targets and additional objectives, respectively. This is done either to encourage bringing in more work, to receive more income, or to ensure the completion of research projects in the plan. Each unit can decide its own priority based on its own situation. The other way is to bundle planned and unplanned projects together to arrive at a goal. Only one percentage is set for bonus payoff. This is a more convenient way to manage projects. In addition, it can prevent laboratories and shops from diverting costs incurred in contracted work of their own to projects planned by the institute.

b. A total duty responsibility system can be implemented with service-oriented laboratories and shops such as information research offices, instrument laboratories, chemistry laboratories and machine shops. (Their assignments are mostly service-oriented in support of major laboratories and shops in the institute. They can also accept outside work to receive technical service and service income.) The personnel, positions, and resposibilities are fixed. They receive compensation for some of the services rendered. On the basis of overall evaluation, bonus is given based on the completion status of the contracted tasks. A portion of the income from external services rendered is set aside for the employees as well.

2. Contract Method Based on the Implementation of Economic Objective Management

Because of the need to gradually reduce government support to achieve economic independence, research institutes in the technology development mode can implement the economic objective management system. The net income of the institute should be determined based on the amount of operating expenses to be saved each year. Based on factors such as the total wages of the people working on the first line of research and production, fixed capital, occupied area and liquid assets, the economic goal of the entire institute is broken down level by level to determine the amount to be undertaken by each unit, including directive research and production assignments. This method can stimulate the research laboratories and machine shops to actively tap into potential resources, save expenses, and add new projects to make the institute economically independent. Nevertheless, too much stress on economic

objectives can make the institute go astray from the direction of scientific research.

3. Contracting Single Project

Some important research projects which involve several departments can be contracted to the task groups. By implementing the system of fixing the assignment, accomplishments, schedule, expenses and bonus in the contract, these projects can be directly managed by the institute. If other laboratories or shops are involved in some tasks, they can sign subcontracts with the task team. The leaders of such teams must be chosen by the institute. When appropriate, we can also try a bidding method.

III. Organization Management with Implementation of Technical Economic Responsibility System

The implementation of a technical economic responsibility system with lateral and serial contracts for research projects will make it easier to organize research based on systems engineering methods. It will also facilitate the coordination of various tasks. However, we should not neglect management because we implement the contract system. On the contrary, because economic and management concepts are brought into the domain of research, management will have to cover a wider range. The work becomes more complicated which requires better management. Specifically, we have to pay attention to the following points:

First, in the past, our primary concern was focused on technical feasibility and applicability and was not concerned with economics. To implement the technical economic contract system is to combine both for proof of technology and economics in order to ensure the accuracy of the research budget and the economic benefit of the project.

Second, there are more sources for projects after we make research face the society which adds a new dimension to organization management. The utilization and balance of research resources becomes more complex.

Third, as we implement the system to combine responsibility, authority and economic interest, to link technical accomplishments to economic gains, the personal welfare of the technical staff is affected. When the work is contracted, it will require tighter management and more rigorous inspection and review.

Fourth, due to the exploratory and uncertain nature of research, no matter how detailed the contracting work is done, there will be many unforeseen problems which require immediate coordination by the management.

Fifth, after implementing the contract system, each department is more concerned about its own interests and tends to neglect the overall picture. For instance, departments with general processing and testing equipment are happy to accept external work for additional income. They are not enthusiastic about assignments within the institute. Some departments will overload the equipment for more money. Some task groups would rather go

outside because they feel the institute charges too much. Thus, the institute loses some funding. In order to save money, some task teams do not do enough experiments. Therefore, we must perfect the structure of the institute with specific reference to the problems emerging after the implementation of the contract system so that internally it is balanced and coordinated. Special favorable internal processing and testing rates must be established to promote collaboration and unity among all departments so that the institute is still one entity. In addition, management of technical quality must be strengthened.

The implementation of the technical economic responsibility system involves everyone. It requires the strengthening of three functional departments--planning, finance and maintenance. Furthermore, we must establish an effective technical control and command system.

The research planning department must handle the relations between what's needed and what's feasible, overall and local, focal points and general issues, progress and quality, and long term and short term well. It plays a leading role in assigning tasks, issuing contracts and rewarding accomplishments. The finance department must regulate, monitor and serve the institute to organize and manage the cost accounting work. In order to match planning with economic management to allow the proper management and utilzation of research funding, we need dedicated organizations and personnel to manage research funds. In general, we may set up a technical economics office under the planning department. The maintenance department must properly manage the instruments and equipment to meet the requirements of the new system.

In order to make sure that technical and quality-related management work such as development planning, project demonstration, and technical coordination and review is done properly to ensure the quality of research, we cannot weaken the technical command functions headed by the chief engineer and chief designer in implementing the contract system. Moreover, it requires a close coordination with the administrative management system.

The overall research and production dispatch system is an important part of the administrative command system. Its duty is to integrate the responsibility and authority of the department which ensures the resources needed in the research into the assignment to effectively utilize them to guarantee the success of the project. A main dispatch office may be established under the research planning and management department. It may be comprised of leaders from the planning department, maintenance departments, laboratories and shops to form a central command system centered around research and production. The chief dispatcher, acting on behalf of the director of the institute, exercises the power to issue orders on regular or emergency basis to ensure the completion of the assignments. A temporary or emergency order may be considered as a supplement to the original contract. Emergency orders should be approved by the director of the institute.

In various stages of research, we must closely combine the technology with economics. In the proof of feasibility stage, we should fully demonstrate both technical and economic feasibility by involving technical, planning and

economic talents to choose the optimal plan. In the design development stage, cost must be controlled by value engineering and cost-effect analysis methods. The allocation and utilization of research funding must be broken down, tracked, accounted for and analyzed in order to reduce costs in various stages. In the accomplishment certification stage, not only technical review must be made, but also economic and social benefits must be evaluated. Only by doing so, the technical economic responsibility system can be fully effective to improve the economic welfare of the institute.

The implementation of the technical economic responsibility system is an important step for a research institute which is changing from a pure research mode to a research and production management mode. Systematic reforms in the leadership system, organization structure, wage system, planning system, internal relation structure and political ideology must be made to make the transformation effective.

IV. Principles to Follow and Relations to Keep in the Reform

When the institute implements reform, we must insist that the direction of research is the most important issue. We must always think based on the goals of achieving more accomplishments, training more professionals, and creating more social and economic benefits. We must place the assignments given by our government and our superiors first. In addition, we should pay attention to strengthening our political ideology and spiritual civilization. We must insist on the principle of distribution based on work. The following three relations must be properly handled:

1. Proper Treatment of the Relation between Government, Collective Entity and Individual in Implementation of Consolidation of Responsibility, Authority and Interest

The core of the technical economic responsibility system is "responsibility." We must determine "authority" and "interest" based on "responsibility."

In the area of "responsibility," in the reorganization within our ministry in recent years, a comprehensive technical post responsibility system has been set up. It is a basis for implementing the technical economic responsibility system. However, it still must be perfected based on the new situation. In the area of "authority," the Ministry issued a ruling in September 1984 to expand the autonomy of individual business units. More autonomy is given in areas such as planning, personnel, finance and discipline. In terms of leadership system, most institutes employ a director responsibility system. In addition, the authorities of research teams and shops are also expanded. Some attempts were made to organize task teams by free choice. These measures also facilitated the implementation of the new contract system. In the area of "profit" it is primarily done through keeping a fraction in the institute and distributing bonuses to individuals. The Chinese Government specifies the bonus exemption limit and the bonus taxation method. Each operating unit also has rules and regulations governing bonuses. In terms of bonus allocation, the size of the bonus will certainly affect individual enthusiasm. Nevertheless, the key is to overcome the idea of even distribution. It should be allocated based on performance. The bonus gap should be widened

reasonably. Currently, bonus allocation is made based purely on profit. Due to the unreasonable social value system, different profit margins for each product, different environments, and other factors, this method may result in unequal rewards for equivalent amounts of work. Based on a survey, the difference is of the order of six- to eightfold. Such unreasonable gaps will affect the enthusiasm of some employees. In order to minimize this gap and to maintain relative internal balance, some institutes also collect a bonus tax from the basic departments based on the method implemented by the government to regulate the imbalances.

When we handle the relation between our country, the institute and an individual, we must strengthen the political ideology work to rectify the misconception that "money is everything." We must combine the evaluation of the technical economic responsibility system with the realization of spiritual civilization. We have to link the evaluation results with performance appraisal and promotion so that the consolidation of responsibility, authority and welfare is realized in a wider perspective.

2. Careful Handling of the Relation between "Building Foundation" and "Catching up With the Norm" with Economic Benefit in Determining the Guiding Business Strategy

After we opened up the institutes and expanded their authorities, there are two situations to be concerned about in the choice of tasks and in the guiding business strategy. One is that tasks related to "foundation building" and "achieving the norm," because of the degree of difficulty and length of duration, are not economically attractive in the short term. Nobody wants to undertake such assignments. Everyone is interested in tasks with short cycle, high profitability and of appropriate technical standards. In some cases, people abandoned research and got into business to make money. The other extreme is to be detached from current resources and blindly pursue leading high technology items by ignoring the economic benefits of the short term, appropriate level, profitable projects. Both extremes must be avoided.

When the relation between "level" and "economic benefit" is treated, we must base on an analysis of the specific situation. Institutes with better foundation and resources, under the premise of facing economic construction and emphasizing economic benefit, must strengthen their involvement in the exploration of new technology and focus on long range projects and technology reserves in order to maintain their advantages. Institutes of weaker foundation and poorer resources must be practical. They should realize that although the majority of those short term, appropriate level projects does not belong to high technology, yet they are small, highly specialized, highly profitable technologies needed to vitalize the economy.

During the early stage, regardless of the foundation of the institute, the desire to improve the economic benefits is more urgent. It is natural to do the easy and profitable tasks first. This is not only a current need but also an unavoidable process in the transformation from a closed to an open type of research institute. During this process, we can adjust to the new management system, explore new avenues, get into new habits, and accumulate required experience. However, as the technical business grows, low level projects will

be less competitive. Research institutes will be forced to raise the standards and improve technology reserves.

3. Appropriate Treatment of Relation between Fundamental Mznagement and Reform

Some fundamental management is required to implement the technical economic responsibility system. Through the reform, fundamental management can be further perfected. These two things are complementary. In reality, once we talk about "improve economic benefit" and "be flexible," we are anxious to make money. The existing management system and operating procedure which are still valid and current are being set aside. For instance, a project may be initiated without going through rigorous technical and economic proof of feasibility. In some cases, the quality control system is inadequate, leading to repeated work. In some cases, speed is the only concern and the accumulation of original technical and economic data is ignored. If these things are not rectified in time, the reorganization results over the past several years will be irrevocably lost. Scientific and economic laws must be obeyed for the reform to strengthen fundamental management work.

There is much work in fundamental management. However, based on implementing the technical economic responsibility system, first we must perfect the technical post responsibility system, as well as other rules and regulations, according to the needs of reform. In particular, we must incorporate contents in economic management and development to be implemented thoroughly. Second, we must strengthen the statistical work. We have to hire people, set up a system, perfect the research statistic indicator system, and establish the raw data forms and tables to create a complete statistical network. Then we must accurately calculate the cost. Through projection, planning, control, accounting, analysis and review, the cost and economic benefit of a research product are reflected. We should promote to combine technical and economic considerations to save expenses and reduce cost. To do a good cost calculation, we need to do a thorough inventory, formulate an internal pricing structure and depreciation schedule, define contents covered by the audit, clarify the roles of each functional department in cost management and accounting, establish an audit system and internal billing system, and prepare to keep good original data. The Ministry has already formulated a cost management and estimation method for research organizations. It will be implemented on a trial basis on 1 January 1986. The cost estimation work at research units will be initiated by the implementation of this method to further perfect the technical economic responsibility system.

CSO: 4008/2122
12553

MICROCOMPUTER USE AS FURNACE CONTROLLER DESCRIBED

Beijing DIANZI JISHU YINGYONG [APPLICATION OF ELECTRONIC TECHNOLOGY] in Chinese No 2, 25 Feb 86 pp 6-9

[Article by Wang Dexi [3769 1795 3886] and Song Jian [1345 0256], Research Institute No 13, Ministry of the Electronics Industry: "The Application of Microcomputers in a High Temperature Molybdenum Element Furnace Control System"]

[Text] Introduction

Among semiconductor manufacturing techniques, the sintering of raw ceramic needs to be done in a molybdenum element furnace at temperatures up to 1,750°C. Molybdenum element furnaces are characterized by high temperatures (up to 1,800°C) and high power (tens of kw), and their control systems generally use the manually adjusted SCR output power method. Because the resistance of the molybdenum in the heating elements changes greatly as the temperature changes (as for example in the furnace we use when at 20°C the resistance is 0.017Ω, while at 1,750°C the resistance is 1.5Ω), in order to control the temperature and safeguard the equipment, operations personnel must regularly adjust the output power. Within a furnace operation time of 12 hours, operations personnel may not leave the premises. Nor can the accuracy of temperature control be guaranteed, as it oscillates ±20°C. Because there is always a large flow of protecting H_2 gas in the furnace, this provides an unfortunate factor in controlling temperature. After the system in question used a microcomputer for control, there was a great improvement in performance, where single-point control accuracy reached 1,750°C ±0.5°C, where the constant temperature area within 200 cm is ±3°C, where the rate of product finishing has reached 99.5 percent, and where at the same time labor intensity has been reduced. The system has excess temperature/cut-off thermocouple protection, and will sound an alarm. The rate of heat rise and temperature constant times may be set according to technical requirements, and the temperature can be maintained at any temperature. In addition, as conditions warrant, all set values may be changed without affecting program operation. Temperature control is via the PID adjustment method, where to avoid integral saturation PI and PD disconnect-type control is used. Data collection is via digital filtering. To avoid the difficulty where changes in molybdenum element resistance is too great, the stepped change of mid-values method is used, which allows optimal control of the furnace throughout the temperature range.

II. The System Hardware Composition

System hardware is made up chiefly of a microcomputer, process input channel, process output channel, printer, digital clock timing circuit, alarm circuit, and power supply circuits. The microcomputer is a DJS065A microcomputer, the CPU for which is the MBL6800, which has an instruction set compatible with the domestic DJS-060 series as well as with the imported 6800 series. Here, we have used only the single board computer part of the computer and the interface expansion board. The interface expansion board (I/OC board) has three parallel interface PIA MBL6821's, as well as the user parallel interface on the original board, which provides a total of four chips for the user to use. This computer has two MBM2716 EPROM's, for a total of 4K bytes; 2K bytes of the ROM is written with the monitor program, which leaves 2K bytes to be programmed by the user. There are 4K bytes of static RAM altogether, of which 1K bytes are used as stack for the monitor and the other 3K bytes are available for use. The system hardware flowchart is as shown in Figure 1.

1. Process Input Channel

The process input channel is outlined by the dotted line in Figure 1. This includes circuits for temperature sensing components, A/D converters, and isolating gates.

a. This system is largely used at present for controlling a high temperature molybdenum element furnace, where the regular temperature is 1,750°C, the corresponding temperature sensor for which is tungsten-rhenium thermocoupler, where the thermocouple potential corresponding to temperatures of 0°C≈1,800°C is 0≈28,030 microvolts. The change in thermocouple potential corresponding to each change of 1°C above 1,500°C is 13 microvolts. Because at the time this system was designed there was still no 16 bit A/D converters, we used the 5 bit semi-digital voltmeter BS18A to substitute for an A/D converter. We used the 0.15 V part of the voltmeter, the least bit of which can detect 1 microvolt.

b. Signal Gathering

The output of the A/D converter is a 5 bit BCD coded signal, in all a 20-bit binary numeral, and when a parallel interface expansion board is added to the computer thena sample signal can be input once at the same time. By not using time shared gathering control circuits, but by adding a software digital filter, we have strengthened the reliability of the system.

2. Process Output Channel

As shown in Figure 1, this is composed of the PIA 2 B circuit, the PIA 3 A and B circuits, separator gates, D/A output and display, mid-value output and display, point of inflection display, adder, power source and voltage compensation, and silicon controlled flip-flop circuits.

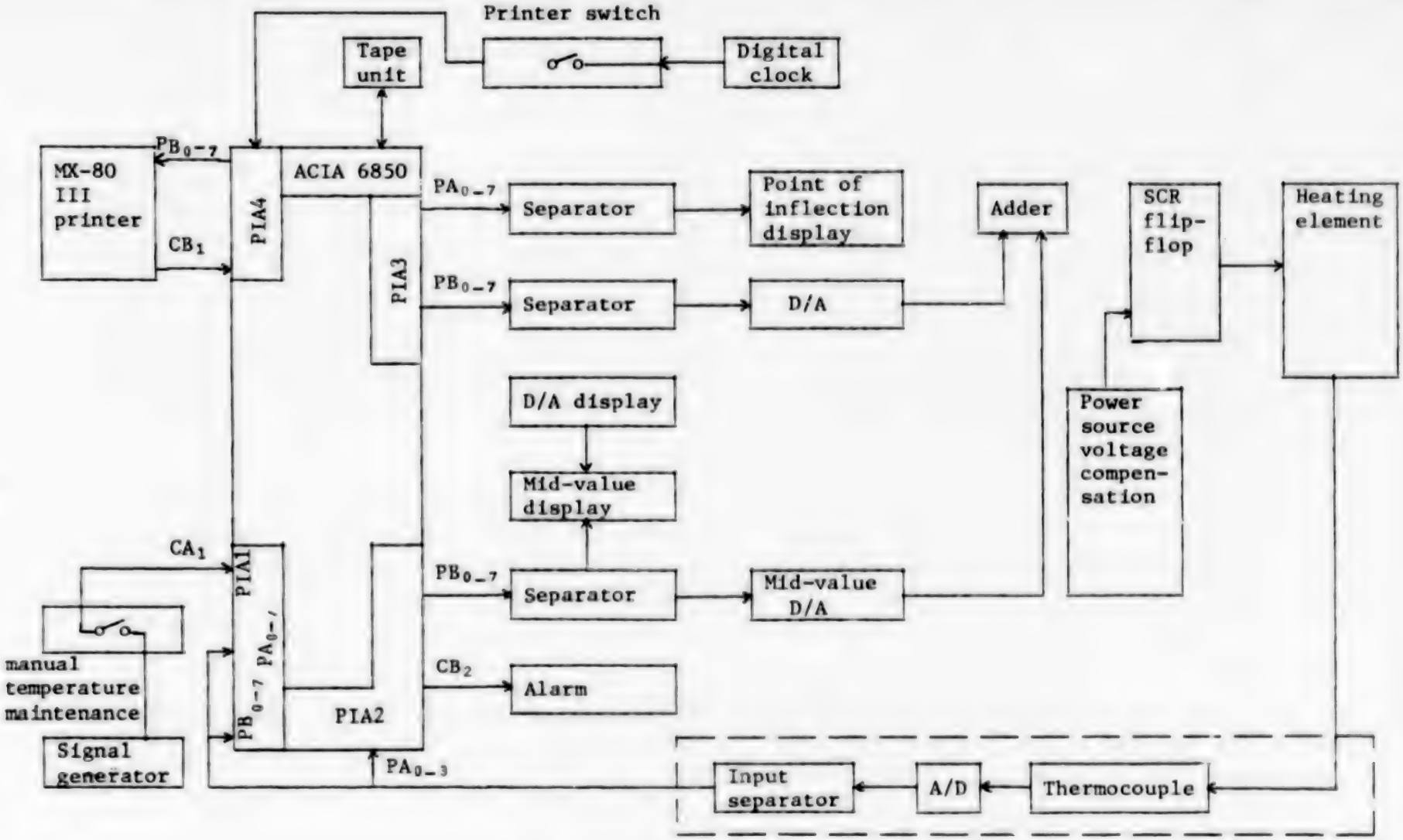

Figure 1. General Diagram of System Hardware

a. Mid-Value Output Channel

Output in this system includes two parts: mid-value and D/A. In fact, mid-value is also D/A, and the D/A does not change for a particular segment of temperature area. Because the molybdenum element resistance will increase 100 times from room temperature to 1,750°C, this is not like controlling an ordinary furnace where full power raises the temperature, but rather the method of depending upon changing mid-values is used to safely reach the temperature goal.

It can be seen from Figure 1 that output is through channel B of PIA and that it is an 8-bit binary value, which means that it can divide the heating power into 255 portions. Passing through the separator gate, one circuit drives an 8-bit LED, which displays the size of the output, and the other circuit connects to the mid-value D/A board. The D/A board is 12 bit, and according to need, we can connect the 8 bits of the PIA to the corresponding bits of the mid-value D/A. Because the 12-bit D/A is greater than the 8-bit output of the PIA, we can in this way flexibly select the size of the output. After the mid-value output is added to the combination of the adder and the incoming D/A channel signal, the output then goes to the silicon controlled flip-flop circuit. Also, fluctuation of the power source voltage is added to the flip-flop circuit through hardware for use in high-speed compensation.

b. D/A Output Channel

Circuits in this portion are basically the same as those in the mid-value output channel, save for the fact that in the D/A output channel the 8-bit binary value output by circuit B of PIA 3 is the amount of adjustment output by the computer after the PID operation, and normally that is fluctuating. Because the D/A board is 12 bit, power trimming can be as fine as 1/4095, which is beneficial to ensuring control accuracy.

c. Point of Inflection Display Channel

This outputs an 8-bit binary value through circuit A of PIA 3 and drives eight LED's through the separator gate. It displays which temperature areas are currently rising in temperature or are constant in temperature. This can display the rising and stable temperature states at eight points of inflection.

3. Interactive Equipment

a. DJS-065A Microcomputer

After the system is operational, beginning from the left of the computer display the first four positions will always display a hexadecimal value for the furnace temperature, which will correspond to the decimal value on the digital voltmeter. When the parameters need revising during operation, the STOP button may be pushed, which will temporarily halt operations. At this time, output will be maintained unchanging and the parameters can be revised or data can be examined. When finished, it begins again from the temporary halt program, and the system continues to operate.

b. MX-80 III Printer

We have selected the MX-80 model III dot matrix printer, and after the digital clock has generated a timing interrupt signal, the printer then prints out the millivolt value corresponding to temperature value at that time, and will at the same time print out the temperature curve.

The timing signal can be set on the clutch plate from 1 to 60 minutes, and if arbitrary printing is needed the clutch plate can be moved to print out the millivolt values of the temperature for that moment. If printout is not needed, the printer switch can just be turned off.

c. Other

This system is also fitted with manual and automatic switching. When extra-ordinary conditions arise (such as excess temperature or thermocoupling), sound and light displays will automatically output that voltage has dropped to 0 volts. At this time, the situation can be handled by operations personnel by turning off the machine or switching to manual adjustment of output power.

III. Mathematical Modeling of the System

1. Adjusting Object Characteristics and a Flowchart for Controlling the System Transfer Function

Ordinary electric heating furnaces are first-order inertial links, and this high temperature molybdenum element furnace is no exception, also being of the first order inertial link. Its transfer function is:

$$W_t(S) = K_t e^{-\tau_t S}/(1 + T_t S) \qquad (1)$$

By measuring the rising curve of the furnace through experimentation, the amplification multiplier K_1 of the systemtransfer function can be found to be 10, the time constant T_1 = 600 seconds, and the delay time τ_1 = 30 seconds.

The system transfer function flowchart is shown in Figure 2.

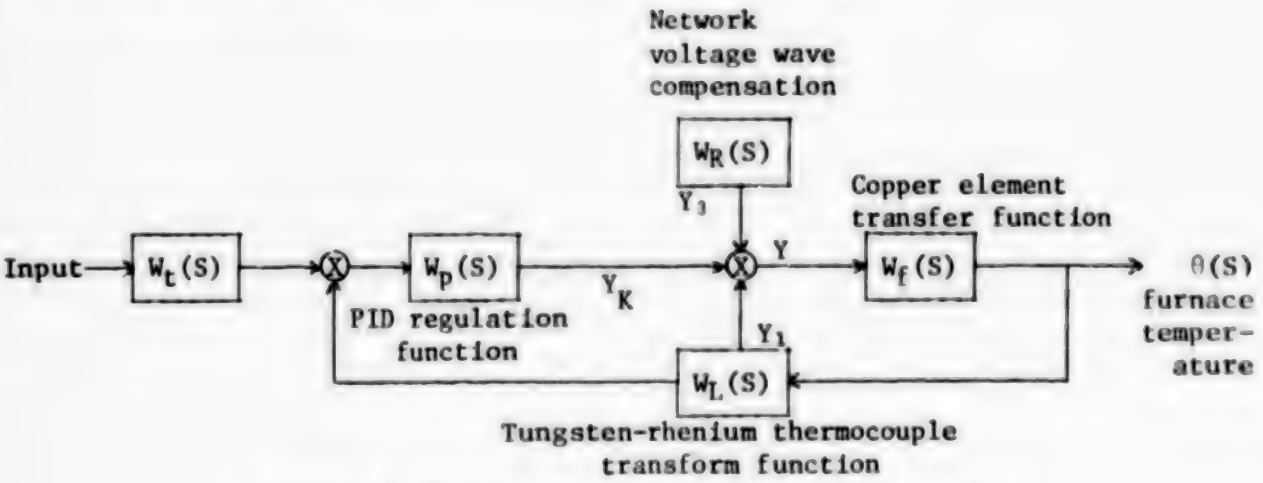

Figure 2. Flowchart of System Transform Functions

In the figure, $W_t(S)$ is the input transfer function and is the group of broken lines determined by the process curve; $W_L(S)$ is the thermocouple change transfer function; $W_R(S)$ is the power network voltage fluctuation compensation function; $W_f(S)$ is the transfer function for controlling the target high temperature molybdenum element furnace; $W_p(S)$ is the transfer function of the microcomputer's PID operation.

The overall controlled output quantity is:

$$Y = y_1 + y_k + y_3 \tag{2}$$

where y_1 is the mid-value quantity and a particular corresponding segment temperature does not change value. y_3 is the proportional feedback value determined by the hardware. The key here is to find the value y_k in the PID operation of the microcomputer.

2. Regulation Rules and Digital Filter for Sampling Data

The ideal method of regulation for first-order inertial systems is proportion-integration-differentiation, that is, the PID regulation method, and the ideal calculation method by which to simulate regulation is:

$$Y = K_p[e + (1/T_1)\int edt + T_d(de/dt)] \tag{3}$$

The PID form of calculation for the discrete sampling equation is:

$$Y_k = K_p\left\{ e_k + (1/T_1) \sum_{j=0}^{k} e_j \Delta T + T_d \ (\Delta e_k/\Delta T) \right\} \tag{4}$$

Y_k -- regulation value for PID K-order output
K_p -- proportional coefficient
T_1 -- integration time
T_d -- differentiation time
ΔT -- sampling time
e_k -- the deviation signal obtained by K-order sampling
$\Delta e_k - e_{k-1}$

where e_k is the deviation between the sampled measured value and the given value. In general, this value will be rather small when the system has entered operations in the vicinity of stable values. Therefore, interference cannot be neglected. Sampling is as in the following digital filter equation, which basically prohibits the effects of interference. We proceed this way with one signal; that is, we successively sample five times, then eliminate the largest and the smallest, then take the average value of the three remaining mid-values as the value at this time. But the difference e_k between this value and the set value is not taken as the deviation value at this sampling. Rather, the deviations of the preceding three occasions are averaged with this deviation and substituted for the deviation value at this time. Showing e_k, we get

$$\bar{e}_k = (e_k + e_{k-1} + e_{k-2} + e_{k-3})/4 \tag{5}$$

$$\Delta\bar{e}_k/\Delta T = (e_k - e_{k-3} + 3e_{k-1} - 3e_{k-2})/6\Delta T \qquad (6)$$

$\Delta\bar{e}_k/\Delta T$ is the average value for deviation differentiation, so substituting first (5) then (6) in equation (4), we get:

$$\begin{aligned} Y_k = K_p\Big\{&(e_k + e_{k-1} + e_{k-2} + e_{k-3})/4 \\ &+ (\Delta T/T_1)\sum_{j=0}^{k} e_j + T_d(e_k - e_{k-3} \\ &+ 3e_{k-1} - 3e_{k-2})/6\Delta T\Big\} \end{aligned} \qquad (7)$$

where K_p, T_1, and T_d can be roughly set up beforehand through K_f, T_f, and τ_f of the furnace transfer function as follows:

$$T_1 = 2\tau_f = 60; \qquad T_d = 0.5\tau_f = 15;$$
$$K_p = T_f/(0.85K_f\tau_f) = 2.15$$

Accurate adjustments require that in actual practice optimal parameters be obtained, so at 1,750°C our final adjusted values are:

$K_p = 4$; $T_1 = 80$ seconds; $T_d = 20$ seconds.

IV. Applications Software

1. Main Temperature Control Routines

The flowchart for the main routines for controlling temperature is shown in Figure 3, which we now explain in the following points.

a. After PIA initialization and clearing of the working elements to 0, there is a delay of 2 seconds to allow the entire regulation period to be 3.2 seconds. This lets it match the control target and will also leave some time when in the future we control several furnaces.

b. Sampling of the temperature millivolt values is continued for five times (separation being 200 ms because the sampling period of the A/D converter is 200 ms), and after these five values have been digitally filtered they are used for identification. If this value is very small or equal to 0 it indicates that the thermocouple has already burned off or that there has been some other malfunction. The mid-values will be turned off, the D/A converter will be turned off, and an alarm will be sounded. If this value is greater than the number of millivolts in the thermocouple corresponding to 1,800°C, then this indicates excess temperature, and the mid-values and D/A will be turned off immediately, and an alarm sounded.

c. The final routines determine in order whether 1,500°C?; 900°C?; 600°C?; or 300°C? If the temperature is lower than 300°C, the production process does not need a rising temperature slope below 30°C, and also because at this time the furnace molybdenum resistance is quite small. To reliably raise the

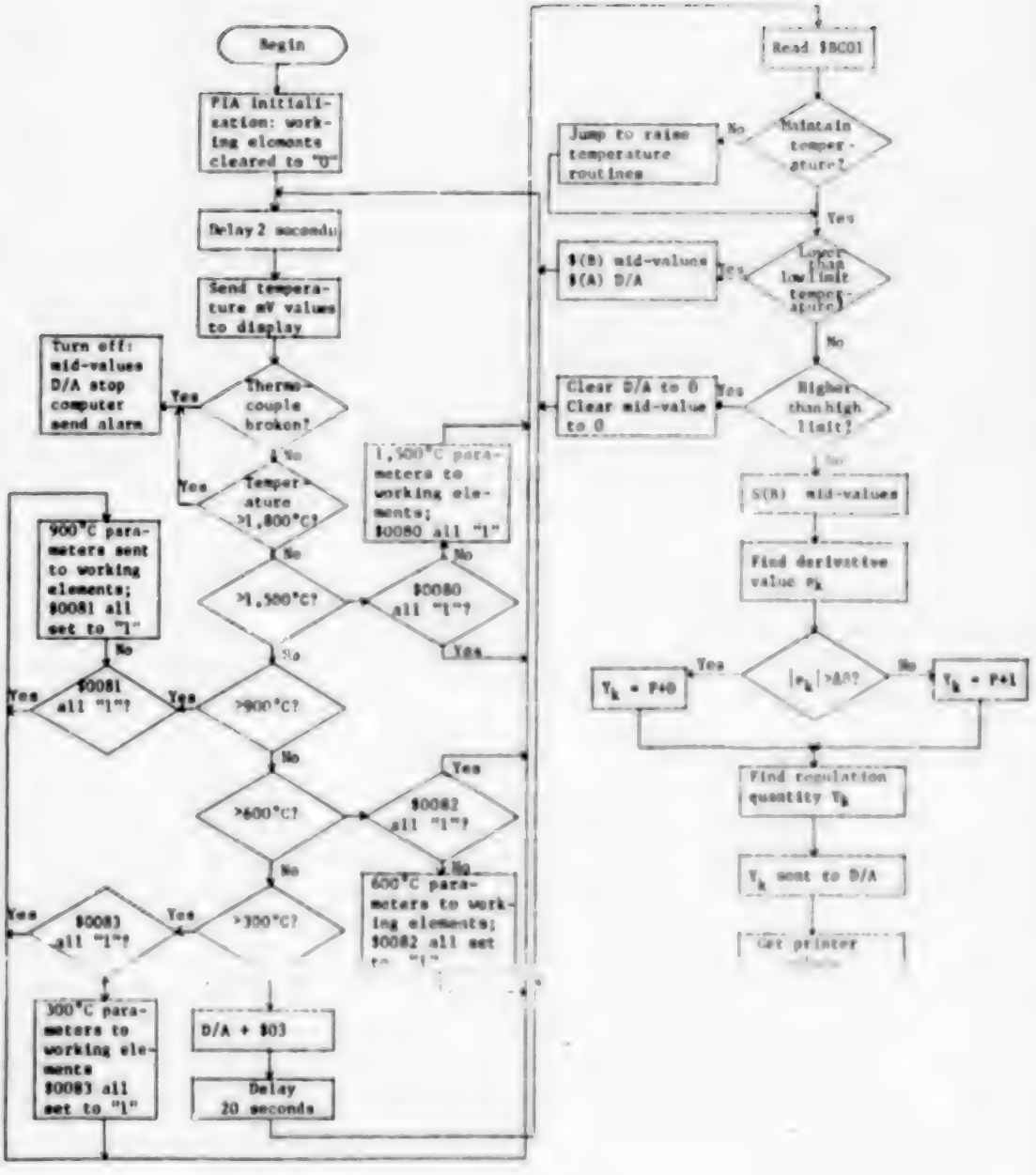

Figure 3. Flowchart of Temperature Control Routines

temperature, the method of adding $03 to the D/A every 20 seconds is used to gradually increase the output power. When the temperature has exceeded 300°C, the entire temperature process is divided into four parts, which allows each segment to correspond to different mid-values (stored as element $B) and D/A (stored as element $A), ensuring that the power will not become too great and burn components.

d. Determines to which segment a temperature corresponds, then after filling in the parameters for this segment in the working element, by distinguishing whether the high bit of control register BC01 is 0 or 1, it is determined whether it is necessary to raise the temperature or to maintain it. If an 0, it indicates that there is no pulse input to jump to the raise temperature routine. If a 1, it indicates that there is a pulse input and processing is to be as needed for maintaining the temperature. Please note that at the end of the routines to raise temperature, they return to the temperature maintenance routines.

e. After jumping to the temperature maintenance routines, it is first determined whether the current temperature is lower than the low limit temperature θ_{low} that has been set. If it is lower than θ_{low}, then the mid-values and D/A are turned completely on (the mid-values and the D/A of the corresponding segment are not the same), which allows a rise in temperature at full speed; when the current temperature is higher than the upper limit temperature θ_{high} that has been set, then the mid-values and D/A are turned completely off for a reduction of temperature at the greatest speed.

Only when the temperature is between the set values θ_{low} and θ_{high} can the routines enter the normal range for controlling temperature, solving for the deviation value e_k. If the absolute value of e_k is greater than 5°C, PD control is used; if less than 5°C, PI control is used, which allows for a better control process. The control value Y_k is derived from PID calculations. It is used to regulate the furnace heater flow I_3, the total heating current of the furnace being composed of three parts:

$$I = I_1 + I_2 + I_3 \tag{8}$$

where I_1 is the mid-value current, corresponding to the temperature within a particular range, this current does not change. I_2 is the compensation current as determined by the hardware and the power source voltage reciprocal. I_3 is the control current as calculated by the microcomputer through PID calculations. Corresponding to any particular temperature, when the deviation e_k is 0, any value may be present. Above 1,500°C, the system routines are preset to 88, and when this value is added to or subtracted from the calculated Y_k, the result is sent to the D/A, which is the I_3 that we have derived.

f. The raise temperature routines rise linearly according to the set value, the furnace temperature reached by the principle of rising. The purpose is to allow the rising temperature curve to fit the process requirements.

2. Printer Routines

This temperature control system is provided with an MX-80 III printer, a dot matrix printer that is a product of the Japanese Epson Co. and that has been modified by the Tianjin Hongxing Plant. Printing is by means of interrupts generated to the computer. This computer provides the user with a screen interrupt IRQ (active low), as shown in Figure 1, and the signal to print is a timing signal (adjustable from 1 to 60 minutes) generated by the digital clock. Output generates an interrupt from the PIA 4 CA1.

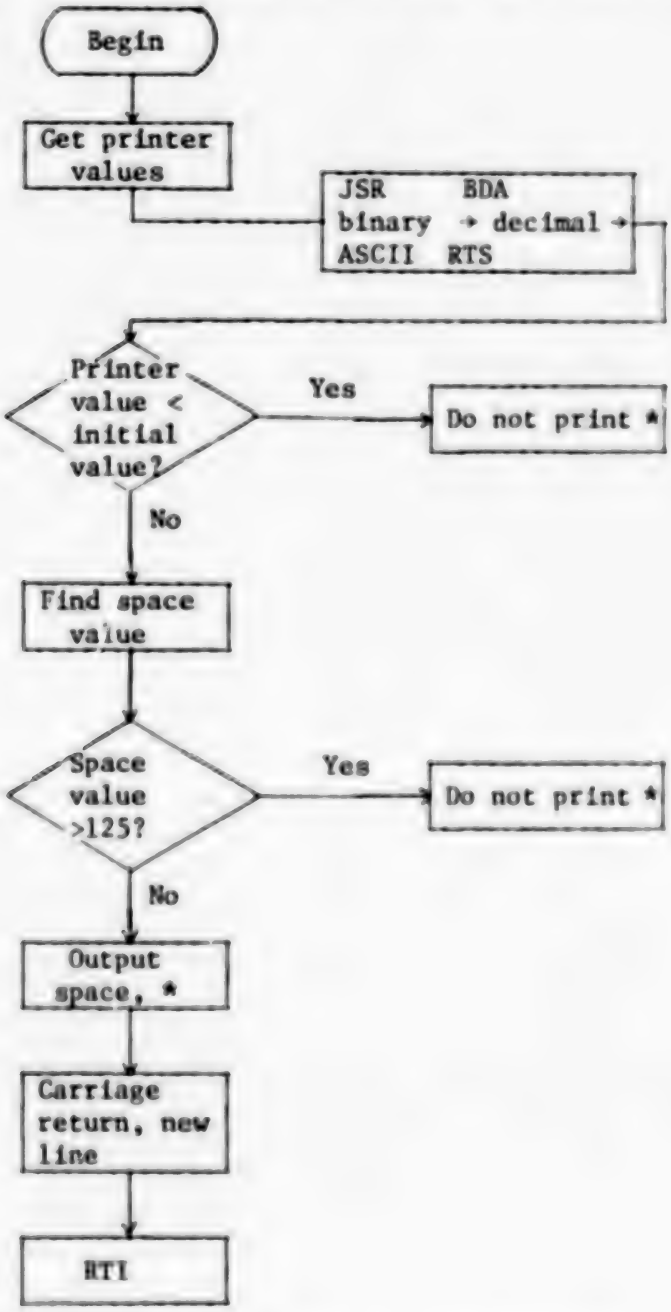

Figure 4. Flowchart of Print Routines

A flowchart for the printing routines is shown in Figure 4, some points about which we explain here:

a. The printer can only receive ASCII code, so after the binary values have been changed to decimal, they must still be changed to ASCII before outputting to the printer.

b. Because we are using compressed printing, there is a maximum of 132 characters [in a line], while the millivolt values for the temperature are five place decimal values, which leaves 127 character positions. We have allowed the largest available space to be 125, the hexadecimal value of which corresponding routine is $09C4.

c. The printing format is to first print out the decimal value of the millivolt value of the current temperature, after which is printed an asterisk. The position of the asterisk is determined by the following formula:

$$M = (T - A)/C \qquad (9)$$

where M -- the output space value
T -- printed temperature microvolt value
A -- initial microvolt value
C -- the microvolt value represented by each space. These routines assume 20 microvolts.

We can see from equation (9) that there will be an asterisk printed after M number of spaces.

The initial value is chosen by the operations personnel, where it is placed at addresses $0210 and $0211, and if less than the initial value or exceeds 125 spaces, then it is not printed.

The printing routines inventory has been omitted.

V. Conclusions

The temperature controlling accuracy of this terminal is ±0.5°C (600≈1,750°C); it can run for long periods. With slight modifications, this software and hardware can control several devices by itself. But as microcomputer prices get lower and lower, from the point of view of highest reliability we still hope to develop microcomputer single installation control systems.

REFERENCES

1. "DJS-065A Microcomputer Instruction Manual," Tianjin Radio Factory No 2, 1982.

2. "Computer Controller Technology," Nanjing Academy of Engineering, 1980.

3. "Microcomputers and Their Applications," Department of Electrical Engineering, Hunan University, 1981.

5. "Microprocessor Devices and Microcomputers," Qinghua University, Li Sanli [2621 0005 4539], 1981.

6. "MX-80 Type III," Operations Manual, Epson.

12586/9365
CSO: 4008/1075

MICROCOMPUTER CONTROLLED ANALOG TESTING SYSTEM DESCRIBED

Beijing DIANZI JISHU YINGYONG [APPLICATION OF ELECTRONIC TECHNOLOGY] in Chinese No 2, 25 Feb 86 pp 18-20

[Article by Wei Fengwei [7614 7685 5633]: "Microcomputer-Controlled Analog Quantity Testing System"]

[Text] In any special field there must be accurate, error-free testing of analog electric quantities, and this must be quick and the instrumentation light and convenient. This is quite a high requirement for automated test equipment. By using microcomputers in the testing and control of analog quantities we can easily realize this requirement. Regarding the microcomputers, all they need are some hardware interfaces together with the corresponding testing software and they can then quickly and accurately accomplish the testing requirement in accordance with pre-arranged routines. They can also generate an alarm signal when volt or current have exceeded a standard. They can provide the location of the error, and the test results can be completely output to display or printer for file storage and analysis.

I. A Brief Description of the Testing System

The testing system is composed of the five parts that are the object to be tested, the controller instrument that is microcomputer based, the test instruments, a power supply, and output equipment. A diagram of the analog quantity test system is shown in figure 1.

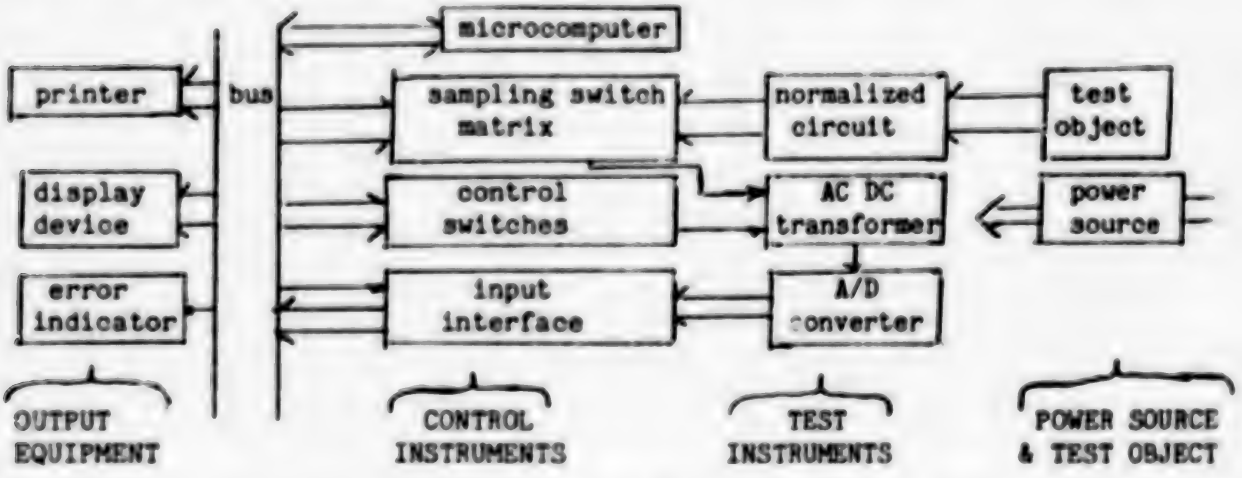

Figure 1 Flowchart of Analog Quantities Test System

Control commands are generated by the user program in the EPROM on the microcomputer, which allows automated testing of multiple circuits and various kinds of signals. Each signal that is tested comes in through cables to the test instrument's signal normalized circuit, gated through multichannel analog switches and gates, sequentially sent into ac/dc transformer circuits and dual integrated A/D converters, and is then sent to the microcomputer via an input interface where it undergoes data processing before being output for display, when the test results are printed out. A partial power source schematic for this automated test system is given in figure 2.

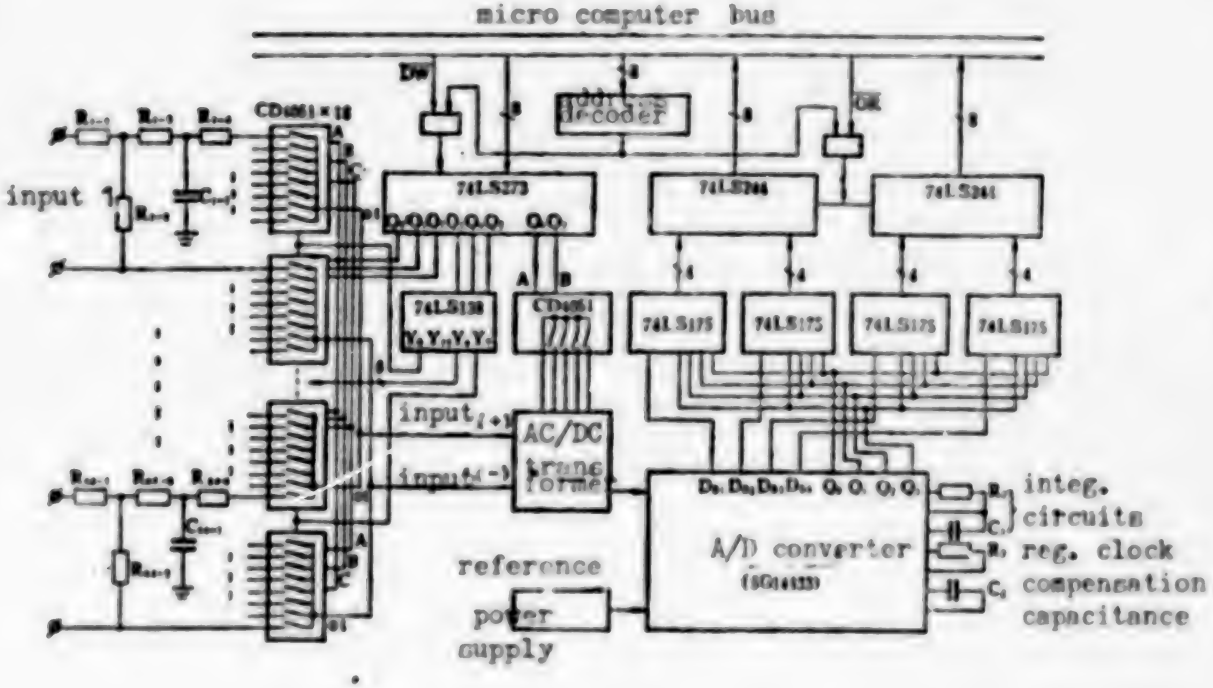

Figure 2 Power Supply Schematic

a. The object of testing

The objects of testing can be electric signals that are the output from power supplies for electronic equipment and from voltage, current, and signal sources, as well as working points on an electronic circuit; all output current not less than 50 microamps; DC voltage signals of 0 + or - 40 volts; effective values of 25 volts of low frequency sinusoidal voltage; peak values of 40 volts of low frequency square waves, all of which can be tested quite

accurately in this system. Length of the transmission cable is determined by actual conditions, the only requirement being that the internal resistance be as low as possible. Theoretically, the voltage values to be tested may be raised without affecting the tested accuracy. But if the tested source load capacity is quite weak, during the process of transmission the signal will be affected by interference, which will affect the accuracy of the test results.

b. The controller

The controller is composed of three parts: the microcomputer, a sampling decoder switch matrix, and an input interface.

The microcomputer used is a Z-8000 16-bit single board computer. But the TP-801 8-bit computer can also be used.

Sampling control is achieved through the 8-bit data lines provided by the microcomputer. The D6 and D7 among them are the status control bits, which two bits can decode four different codes. It can select four different working states of AC-DC transformer circuits: afterpulse, maintain peak value, maintain negative peak value, and maintain. Lines D0 through D5 are the sampling gate controller bits, through which can be decoded 64 different codes, used for controlling an 8 X 8 switch square matrix. There can be automatic gating and testing of signals on 64 circuits. The testing system described in this paper actually uses 40 circuits, the other 24 being for future use. The switch matrix uses the non-contacting electronic multiplexing analog switch CD4051.

The input interface is a 16-bit parallel input interface. Two levels of transfer have been designed for this system, with four 4D flip-flop 74L8175's acting as data buffers; two 8-bit tri-state latches, 74L8244, latch the computer's data bus.

c. The test instrument

The test instrument is made up of a normalized circuit, AC-DC transformer circuits, and an A/D converter.

The normalized circuit is actually a system input circuit that has been designed as an RC network with filter, current-voltage converter, and voltage level conversion functions. By adjusting the R1-2 ratio we can select the sampling ratio, allowing the input signal to uniformly become a voltage signal within a particular amplitude, to prepare for gating and testing.

The A/D converter is the key link in the test instrument. We have used the dual integrated A/D converter, 5G14433. This device is a product of the Shanghai Component Factory #5, and outputs BCD code. It uses analog zeroing, digital zeroing, repeated analog zeroing, integration of input voltage, and

accomplishes first-order conversion of analog quantities-digital quantities for reference voltage integration, integrator constant-current discharge, and for counting within the current discharge time. R2 in figure 2 is used to adjust components connected to the clock frequency of the converter, as the clock frequency determines the speed of the A/D conversion. The conversion speed of this system is 4 times per second.

The AC-DC converter is a dual integrated A/D converter 5G14433 designed advance circuit. It function is to convert the normalized voltage signal to be a DC voltage signal of less than 2 volts, to prepare for modular conversion. The working process for the AC-DC converter is controlled by the computer, and four working states are automatically selected according to the requirements of the test signal.

d. Power supply

For the power supply a floating, dual shielded secondary power source is used.

e. Output equipment

1. A digital display device on the microcomputer; 2. a printer.

f. Functional set-up of the system

1. Sampling of the input signal is gated through control of the microcomputer, automatically gated according to the user-designed program.

2. Working states of the AC-DC converters are controlled by the microcomputer, automatically programmed to switch over.

3. Various reset coefficients and standard values for tested electrical quantities are programmed into the EPROM, so data handling proceeds automatically.

4. Actual values of tested signals can be read directly from the display device or from the printed results, the dimensions being identical with reality.

5. Automatic adjustment of zeroing.

6. Automatic initialization and both manual and initial reset.

II. A Flowchart of the Test Routines

A flowchart of the test routines is given in figure 3.

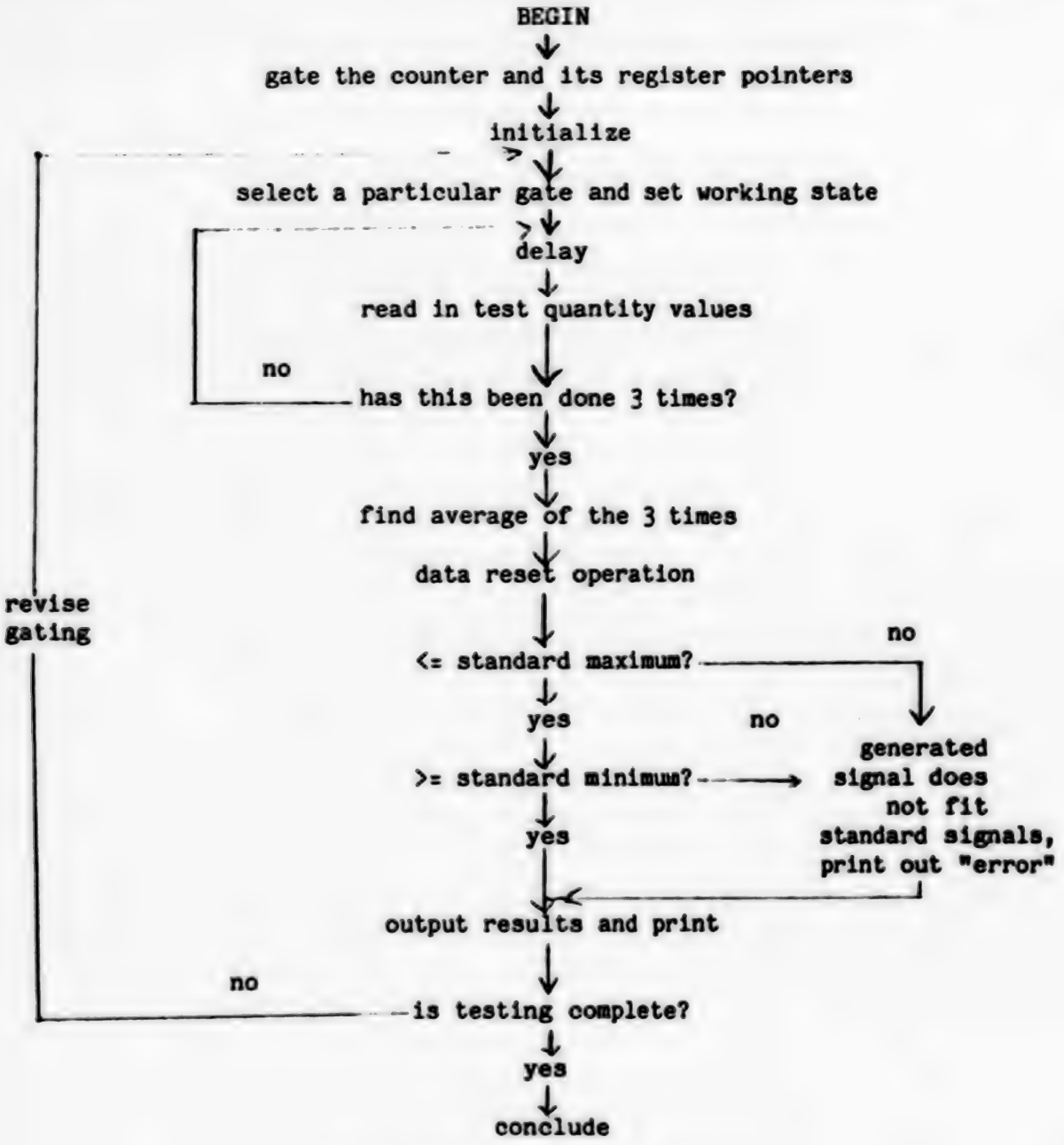

Figure 3 Flowchart of Testing

III. Further Developments of System Applications

What we have discussed above is an automatic testing system controlled by a microcomputer. It can also be used for multimonitoring or relative constant control of physical quantities such as temperature, speed, and water pressure. As long as each monitoring point (or control point) of the object to be tested is equipped with sampling devices and electrical quantity converting devices that can convert the physical quantities to electrical quantities, it will work. The flowchart of the routines used for monitoring is shown in figure 4. The portion indicated by dotted lines in the figure are the places in the

program process and monitor testing program process that are not the same when used for relative constant control, the identical portion having been abridged.

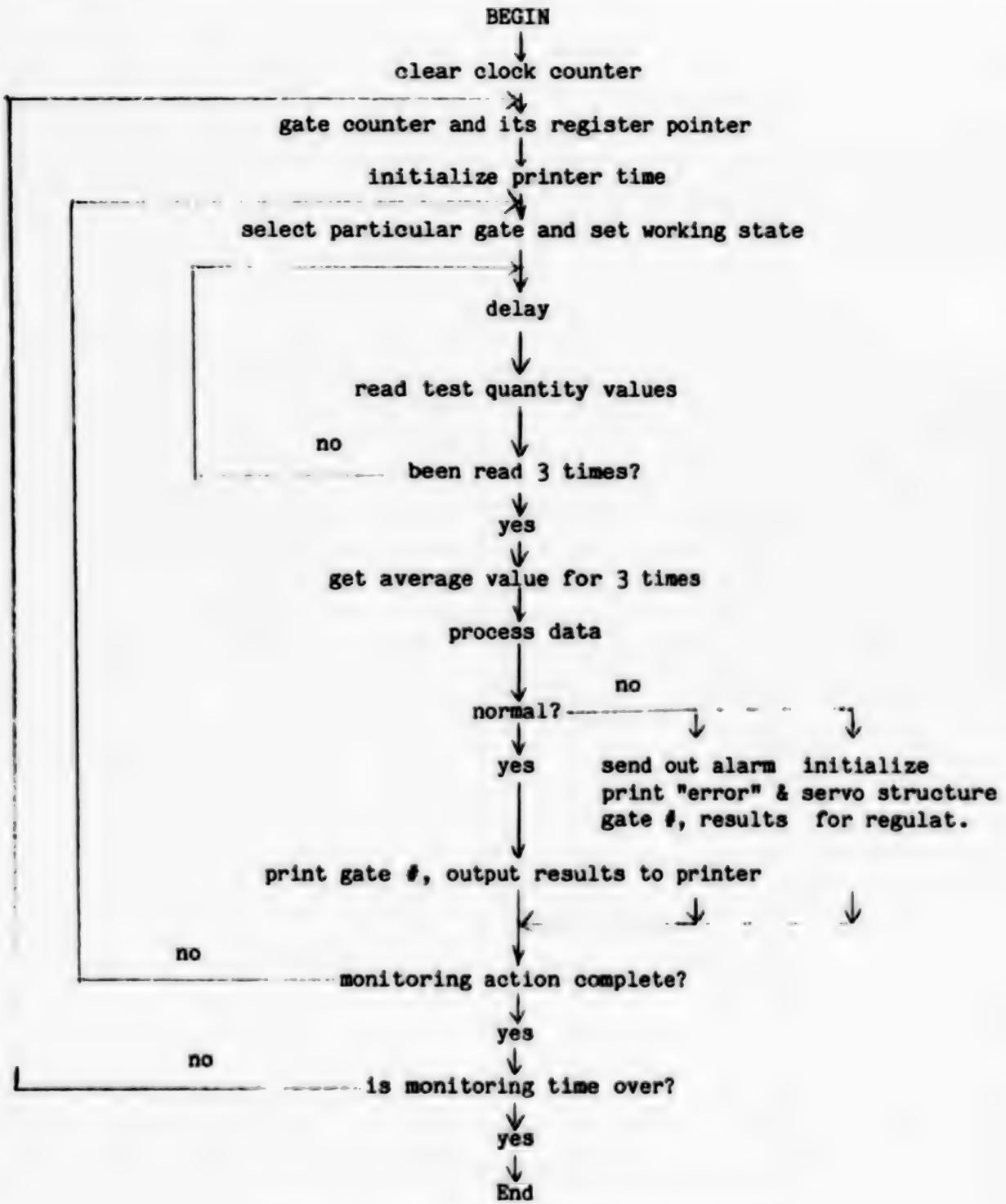

Figure 4 Flowchart of Monitoring Routines

IV. System Anti-Interference Measures

Whether it is the testing of analog quantities or the process of monitoring or controlling, when examining the strengths and weaknesses of a system anti-interference capability is an important index. If the system is operating under harsh conditions, the relative strength of its anti-interference capability not only directly affects the reliability and accuracy of output results, but it even concerns the success of the system. To improve anti-interference capabilities in this system, we have taken the following measures:

a. We have chosen a dual integrated A/D converter that is highly resistant to interference;

b. Filtering links have been added to input circuits to prevent random high frequency pulse interference;

c. The microcomputer and test instruments both have high level shielded, floating secondary power supplies and automatically loop back to prevent common mode interference;

d. The differential input method is used to prevent ordinary state interference;

e. The transmission cable has twisted-pair shielded wire, and the test circuits are shielded, all of which prevents cross interference.

Experiments have shown that anti-interference measures used in this system are effective. When transmitting over a 150 meter line, test accuracy of the system is not degraded.

12586
CSO: 4008/1075

DISPOSAL OF SOLID RADIOACTIVE WASTE OF NUCLEAR POWER PLANT

Chengdu HE DONGLI GONGCHENG [NUCLEAR POWER ENGINEERING] in Chinese Vol 7, No 2, Apr 86, pp 35-38, 74

[Article by Yu Shicheng [0151 0013 6134]]

[Text] I. Introduction

During the operation of a nuclear power plant, most of the released radioactive elements with the exception of the low-poison group such as inert gases and tritium, are contained in th radioactive solid wastes. Therefore, management of radioactive solid waste is an issue of great importance.

The treatment of radioactive waste involves converting the waste materials into a form that is suitable for shipping, storage and disposal (including condensation, compression, solidification and packaging). The disposal of radioactive waste is to properly seal and store the waste so that before the radioactive elements decay to a sufficiently low level, they will be isolated from the human and biological cycles, and will never cause harm to human beings.

In 1983, the International Atomic Organization held a conference on radioactive waste management in Seattle, where 31 countries and 9 international organizations participated. It was generally believed that the basic technical problems of disposing low-radiation level waste materials had been solved, but further improvements are required to develop a complete waste disposal system[1].

II. Unique Features of Radioactive Solid Waste from Nuclear Power Plant

It should be pointed out that the radioactive solid waste from nuclear power plants does not include the exhausted fuel elements from the reactor or the high-radiation glass byproduct from processing exhausted fuel elements. A small amount of high-radiation waste such as replaced reactor parts are stored with the exhausted fuel elements where they undergo decay and then shipped out of the plant.

A small amount of solid waste (e.g., contaminated equipment and parts) may be treated as non-radioactive waste or reused after decontamination or storage and decay. Most of the solid wastes (e.g., solidified residual liquid from evaporation, filtered slush, filter core, wasted resin, burned ash, or other types of dry waste) contain more than 90 percent of the radioactive elements. These solid wastes are primarily low to medium radioactive elements with relatively short half lives and exhibiting $\beta - \gamma$ radiation; the content of super uranium, long half-life elements exhibiting α radiation is very low. The level of activated corrosive products such as ^{58}Co ($T_{1/2}$ = 71 days), ^{60}Co ($T_{1/2}$ = 5.3 years), ^{55}Fe ($T_{1/2}$ = 2.7 years), ^{59}Fe ($T_{1/2}$ = 45 days) is quite high, but because of their short half lives, generally they will have no adverse effect after storage for 50-100 years. The radioactivity after storage primarily comes from fission products ^{90}Sr ($T_{1/2}$ = 28.5 years) and ^{137}Cs ($T_{1/2}$ = 30.2 years).

The annual output of solid waste from a nuclear power plant depends on the reactor power, the type of reactors, the operation and management of the power plant, the condition of maintenance and repair, and the waste treatment techniques [2]. The amount of solid radwastes produced by a 1 million kW light-water reactor in the U.S. is 400-1300 m^3 per year [3]; a similar reactor in Japan produces (600-1000 m^3 solid radwastes per year [4]; and a 900,000 kW PWR of the French Framatome Atomic Energy Co. produces 400-500 m^3 solid radwastes per year.

The above discussion shows that the unique features of solid radwastes from nuclear power plants are: large volume (a 1-million kW PWR power plant produces 400-600 m^3 solid radwastes per year; a BWR power plant with the same reactor power will produce 70 percent more), and low specific radioactivity, most of which is attributed to short half-life nuclear elements with $\beta - \gamma$ radiation. According to the law of radioactive decay, the level of radioactivity is reduced by a factor of 1,000 after 10 half lives and by a factor of 1 million after 20 half lives. In other words, the radioactive waste must be isolated from human and bilogical cycles for 300-600 years.

III. Ocean Disposal

Ocean disposal of solid radwastes has the following merits:

1) The ocean is isolated from human environment;

2) The structure of the ocean floor used for waste disposal is geologically stable;

3) Because of the lack of free oxygen near the ocean floor, the waste containers can remain intact for a long period of time without suffering oxidation;

4) The ocean emits a high level of natural radiation, even if there are leaks of radioactive elements from the disposed wastes, they will be absorbed in the fluctuations of natural radiation.

The Nuclear Energy Office of the Organization of Economic Cooperation and Development had studied the problem of ocean disposal of low radiation solid wastes, and had established guidelines and clearly defined monitoring responsibilities. Disposals of nuclear wastes in the Atlantic Ocean had been monitored by an international organization; specifically, at a depth of 5,000 m, five member nations had disposed 35,000 waste containers with a total weight of 11,000 tons and total radiation level of 8,000 curies. Subsequently, eight European countries (France, West Germany, Belgium, Italy, Holland, Switzerland, Sweden and Great Britain) participated in 11 ocean disposals; the average depth of disposal was 4,500 m [5].

In order to prevent the radioactive wastes from polluting the ocean, a conference was held in 1972 in London to discuss a treaty on ocean disposal. The treaty requires that each country establish a national-level organization to control the ocean disposal of wastes, ban the disposal of high-radiation wastes, and that disposal of low and medium radiation wastes must be approved and managed by a special office. It also establishes specific regulations for selecting the disposal sites, and requires that they must be at least 4,000 m deep, and must be away from continental mounts, deep-sea resources and underwater cables [6].

Based on an assessment of the radioactive ecology of disposed radwastes in deep ocean regions, the International Atomic Energy Organization has banned the ocean disposal of high-radiation wastes; all radioactive elements are classified, and those which exceed the threshold are banned from ocean disposal. An inspection of the disposal site in the northeast Atlantic Ocean shows that it meets the requirements established by the International Atomic Energy Organization.

Between 1946 and 1970, the United States opened more than 50 ocean disposal sites, 90 percent of the waste materials and 95 percent of the radioactive elements are concentrated in four of these sites, but they did not meet the specifications of the London treaty or the Organization of Economic Cooperation and Development. Since the method of shallow ground burial of solid radwastes was successfully developed by the Department of Energy, in 1970 the United States decided to stop ocean disposal of radioactive wastes in order to protect the ocean environment. In an environmental assessment of the four disposal sites, containers were retrieved from the ocean floor ranging from 2,800 m to 3,800 m in depth; careful inspection showed that the containers were compressed toward the center, and there were small amounts of radioactive elements surrounding the container; however, there was no evidence of damage to human beings or the ocean environment[7].

In 1949, Great Britain began disposing packaged containers of low-radiation solid wastes in the Atlantic Ocean; between 1967 and 1971, it participated in the experimental joint ocean disposal project sponsored by the Nuclear energy Office of the Organization of Economic Cooperation and Development, and accepted international monitoring. By the end of 1983, the total amount of ocean disposed waste materials reached 77.53 tons. They believe that ocean disposal will not lead to detectable danger, and therefore will continue to do so. They plan to invest in the renovation of disposal ships and installation of satellite navigation equipment; the amount of disposed radwaste is expected to increase at a rate of 20 percent per year.

In order to assess the safety of ocean disposal, Japan conducted high-pressure filtration tests and container integrity tests under simultated 5,000-m deep ocean conditions. It also conducted safety inspections of disposal sites.

In 1983, the London Waste Disposal Treaty Conference passed a resolution to ban ocean disposal of radioactive wastes, but this resolution had no real restraining authority. Protecting the ocean environment and preventing radioactive pollution has become a problem that is of concern to every nation in the world; a final resolution is expected to be reached during an international conference in 1985.

IV. Land Disposal

Land disposal of radioactive solid wastes is an effective method to protect human beings and the environment [8]; it accounted for 99 percent of the radwaste disposals in the past [9]. There are three different approaches to land disposal.

1. Shallow Ground Burial

The shallow ground burial approach is to bury the radioactive solid wastes in a trench which is 30-240 m long, 6-12 m wide and 6 m deep. The waste container is first covered with 1-3m of dirt then with a layer of clay; a stone or metal market will be erected to indicate the volume and radiation intensity of the disposed wastes. The United States has 6 commercial disposal sites which can accommodate 764,000 m^3 of solid wastes. Currently, all the low-radiation solid wastes produced by the nuclear power plants in the U.S. are disposed using the shallow ground burial approach. At some of the earlier burial sites, because of the crude construction and site selection, and poor packaging and management, there was evidence of leakage of radioactive elements. Upon detection by the monitoring system, the disposal sites were closed down immediately to avoid further damaging effects on the public and on the environment.

The construction and utilization of shallow disposal sites can be divided into four stages: 2-3 years of building the site facilities and digging the trenches; 15 years of disposal service; 150 years of monitoring and limiting land use after closing down the disposal site; after that the land can be used without any constraint. Because of the different conditions of hydrology and geology, the cost of building a disposal site differs considerably from one country to another.

In Great Britain, the Nuclear Industry Radioactive Waste Commission divides the waste materials designated for shallow ground burial into different categories; low-radiation wastes can be directly placed in storage tanks; medium-radiation waste tanks must be shielded with cement before shipping; waste materials with high β-γ radiation are stored in tanks and shipped to the disposal sites in shielded containers. The design guidelines for the burial trenches are:

a) selecting a trench site with the proper geological structure of with clay soil;
b) the sidewalls and bottom of the trench must be inclined;

c) water drainage ditches must be constructed around the burial trench;
d) monitoring holes must be installed in the vicinity of the trenches.

The first type of burial trench is 150 m long, 8 m wide and 6-9 m deep. The bottom of the trench is inclined toward the water pit, and is covered with a layer of 1-m thick gravel and sand for water drainage. When the waste materials reach a height of 3-5 m, they are covered with clay to minimize water infiltration.

The second or third type of trench is 70 m long, 20 m wide and 19 m deep. The bottom of the trench is inclined toward the water pit, and covered with a layer of porous cement; the water pit is equipped with monitoring tubes, and the trench walls are constructed with steel reinforced concrete. The shielded waste tanks are lowered into the trench using a fork lift; after reaching a height of 8 m, they are covered with a 1-m thick steel-reinforced concrete and coated with a layer of water-resistant asphalt, then filled with a layer of 3 m-thick packed clay. On top of the trench is a 1 m-thick steel reinforced concrete structure covered with a layer of of 5 m-thick packed clay to prevent rain water from entering.

In France, the disposal of solid radwastes from nuclear power plants is the responsibility of a national radwaste management bureau. The [wangshen] radwaste storage pool located in northwest France has a storage capacity of 400,000 m^3; since storage began in 1969, 200,000 m^3 of it has been filled. In France, the solid radwastes produced by a nuclear power plant are stored inside the plant for 15 days before being shipped to the national waste pool for disposal.

2. Storage in Abandoned Mines (or Caves)

This form of storage is primarily used by small, densely populated European countries with stable geological structure. The abandoned [Hesai] salt mine in the northeast part of West Germany is free of ground water and geologically stable; it has an area of 4.2 square kilometers. In a region 490-750 m below the surface, 130 chambers were excavated with a total capacity of 3.6×10^6 m^3; they can accommodate 140,000 barrels of low-radiation wastes and 1,300 barrels of medium-radiation wastes.

Abandoned mines generally have sufficient depth to have any effect on human activities. But they were designed and constructed to meet mining requirements; whether they are safe for disposal of radioactive wastes remains to be investigated.

3. Storage at the Plant Site

In technical report No. 198 of the International Atomic Energy Organization, "Guidelines for Safe Treatment of Radioactive Wastes of Nuclear Power Plant", the feasibility of plant site storage was confirmed. The guidelines stated that "for a reactor location with favorable hydrological and geological conditions, it is feasible to use shallow ground burial to dispose certain radwastes at the plant site." Japan has accumulated 460,000 barrels of solid radwastes stored at the reactor sites. The United States had also suggested plant site disposal plans because of increasing disposal costs due to shut-down of three of the four disposal sites in the eastern part of the country.

Final disposal of the solid radwastes and the plant will take place when the nuclear power plant reaches retirement age. Great Britain on the other hand, believes that plant site storage of solid wastes can be considered a form of final disposal.

The long-term process of radwaste disposal may be affected by natural processes or by human activities, which cause radioactive elements to enter the human environment through water infiltration and diffusion. Because of the difficulty in finding an ideal disposal site, man-made screens (e.g., engineering structures) are often used to enhance the isolation effect and the depth of burial is increased to improve safety. The disposed solid wastes must meet the following requirements:

a) there must not be any leakage of liquid or gas; the U.S. Nuclear Regulatory Commission specifies that the amount of free liquid in a waste tank must be less than 1 percent;

b) the container must have sufficient strength to withstand loading, unloading and docking operations; generally, 200-liter steel tanks with wall thickness of at least 1.5 mm are used; Japan specifies that the waste tanks must be able to withstand a load of 5 tons; the United States specifies that the containers must remain corrosion resistant for 20 years and they must be retrievable;

c) the content of super uranium α radiation in the disposed wastes must be strictly controlled.

Solid radwastes of nuclear power plants have much lower screening requirements for the disposal sites than high-radiation, long half-life waste materials. They can be disposed in shallow or medium-depth trenches, and that the heat generated due to decay can be ignored during the disposal period.

V. Suggestions

Disposal of solid radioactive waste of nuclear power plant is an important part of waste management, and directly affects the cost of waste management. During the disposal period, the effect of radiation on the environment and on human beings must be kept "as low as feasible." Disposal of solid radwaste not only is a costly task but also requires the allocation of a large amount of land; therefore, reducing the volume of the waste material is a critical issue of waste management in countries with high developed nuclear power capability as well as in developing countries.

Disposal of solid radioactive waste of nuclear power plant is a complex problem which has technical, economic and social implications. In view of the unique characteristics and far-reaching effects of radioactive wastes, any policy concerning the disposal of radwastes must be proclaimed in the form of national laws or regulations so they will be enforced with sufficient authority. A national radioactive waste management organization should be set up to establish the necessary regulations and standards including radwaste management procedures, waste classification standards, and performance test standards; it should also be responsible for such tasks as mapping the

hydrological and geological structures of the earth stratum, studying the mechanism of migration of nuclear elements, selecting appropriate disposal sites for land burial in order to support China's nuclear power industry. Environmental protection is a basic policy of this country; therefore, economic development and urban/rural development must be coordinated with environmental de lopment in terms of planning and implementation in order to reach a bala..ce between economic benefits, social benefits and environmental benefits.

3012/9869
CSO: 4008/77

RECYCLING URANIUM AND PLUTONIUM IN LIGHT WATER REACTOR

Chengdu HE DONGLI GONGCHENG [NUCLEAR POWER ENGINEERING] in Chinese
Vol 7, No 2, Apr 86 pp 39-48, 54

[Article by Zheng Hauling [6774 5478 6875]]

[Text] I. Introduction

The UO_2 elements in a light water reactor (UO_2-LWR) produce approximately 1 percent industrial plutonium after irradiation; most of the plutonium produced are ^{239}Pu and ^{241}Pu, which can be used as fuel for theremal neutron fission. Since the 1950's, western countries in Europe and North America have conducted studies and industrial tests of the recycled utilization of treated nuclear residues of UO_2-LWR. In 1957, the first manufacturing plant of mixed uranium and plutonium oxides (MOX) began operation; in 1963, the first batch of experimental MOX elements were tested with BR_3 irradiation in a reactor. By January 1984, 13 PWR's and 12 BWR's were using MOX elements with a maximum burnout value of 71 GWD/TU[1].

Since the beginning of the LWR industry, recycling U and Pu has been a topic of great interest because of the low utilization rate of LWR fuel and the limited uranium resources. While building FBR is one way to solve this problem, a completely new industrial system which has more stringent requirement than that of LWR must be developed. It is estimated that such a system will not be commercially available until around 2025, and even then its initial economic benefits will not be able to compete with LWR's. Consequently, suggestions have been made to use a MOX-LWR fuel cycle strategy during the LWR and LWR-FBR transition period, i.e., using the retrieved uranium and plutonium from LWR post-processing to make MOX-LWR elements, which can then be reused in LWR's. The author believes this to be an effective approach to improve the fuel utilization LWR, to develop new sources of fuel, and to speed up the accumulation of plutonium for FBR's.

II. Recycling of Uranium and Plutonium in LWR's

1. Recycling of Plutonium

The industrial-grade plutonium (also called primary plutonium) produced from burning UO_2-LWR in LWR's amount to approximately 0.9-1 percent of the total reserves of heavy metals. It contains approximately 1 percent of ^{238}Pu, 58-68 percent of ^{239}Pu, 20-30 percent of ^{240}Pu, 9-10 percent of ^{241}Pu, and 2-6 percent of ^{242}Pu. Primary plutonium can be mixed with depleted uranium, natural uranium and retrieved uranium from post-processing to produce MOX

elements, which are reusable in LWR's. Energy will be released from thermal neutron fission of ^{239}Pu, ^{241}Pu and ^{235}U, and the neutrons will again be captured by ^{238}U, ^{238}Pu and ^{240}Pu to produce fissionable plutonium (^{239}Pu, ^{241}Pu). Therefore, by burning recycled elements, there is no intrinsic or quantitative reduction in the fissionable plutonium; in other words, there is no intrinsic change in fissionable contents between secondary plutonium (from MOX elements) and primary plutonium, or between tertiary plutonium and secondary plutonium. This is the basic difference between plutonium and ^{235}U in the UO_2 fuel elements.

Fig. 1 shows the composition of plutonium isotopes at various stages of recycling. After the fifth recycle, the proportions of plutonium isotopes remain unchanged; they do not vary with the number of recycles or with the type of uranium used (natural uranium, depleted uranium, or retrieved uranium from post-processing). The "equilibrium" isotope contents are shown in Table 1[2].

Fig. 2 shows a plot of the variation of fissionable plutonium (Pu_{fis}) as a percentage of the total plutonium with the number of refuelings in the reactor. Initially, Pu_{fis} is about 77 percent of the total plutonium, then it gradually decreases and stabilizes at about 60 percent after 20 refuelings. This "equilibrium composition" of industrial plutonium is totally acceptable for maintaining the production of MOX-LWR elements.

Table 1. Pu Isotope Content After Fifth Recycle of MOX Elements

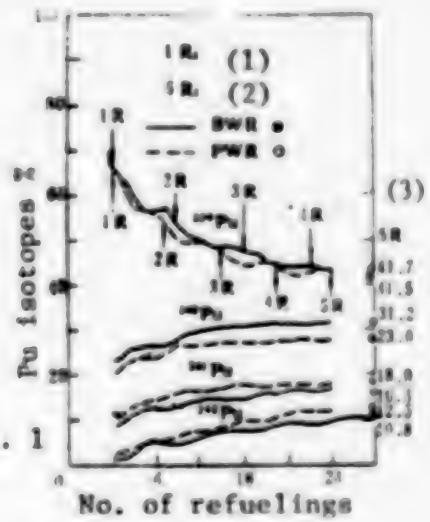

Fig. 1

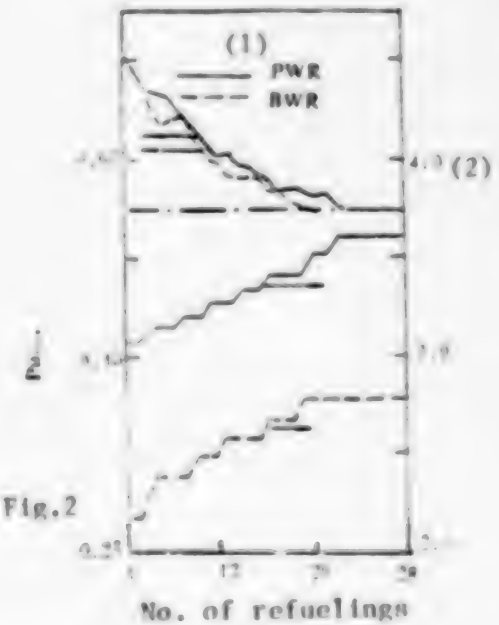

Fig.2

Fig. 1. Composition of Recycled Pu Isotopes in MOX Elements

Key:

(1) 1R: 1st Pu recycle
(2) 5R: 5th Pu recycle
(3) equilibrium composition of Pu isotopes, percent

Fig. 2. Variation of the Proportion of Fissionable Plutonium with Number of Refuelings

Key:
1. use of natural uranium as basic fuel
2. weight of Pu_{fis} in MOX elements

The key considerations for optimum recycling of industrial plutonium are the following: a) the plutonium should be allowed as much time as possible in the reactor to maximize energy production; b) the elements should have an adequate cooling period after being removed from the reactor to ensure disintegration of the short-half-file fission elements in order to reduce the level of irradiation during post-processing; c) the ^{241}Pu should be utilized as much as possible in the reactor before significant decay ($T_{\frac{1}{2}}$=14.4 years) occurs.

Based on the above considerations, the Nuclear Industry Service Co. (NIS) of West Germany suggested that the safest and most economical approach is to have a 2-year period outside the reactor, which includes 1 year of cooling and decay and 1 year of post-processing and element production.

The standard operation for both PWR's and BWR's is to have one refueling per year; in PWR, one-third of the fuel is replaced each time, and in BWR, one-fourth of the fuel is replaced, hence the plutonium recycling periods are respectively 5 years and 6 years. If the life of a reactor is 30 years, then PWR's can be recycled 6 times, BWR's can be recycled 5 times.

The initial proportion of MOX elements in the reactor core is only 3 percent for BWR and 4 percent for PWR. As the number of cycles increases, plutonium production also increases; by the 20th refueling, plutonium consumption and production reach an equilibrium, i.e., the so-called SGR (self-generated recycling) condition, and the proportion of MOX elements becomes approximately 30 percent. Table 2 shows the data of fuel elements for different refuelings; the data do not vary significantly if natural uranium is replaced by depleted uranium or post-processed uranium.

Table 2. Fuel Element Data in a Reactor (Natural Uranium)

表2 反应堆换料元件数据（天然铀基料）

No. of refuel.	$(u+Pu)_{fis}$, Wt%		No. of MOX elements		MOX proportion		Pu_{fis}/Pu_{tot}	
	BWR	PWR	BWR	PWR	BWR	PWR	BWR	PWR
4	2.9	3.8	28	8	3	4	0.75	0.77
8	3.1	3.9	48	12	21	21	0.69	0.71
12	3.3	4.0	56	20	25	27	0.64	0.65
16	3.4	4.1	60	16	28	27	0.62	0.63
20	3.5	4.2	60	20	30	29	0.60	0.61

Based on the "optimum self-generated recycling; mode of operation, plutonium remains inside the reactor for 20 or 18 years of the 30-year reactor life, i.e., more than three-fifths of the time it is producing energy for power generation. However, if the current "delayed plutonium recycling" mode of operation is used, during each cycle it remains outside the reactor for 7 years, plus 1 additional year required for post-processing and element production, i.e., the period of storage and processing outside the reactor is four-fifths of the reactor life. Clearly this is undesirable from the point of view of both economy and safety.

2. Recycling of Uranium

Most of the uranium in the UO_2 elements from a LWR contain ^{238}U and 0.8-0.9 percent of ^{235}U, both of which can be returned to the LWR without much difficulty, but there are also accumulations of ^{232}U, ^{234}U and ^{236}U in the retrieved uranium. Although the ^{232}U content is very low, its strong γ radiation requires special protective measures and the necessary modifications of the industrial flow process [3]. ^{234}U and ^{236}U have strong neutron-absorption capability, hence the presence of ^{234}U and ^{236}U tend to reduce the reactivity of the elements, which can only be compensated by increasing the fuel content.

In terms of ^{234}U and ^{236}U, the first uranium recycle can save 15 percent of natural uranium, but the second recycle can only save 3 percent of natural uranium, hence its economic benefits are limited.

The above discussion shows that from the point of view of cost effectiveness and minimizing processing difficulties, uranium should be recycled only once.

3. Experience of Using MOX Elements in LWR

There are generally two types of MOX modules used in a LWR:

a. "Plutonium Island" Type Modules. In this case, the MOX elements are placed in the center of the reactor core, with enriched UO_2 elements placed around the periphery. This type of module is suitable for BWR's or reactors with large water gaps between the modules.

b. "All Plutonium" Type Modules. This type of module contains only MOX fuel elements and is used primarily in PWR's. In this type of reactor, the effects of guide tubes on flux and peak value coefficients can be corrected by properly selecting the enrichness distribution diagram.

In a typical PWR module, approximately 60 percent of the MOX elements are highly enriched (3.9-4.6 percent fissionable materials), 8 percent are slightly enriched (2.4-2.8 percent fissionable materials); and the remainder are moderately enriched (3.2-3.9 percent fissionable materials).

In a typical BWR module, approximately 50 percent of the MOX elements are highly enriched (3.2-4.6 percent fissionable materials), the other 50 percent are slightly enriched (2.6-3 percent fissionable materials).

With regard to reactor core management, one can follow a procedure similar to that used in UO_2-LWR, i.e., first select the characteristic parameters of the highly enriched elements of the MOX fuel, then determine the number of MOX rods of each module, and finally determine the number of fresh refueling modules.

In order to avoid the formation of power peaks on the boundary between the MOX elements and the UO_2 elements, generally there is a buffer zone in the low-enrichment MOX region.

The MOX element has a melting point 20°C lower than that of the UO_2 element, and its thermal expansion is approximately 1 percent larger; in addition, its γ self-screening effect is better and its heat production is higher. These properties partially compensate for the poor thermal properties of the MOX fuel.

The release of gas from fission products and the expansion of UO_2 or MOX particles are not affected by adding Pu to U, but they are affected by the microcrystalline structure[1].

When the power exceeds 430 W/cm, the plutonium in the fuel rod begins to shift toward the high temperature region; but this is not a problem in MOX-LWR because its linear power level generally is less than 430 W/cm; also, the self-screening effect tends to lower the temperature at the center of the MOX-LWR.

Based on its 20 years of experience, the BN Co. in Belgium found that: 1) MOX fuel contained in a stainless-steel shell performs better than UO_2[4]; 2) there is less mechanical interaction between the MOX fuel plates and the shell than UO_2 fuel elements; 3) MOX has better creep characteristics than UO_2 because of the smaller plate-shell interaction; 4) MOX has slightly lower production of ^{135}Xe than UO_2. ^{135}Xe is an extremely strong neutron absorber, but the effect on reactivity is quite small because MOX has larger neutron absorption cross section than UO_2, thus LWR's using MOX elements operate more steadily; 5) MOX elements cause the moderator temperature coefficient to become more negative, which may result in a slight loss of the reflectivity margin when the reactor is shut down [5]; 6) because of the more negative Doppler coefficient and moderator temperature coefficient of the MOX elements, the power of MOX-LWR decreases more slowly than UO_2-LWR; this leads to better self-screening and better self-modulation; 7) the γ scan spectrum of discarded elements showed evidence of good power distribution when the burnout of "plutonium island" elements is very high [6].

A study done by CEA of France showed that in a mixed loading of MOX-UO_2 elements, the neutron flux is discontinuous, therefore, the reactor physics method of calculation should be modified [7].

The research done by Sweden showed that the slow neutrons emitted by plutonium isotopes are two-thirds less than those emitted by uranium isotopes. Therefore, MOX elements will respond faster to a change in reactivity than UO_2 elements. This would have an undesirable effect in case of an accident such as ejection of control rod in PWR or dropping of control rod in BWR, but because of the large negative Doppler coefficient, the accident will terminate very quickly [8].

Fig. 3 presents a reactivity equilibrium diagram of PWR proposed by the West German Power Plant Union (KWU); it shows a comparison of reactivity in a PWR when different fuel elements are used [5].

Fig. 3 Reactivity Equilibrium Diagram for Different Fuel Modules in a PWR

Key:
(1) emergency shut-down Doppler effect
(2) reactivity due to decreasing coolant temperature
(3) returning to critical state
(4) reactor shut-down margin
(5) jammed control rod

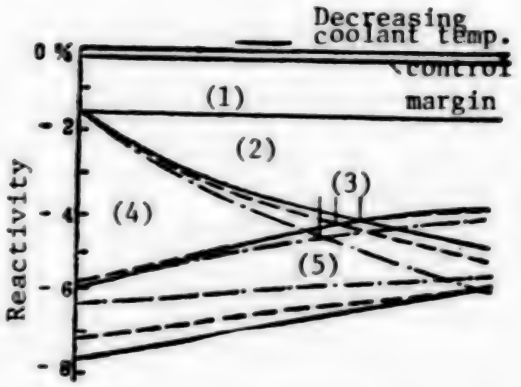

III. Fuel Cycle

The fuel cycle is generally divided into the front and rear segments. The front segment includes mining, mineral processing, enrichment and element fabrication; the rear segment includes temporary storage of nuclear residues, post-processing, conversion, waste treatment and permanent disposal. The recycling of U and Pu in LWR reduces the load on mining, processing and enrichment of natural uranium, but it poses some new problems for element fabrication, post-processing and conversion. This section briefly discusses the difference between MOX and UO_2 and the resulting effect on fuel cycle industrial units.

1. Post-Processing

The main differences between MOX and UO_2 elements with the same burnout and the same cooling period are: a) MOX elements have different levels of fission products, approximately 30-70 percent higher in ^{106}Ru, ^{106}Rh, ^{85}Kr and ^{129}I, and approximately 10 percent lower in ^{95}Zr-^{95}Nb; b) MOX elements have different levels of the actinium series--3 percent less in U, 1-3 times more in Pu, Am and Cm; c) there are also differences in physical-chemical properties such as thermal property, heat-conductivity, solubility, melting point, and density. These differences have the following effects on post-processing:

(1) Segment Processing. There are no major changes in such procedures as transportation, fuel removal, storage, disassembly of modules and cutting of fuel rods between MOX-LWR elements and UO_2-LWR elements.

The dissolving of MOX waste elements is a major problem. If the conventional method of mechanically mixing the UO_2 and PuO_2 powder is used, there will be a large particles which are difficult to dissolve even in boiling, high-concentration HNO_3 solution. The best way to solve this problem is to choose a fabrication process for MOX such that the U and Pu atoms can be interchanged in the lattice. Research showed that the following process is quite satisfactory: a) grinding the UO_2 and PuO_2 particles to a highly refined powder (less than 0.5) and carefully mixing them; b) applying the conversion process to the mixture.

(2) Extraction. The Pu content in MOX is 2-3 times higher than that in UO_2, but since the distribution ratio of Pu(IV) in the 30 percent TBP-OK is smaller, appropriate measures must be taken if the level of Pu loss in the extracted liquid waste is to be maintained at the same level of U loss in processing UO_2 fuel. If the number of extraction stages is increased or the extraction stage is lengthened, then high-acid (>3M) operation should be used between the extraction stage and the washing stage instead of $2MHNO_3$, so that Pu(IV) can be extracted into the organic phase. High-acid operation will reduce the cleaning action for Zr/Nb, but will enhance the cleaning of Ru/Rh; hence it is compatible with the variation in fission product spectrum (Zr, Nb less than 10 percent, Ru, Rh greater than 70 percent).

The separation of U and Pu can be accomplished by existing reduction techniques, but most of these techniques can be improved, or a combination of two different techniques can be used [9].

The same purification process is used for plutonium as in UO_2-LWR, i.e., the electrolysis reduction process. But because of the 2-3 times increase in plutonium content, the design of post-processing plant for UO_2-LWR should be modified to avoid adverse effect on its processing capability.

In the purification of uranium, it is required that the total α specific radiation of the uranium product be less than 15,000 dpm/gU. Because of the increased super uranium content in the wastes of MOX-LWR the purification process must be strengthened to improve its cleaning ability.

(3) The Three Wastes of Post-Processing. Sixty to seventy percent of the total tritium is collected on the shell of the MOX-LWR elements, which is 30 percent more than UO_2-LWR. The structural components and the head and tail blocks of the fuel modules do not differ from those of UO_2-LWR. The amount and radiation level of the dissolved residues are approximately the same as those of UO_2-LWR. The concentration of fission products in the high-radiation liquid waste is approximately 20 percent higher than that of UO_2-LWR, and the amount of heat released is also higher; this will have an effect on the heat released is also higher; this will have an effect on the heat dissipation and cooling desing of the HAWC container. When glass solidifies, its envelope volume must be reduced. Because of the large plutonium content, the amount of medium and low radiation liquid waste will increase, and the amount of plutonium loss in the liquid waste is 1 percent less than that of UO_2-LWR. The amount of escaped volatile nuclear elements is also higher than that of UO_2-LWR, specifically, ^{3}H is 30 percent higher. ^{85}Kr is 40 percent higher, and ^{129}I is 30 percent higher. There is an obvious drop in solvent effectiveness due to increases in α dosage and in β/γ dosage; therefore, the solvent processing technique and equipment must be chosen with care.

(4) Feasibility of Post-Processing. The above analysis yields the following conclusions: a) there is no basic difference between MOX-LWR and UO_2-LWR post-processing except for quantitative variations; b) the post-processing of MOX-LWR waste elements can be accomplished by making simple modifications to the existing methods for processing UO_2-LWR.

2. Conversion

The process of transforming $Pu(NO_3)_4$ and $UO_2(NO_3)_2$ obtained from post-processing or a mixture of the two into PuO_2, UO_2 or $(Pu,U)O_2$ is referred to as the conversion process. It is an essential link between post-processing and element refabrication. There are two approaches used to produce $(Pu,U)O_2$: "conversion followed by mixing" and "mixing followed by conversion".

(1) "Conversion Followed by Mixing". This approach involves first converting uranium and plutonium into MO_2, then mixing them; it has been in use for almost 30 years. In the early days, the MO_2 particles were large in size and poor in uniformity; they were difficult to dissolve even in boiling high-concentration HNO_3 solution. Only by adding HF to HNO_3 was it possible to reduce the insoluble residues to a level of less than 1 percent, but the introduction of HF leads to severe corrosion of the equipment. Subsequently, it was discovered that the above difficulties can be overcome by pulverizing the MO_2 particles to a size smaller than 0.5μ so they are in a free flowing state.

(2) "Mixing Followed by Conversion". This approach involves first mixing $Pu(NO_3)_4$ and $UO_2(NO_3)_2$, then converting the mixed solution into $(Pu,U)O_2$. This method provides a direct and simple way to dissolve MOX. Currently, three such techniques are being studied extensively: the sol-gel technique, the direct denitration technique, and the joint precipitation technique.

(i) The sol-gel technique. Based on the requirement of reactor core design, the $Pu(NO_3)_4$ and the $UO_2(NO_3)_2$, solutions are mixed according to a prescribed proportion and evaporated in vacuum; then, by adding a certain amount of reagent to the mixture and passing the mixture through a pulse jet nozzle, "gel balls" are formed. Finally, they are washed with NH_4OH, dried, inspected, baked, and sintered to produce the raw material for element fabrication.

(ii) The direct denitration technique. In this case, $(U,Pu)NO_3$ is converted directly into $(U,Pu)O_2$ in either a vulcanization bed or a microwave oven. Both techniques share the following common features:

a) the mixed U. Pu solution can be converted directly; b) the conversion process is simple; c) the product requires further pulverization; d) very little liquid wastes are produced. But the vulcanization technique has a number of advantages over the microwave technique [12, 13].

(iii) the Joint precipitation technique. This is an advanced technique for producing MOX which uses NH_4OH as the precipitation system. The Pu(IV) oxalate system is ideal for plutonium conversion, but it is not suited for joint preciptiation because the oxalate of Pu precipitates faster than that of U, thereby causing changes in the MOX composition. The Alkem Co. of West Germany developed the AUPuC process which uses NH_4OH to produce a solid mixture is then filtered or directly sintered with the slush in a vulcanization bed.

The precipitated MOX powder, like the product from microwave denitration, are small in size (0.67μ) and have large surface ration (9.5 m^2/g); they are also highly reactive and can readily be made into tablets. The precipitation

technique produces about twice as much ammonium nitrate waste water as the sol-gel technique. The joint precipitation technique has been used by some countries, and each batch produces approximately 1-2 tons of fuel [1].

3. Element Fabrication

Most of today's large-scale MOX-LWR element fabrication processes are based on the "conversion followed by Mixing" method. The procedures are similar to those used for UO_2 element fabrication, and the equipment are essentially the same.

In recent years, the United States had established a "Consolidated Fuel Post-Processing Plan' (CFRP) under which the Oak Hill Laboratory, the Hanford Laboratory and the Pacific Northwest Laboratory are jointly studying the "gel ball-tablet" technique, and have already produced high-quality elements with high density (90-96% TD), good microcrystalline structure and high mechanical strength.

There are other techniques in which the gel balls from the sol-gel technique are sintered and inserted into the fuel tubes through vibration to form the element rods. Practical experience with this technique is still quite limited; the United States plans to use it as the technique for advanced fuel fabrication in the future.

The large amount of plutonium required for the fabrication of MOX elements produces some special problems; specifically, they are: a) the problem of self-generated heat of Pu; b) the problem of dissolving of Pu; c) the problem of hydrogen content; and d) the problem of contamination of plutonium dust [11]. These problems can be overcome by choosing the appropriate procedures, using the proper equipment and materials, and through intelligent design and management.

IV. Safety Analysis

Safety analysis is a complicated issue which covers a wide range of different areas. The U.S. Government and the European Common Entity had organized a special group of scientists who had devoted a considerable amount of effort in carrying out the safety analyses of recycling U and Pu in LWR and publishing an extensive report.

1. Main Conclusions of the European Common Entity

The European Common Entity made the assumption that by the end of this century, the total nuclear power capacity of the Entity will be 150 GWe, and the primary power source will be LWR. It is estimated that at that time, 10 tons of fissionable plutonium will be recycled each year, producing 400 tons of MOX fuel, which is equivalent to about 10 percent of the LWR fuel. These MOX will be recycled in 50 of the 150 power plants; they account for 30 percent of the fuel used in these reactors, which will be operating in a self-sustaining mode, i.e., they produce all the plutonium being recycled. Based on this scenario, the group of European scientists reached the following conclusions: a) with regard to public radiation level, it is 51 personsievert

with recycling, 70 person-sievert without recycling, and the natural background is 400,000 person-sievert, thus the level with recycling is less than the level without recycling which is less than the natural background; b) with regard to individual radiation level for a professional worker, there is a 10 percent with recycling, but the professional group radiation level is reduced by 10 person-sievert per 10 ton of plutonium; c) in any case, the radiation dosage is far below the allowable value specified in the safety standards; d) with regard to non-radioactive environmental effects, there is no significant difference between the recycling case and the non-recycling case in terms of land use requirement, transportation, non-radioactive wastes and heat release.

2. Main Conclusions of the U.S. Government

After several years of detailed analyses and calculations, the U.S. NRC issued a final environmental report which addresses the issues of health protection, safety, and environmental effects. In particular, they compared five different fuel cycling modes: mode 1: immediate post-processing and U recycling, delayed Pu recycling; mode 2: delayed post-processing followed by U,Pu recycling; mode 3: immediate U,Pu recycling; mode 4: U recycling, but no Pu recycling; mode 5: no U or Pu recycling.

The basic assumptions for these estimates are as follows: a) time period: 1975-2000; b) nuclear power capacity: $5X10^{11}$ W by the year 2000; c) total power output: $3.5X10^{13}$ KW·h.

The key results of the report are summarized in Tables 3, 4 and 5. It is seen that: a) the effect of U,Pu recycling in the U.S. on public radiation dosage and on the cancer death rate is only 1 percent of the natural background; b) the differences in the effect on either public radiation dosage or cancer death rate between the different modes are far below the fluctuation levels of the natural background.

Table 3. Effect of U, Pu Recycling on Human Radiation Dosage in the United States

Key:

1. rad dosage, 10^6 person rem
2. mode
3. natural background
4. U.S.
5. professional workers
6. outside residents
7. entire population
8. foreign countries
9. whole world (including U.S.)

Table 4. Effect of U, Pu Recycling on Human Health in the United States

Key:

1. effect on health
2. mode
3. natural background
4. cancer death rate
5. general public in U.S.
6. whole world (including U.S.)
7. genetic defects

Table 5. Effect of U, Pu Recycling on the U.S. Environment*

Key:

(1) other radioactive elements
(2) residue from ore dressing
(3) super uranium solid
(4) high-radiation solid waste

表5 美国U.P.循环工业对环境的影响*

	Environmental Factors	Mode 1.2.3	Mode 5	Mode 6
Resource utilization	land area, acres	3.4×10^{4}	4.0×10^{4}	5.0×10^{4}
	water, gallons	1.2×10^{14}	1.3×10^{14}	1.3×10^{14}
	dissipated heat, BTU	2.9×10^{17}	2.9×10^{17}	2.9×10^{17}
	coal, tons**	8.9×10^{8}	9.0×10^{8}	9.0×10^{8}
	gas, 10^5 BTU	1.0×10^{10}	1.2×10^{10}	1.3×10^{10}
	oil, gallons	2.0×10^{10}	2.0×10^{10}	1.9×10^{10}
	Elec GW·Y	3.8×10^{3}	3.8×10^{3}	3.8×10^{3}
Factory discharge	^{222}Rn	2.3×10^{7}	2.5×10^{7}	2.8×10^{7}
	^{226}Ra	1.1×10^{1}	1.3×10^{1}	1.4×10^{1}
	U	8.7×10^{2}	1.0×10^{3}	1.1×10^{3}
	^{230}Th	3.2×10^{1}	3.8×10^{1}	4.2×10^{10}
	Pu(α)	4.6	3.0	2.3×10^{-3}
	Pu(β)	1.2×10^{2}	7.4×10^{1}	3.8×10^{-3}
	TrPu	1.1×10^{1}	5.3	9.8×10^{-4}
	^{3}H	6.5×10^{7}	6.4×10^{7}	4.7×10^{6}
	^{14}C	1.2×10^{6}	1.2×10^{6}	4.3×10^{4}
	^{85}Kr	1.3×10^{9}	1.3×10^{9}	2.6×10^{4}
	^{90}Sr	1.8×10^{1}	1.8×10^{1}	2.5×10^{-3}
	^{99}Tc	4.5×10^{2}	5.3×10^{2}	—
	^{129}I	1.1×10^{2}	1.1×10^{2}	—
	^{131}I	3.4×10^{1}	3.3×10^{1}	6.0×10^{1}
Factory waste (M^3)	(1)	5.3×10^{7}	5.4×10^{7}	5.4×10^{7}
	(2)	5.9×10^{6}	6.9×10^{6}	7.8×10^{6}
	(3)	1.5×10^{5}	1.3×10^{5}	—
	(4)	6.5×10^{3}	6.5×10^{3}	5.5×10^{4}

* These effects include: mining, ore dressing, UF_3 conversion, U element fabrication, MOX element fabrication, reactors, post-processing, transportation, waste management, and waste fuel storage.

** Includes the coal used by fuel recyling plants and by coal-fired power plants which provide 2/3 of the electricity.

V. Analysis of Social and Economic Benefits

The economic benefits of recycling U. Pu in LWR are quite obvious; even more apparent are the social benefits such as conservation of resources and safety considerations.

1. Savings in Natural Uranium and Separation Power

Because of the different assumptions used by different countries, the estimated amount of savings vary from one country to another. Fig. 6 shows that approximately 35-40 percent of natural uranium can be saved by recycling U, Pu in LWR. For a 1300 MWe PWR, this is equivalent to 80 tons of natural uranium each year.

2. A Good Way to Solve the Pu Storage Problem

The purpose of recycling Pu in LWR is to replenish the depleted uranium; but once it reaches a certain level, power generation can be maintained by the self-generated plutonium, and the plutonium regeneration process will become self-sustaining. This form of "energy-producing storage" is clearly more desirable than the conventional form of storage. The cost savings realized by a 1000 MWe LWR by using recycled Pu over PuO_2 storage are as follows: approximately (1.9-4.8) $x10^6$ dollars per year for 5-year storage; approximately (3.1-6.2)$x10^6$ dollars per year for 15-year storage (based on 1983 U.S. dollar). These data show that it is uneconomical to store Pu for 20-40 years until FBR becomes operational.

Table 6. Savings in Natural Uranium Due to Pu Recycling

表 6 返循环节约天然铀数值

		Pu recyc.	U recyc.	Pu+U recyc.
(1)	(INFCE) (1980)	20%	20%	35—40%
Ger.	(BMFT) (1981.10.)	20—30%	15—20%(一次)	40%
U.S.	(NRC) (1976.9)	—	10%	22%
	(ERDA) (1976.12)	—	—	26%
Japan	[4](NAIG) (1982)	—	17—19%	—
France	(CEA—CEN) (1982)	—	18%	—
Belgium	(BN)[11](1983)	—	—	~35%
(2)	(U.R.G)(1977)	—	—	30%

Key:
(1) International Nuclear Fuel Cycle Evaluation
(2) United Post-Processing Company

3. Moderate Reduction in Fuel Cost

It is INFCE's opinion that from a narrow economic view point, the economic benefits of recycling U, Pu in LWR are quite limited, but if one considers the depleting resources, rising uranium prices, and high cost of developing FBR's, recycling U and Pu will become very attractive.

The conclusion of NRC is: The cost saving of recycling U, Pu over the single-pass mode of operation is about 8.1 percent.

4. Becoming Self Reliant in Nuclear Fuel and Protecting the Fuel Supply

Recycling U, Pu in LWR also helps realizing the goal of becoming self-reliant in nuclear fuel and protecting the fuel supply. This is significant for countries which are developing their LWR industry but have very limited uranium resources.

VI. A Quick Review of China's Strategy on LWR Fuel Cycle

According to China's nuclear power development plan, the near-term efforts will concentrate on building million KW-class PWR's and on developing FBR's. One of the important issues that affects the operation and economic benefits of nuclear power plants is to decide on a fuel cycle strategy. In the following sections, we shall present an analysis of this issue based on China's current conditions.

1. Three Different Modes of Fuel Cycle

During the several decades when LWR's transition to FBR's, there are three possible modes of processing UO_2-LWR nuclear wastes (Fig. 4). Their advantages and disadvantages are summarized below:

Mode 1: a) After several decades of storing post-processed Pu, all the ^{241}Pu, which is 1/7-1/8 of the fissionable plutonium, will become ^{241}Am and lost; b) Because of the strong α, γ, n radiation of ^{241}Am, special production lines must be built to meet super-plutonium requirements, and costly purification procedures will be required for fabricating FBR elements.

Mode 2: a) One seventh to one eighth of the fissionable plutonium will be lost; b) The problems of storage and heat release, corrosion, monitoring, damage and retrieval must be solved.

Mode 3: a) There is basically no loss in fissionable plutonium; b) A 35-40 percent saving in natural uranium and separation power can be achieved; c) The cost of fuel cycle is reduced by 10 percent; d) It contributes toward self-reliance in nuclear fuel and protection of fuel supply; e) The energy of Pu can be fully utilized, i.e., 3/5 of the time before FBR becomes operational, it is used to generate electricity.

The above analysis shows that mode 3 provides the best social and economic benefits.

Fig 4. Three Possible Modes of LWR Fuel Cycle

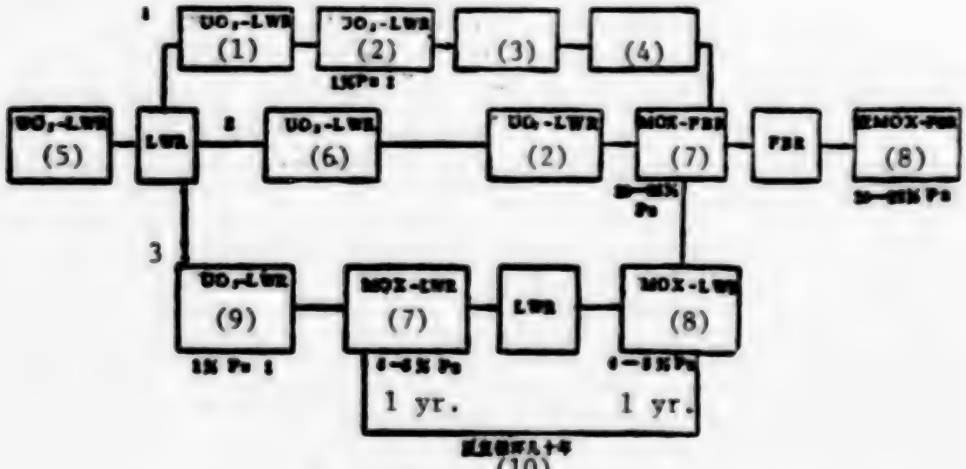

图4 LWR燃料循环的三种模式

Key:

1. storage of waste UO_2-LWR for 5 years
2. post-processing of waste UO_2-LWR
3. storage of Pu for several decades
4. repurification
5. fabrication of UO_2-LWR elements
6. storage of UO_2-LWR for several decades
7. fabrication of MOX-FBR elements
8. post-processing of waste MOX-FBR
9. post-processing of waste UO_2-LWR (cooling for 1 year)
10. recycling for several decades

2. Current Status of China's Nuclear Fuel Industry

(1) Nuclear Resources. China's proven resources that have industrial values can provide enough fuel for military use and for the operation of 15 million-KW PWR's for 30 years [15]. By around 2020, the uranium resources will be mostly depleted [16, 17]. Also, the average grade of China's uranium ore is quite low and the costs of mining and separation power are high.

(2) Post Processing Industry. China's post-processing industry has almost 20 years of operating experience, and has a team of well-trained researchers, designers and operators, who had laid a solid foundation for LWR post-processing.

(3) Plutonium Industry. China has accumulated considerable experience in the operation of the plutonium industry to be able to develop an industry of MOX element fabrication.

(4) Economic Conditions. China is still an economically underdeveloped country with per capita output of less than 400 dollars per year. Therefore, it is not possible for China to spend a great deal of money in this century to develop fast reactors or to devote its resources to large-scale development of PWR nuclear power plants. Under these circumstances, U and Pu recycling is attractive because only a moderate of money is needed for the design, fabrication and inspection of MOX-LWR elements.

Based on the above discussions, the author believes that recycling U and Pu in LWR is consistent with China's current resource, economic and industrial conditions, and is consistent with the guidelines of "becoming self-reliant in nuclear fuel, reducing the cost of power generation"; it is also feasible from technical and safety considerations and provides stimulant for the development of FBR's. Therefore, it is recommended that recycling U and Pu be adopted as China's fuel cycle strategy.

References

13. Hirobumi, Oshima, Journal of Japanese Atomic Energy Society, 25(11) 918-928 (1983)
15. Jian Shengjie, "Nuclear Science and Engineering", 4(1), 1(1984)
16. Lian Peisheng, "Fast Reactor Research", (4) 1(1984)
17. Wen Hongjun, "Fast Reactor Research", (4) 4(1984)

3012/9869
CSO: 4008/77

SINGLE BOARD DIGITAL CONTROL SYSTEM FOR EPITAXIAL REACTOR

Beijing DIANZI XUEBAO [ACTA ELECTRONICA SINICA] in Chinese Vol 14, No 3, May 86 pp 19-24

[Article by Liang Renqiu [2733 0117 7264] and Huang Shengjun [7806 0524 6511] of Qinghua University: "Single Board Direct Digital Control System for Epitaxial Reactor"; manuscript submitted in January 1985, revised manuscript received in August 1985]

[Text] Abstract: This paper discusses the structure and characteristics of a single board digital control system for a vapor phase epitaxial reactor, the mathematical model established, and the two designs for the digital controller. The control software and the operation of the system are also described. The system has already been successfully placed on a production line.

1. Introduction

In manufacturing modern integrated semiconductor circuits, very stringent requirements are imposed on the thickness and dopant levels in the epitaxial layer on silicon. For this reason, the temperature of the silicon wafer in the oven, the gas flow rate and the processing time must be accurately controlled.[1] In other countries, small computers are being used for direct digital control.[2] In 1983, China completed the development of direct digital control by using microprocessors in the laboratory. However, it is too costly. At the end of 1983, Qinghua University and Beijing Electronic Tube Plant jointly developed a direct digital control system for a Chinese made epitaxial reactor, resulting in a single board control system with some special features. The system uses a Model TP-801 single board computer for direct digital control and program control of a vapor phase silicon epitaxial furnace. It was brought on line in late 1984 and has been working satisfactorily to date.

2. Structure and Characteristics of the System

The structure of the system is shown in Figure 1. The single board computer sends out the digital temperature signal. Through the 8 bit D/A converter (DAC), the optoelectronic coupling (isolation) circuit and the switch S, the three phase ac voltage regulating thyristor device can be controlled. The ac output of this device is stepped up, rectified and filtered, and then sent to the LC oscillator which generates a 400 kHz current to heat the epitaxial

furnace. The voltage regulator, step-up transformer, rectifier and filter also form a local negative feedback system to regulate the silicon wafer temperature. The wafer temperature is measured and displayed by a non-contact optoelectronic infrared thermometer.

The system employs seven isolated switching ports. Sampling cycles and processing periods are generated by using 4 channels of the Z80-CTC and some software program. In addition to the 6 and 4 digit displays on the single board computer and thermometer, respectively, the system has a 11 digit display where 4 digits are used to show the processing time, 3 for HCl flow rate and 2 each for PCl_3 and $SiCl_4$ flow rates. The PIO on the computer is used for displaying various epitaxial steps and "flow" platterns for the gases, as well as for an optical-acoustic alarm.

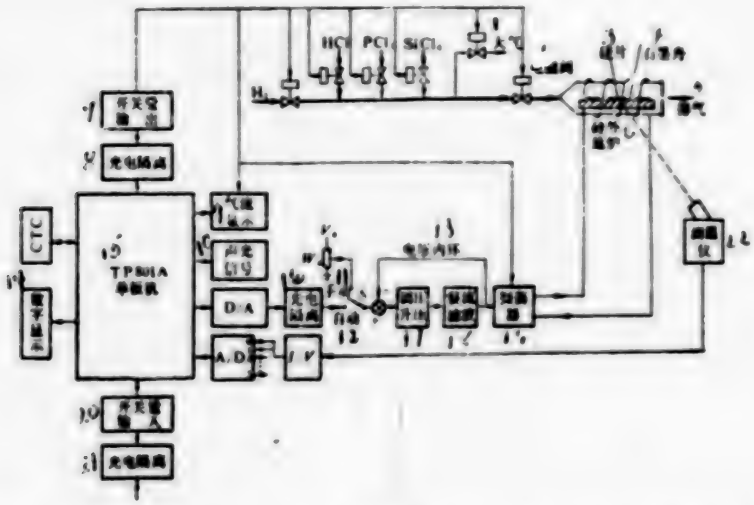

Figure 1. Structure of Single Board Direct Digital Control System for Vapor Phase Epitaxial Reactor.

Key:

1. Atmosphere
2. Electromagnetic valve
3. Silicon wafer
4. Graphite boat
5. Exhaust
6. Silicon epitaxial furnace
7. Switching parameter output
8. Optoelectronic isolation
9. Flow display
10. Photo-acoustic signal
11. Manual
12. Automatic
13. Voltage loop
14. Digital display
15. Single board computer
16. Optoelectronic isolation
17. Voltage regulator
18. Rectifier and filter
19. Oscillator
20. Switching parameter input
21. Optoelectronic insulation
22. Temperature monitor

Based on Figure 1 we know that the system is a serial direct digital control system consisting of an analog inner loop and a digital outer loop. It is also a program controlled system for various valves. The system has the following special features: 1) In the neighborhood of 1200°C, the temperature control error is less than ± 4°C. 2) Through man-machine dialogue, major epitaxial parameters can be changed at any time to quickly change over to another type of integrated circuit with ease. 3) Silicon wafer temperature, processing durations and gas flow rates are digitally displayed. If the temperature exceeds its limits or the computer is out of order, an optical-acoustic alarm will be activated so that the system can immediately be switched to manual operation. 4) A method involving the use of a bias and program switching is used to realize the high resolution conversion of temperature signal by a low resolution ADC. 5) The program and some data are loaded in an EPROM; 6) Effective measures such as low pass filtering, isolation, de-coupling, shielding and grounding are used to resist interference. Even in the presence of intense interference by the 400 kHz high frequency power supply and spatial electric field, it can operate reliably on the production line. 7) The equipment and instruments used, including the DC-8B microcomputer control device, temperature probe and high frequency power supply, are made in China. The costs are very low.

3. Establishment of the Mathematical Model

In order to find a transfer for the epitaxial furnace including the inner voltage loop, the LC oscillator and the temperature measuring device, we created a rising curve digital measurement system as shown in Figure 2. Near the actual operating temperature, the single board computer sends output with sudden increment or decrement. The relevant rising curve is automatically stored in internal memory and then printed out. Based on these data, a curve can be plotted and the transfer function can be determined.[3] Through plotting and computation, the time constant τ_1 is 45 seconds, the magnification factor K_1 is 3.44, and the pure time lag θ is 1 second. The transfer function can be written as:

$$W_{p1}(S) = K_1' e^{-\theta s}/(\tau_1 S + 1)$$
$$= 3.44 e^{-s}/(45S + 1) \qquad (1)$$

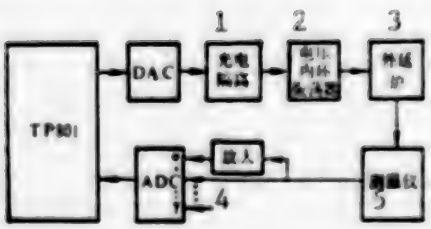

Figure 2. Digital Measurement System for the Rising Curve

Key:
1. Optoelectronic isolation
2. Voltage loop oscillator
3. Epitaxial furnace
4. Amplifier
5. Temperature monitor

Because the pure time lag is very small compared to the time constant, the system can be treated as a first order inertia system whose transfer function is:

$$W_{p1}(S)=3.44/(45S+1) \qquad (2)$$

This is the transfer function measured in channel 1 of the ADC. Because the 0 channel used for PID modulation is also used to amplify the analog voltage to be converted by a factor of 4.4 to raise its resolution, the transfer function for this temperature control channel should be:

$$W_{p0}(S)=K_1'\times 4.4/(\tau_1+1)=K_1/(\tau_1 S+1)\approx 15/(45S+1) \qquad (3)$$

After considering the transfer function $W_h(S)$ of the zero order holder which is formed by the DCA input register, the final complete transfer function is:

$$\begin{aligned} W_p(S)&=W_{p0}(S)\cdot W_h(S)=[K_1/(\tau_1 S+1)]\cdot[(1-e^{-TS})/S] \\ &=15(1-e^{-TS})/S(45S+1) \end{aligned} \qquad (4)$$

T is the sampling cycle in the above equation which is chosen to be 1 second. By performing z transformation for equation (4), the pulse transfer function is obtained.

$$W_p(z)=0.3297z^{-1}/(1-0.978z^{-1}) \qquad (5)$$

If conditions permit, we may use the least square method to conduct off-line recognition to directly dete-mine this pulse transfer function.

4. Digital Controller

Based on the requirement in the epitaxial process, the silicon wafer temperature to be controlled by the system should follow the pattern shown in Figure 3. From room temperature T_0 to point a, the system uses an open loop control to raise the temperature at a slope Δ_1 without measuring temperature. From point a to b, the temperature is checked in an open loop control to increase the temperature at a slope Δ_2. Once the silicon wafer temperature is raised to b (temperature T_R), the system enters the PID modulating mode. It automatically switches channel of the ADC to channel 0 and begins PDI closed loop control. From point c to d, it is the constant temperature segment. It is required to be under PID control to ensure the required accuracy in silicon wafer temperature. After the epitaxial procedure is completed, i.e. from point d to e and e to f, open loop control is used to lower the temperature at slopes Δ_3 and Δ_4, respectively.

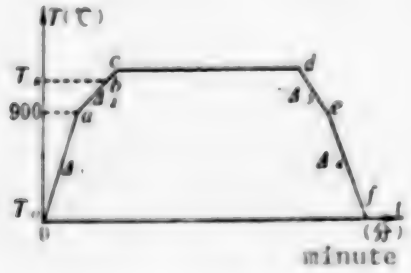

Figure 3

There are many ways to design the digital temperature controller in segments bc and cd. Because the system is a definitive single input/single output system, it is all right to use the conventional PID method or some practical engineering algorithm with pure lag. For instance, it is possible to use the following direct digital design method.[4,5]

Figure 4 shows the block diagram of the structure of the system. D(z) is the pulse transfer function of the digital controller. Y(z), U(z), E(z) and C(z) are the z transformation of the system output, given value, control error, and digital controller output, respectively. The closed-loop transfer function of the system is:

$$W_c(z)=D(z)W_p(z)/[1+D(z)W_p(z)] \qquad (6)$$

From equation (6) we can obtain the pulse transfer function of the digital controller:

$$D(z)=C(z)/E(z)=W_c(z)/W_p(z)[1-W_c(z)] \qquad (7)$$

When the static error of the system is 0, we get the following based on the final value theorem:

$$e(\infty)=\lim_{z\to 1}\{(1-z^{-1})U(z)[1-W_c(z)]\}=0 \qquad (8)$$

Let us assume that the input is a unit step function. The unit step pulse function is:

$$U(z)=1/(1-z^{-1}) \qquad (9)$$

To make equation (8) equal to 0, the closed loop pulse transfer function of the system should be $W_c(z) = z^{-1}$. By substituting equations (5) and (9) into (7), the specific pulse transfer function of the digital controller is:

$$D(z)=C(z)/E(z)=W_c(z)/W_p(z)[1-W_c(z)]=(3.033-2.966z^{-1})/(1-z^{-1}) \quad (10)$$

This is a PI modulated model. By multiplying equation (10) to C(z)/E(z) and then performing an inverse z transformation, we get the following difference equation or control scheme which is suited to be computed on a computer.

$$c(k)=c(k-1)+3.033e(k)-2.966e(k-1) \qquad (11)$$

This is the theoretical design. We mentioned that the closed loop pulse transfer function of the system is $W_c(z) = z^{-1}$. This indicates that the output of the system can vary with respect to the previous input within the same beat

(one sampling cycle). Due to the saturation characteristics of the loops in the system, this is not attainable. The parameters in equation (11) must be corrected accordingly in testing.

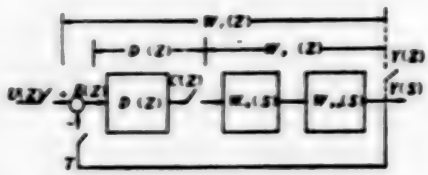

Figure 4. Block Diagram of the Structure

As a result of testing, the parameter expressed in equation (11) were found to be usable. The temperature variation is less than ± 4°C and the transition time is under 45 seconds. The parameter was modified to include $b_2e(k-2)$ term and point differentiation was introduced; i.e. to adopt the following PID modulation model:

$$c(k)=c(k-1)+b_0e(k)-b_1e(k-1)+b_2e(k-2) \qquad (12)$$

The performance is thus improved. Tests showed that there was no overshoot when temperature was raised at a given slope. The static temperature variation was less than ± 4°C and the transition time was under 35 seconds. When a 17°C temperature disturbance was introduced abruptly, the recovery time was under 25 seconds. These specifications can satisfy all technical requirements.

The Dahlin algorithm was also used to design the digital controller[6,7]. Based on this method, when zeroth order register is not taken into account, the transfer function is:

$$W_p(S)=K_1e^{-\theta S}/(\tau_1S+1) \qquad (13)$$

The design is to find an appropriate digital controller D(z) for closed loop control. The closed loop transfer function is an inertia loop and a pure lag loop in series. In addition, the pure lag time is that of the subject, i.e.

$$W_c(S)=e^{-\theta S}/(\tau S+1) \qquad (14)$$

Let the lag time 0 be N times the sampling cycle T, where N is a positive integer, i.e. $0 = NT$. The pulse transfer function of the closed loop system is

$$\begin{aligned} W_c(z)&=\mathcal{Z}[W_c(S)\cdot(1-e^{-TS})/S] \\ &=\mathcal{Z}\{[e^{-NTS}/(\tau S+1)]\cdot[(1-e^{-TS})/S]\} \\ &=(1-e^{-T/\tau})z^{-N-1}/(1-e^{-T/\tau}z^{-1}) \end{aligned} \qquad (15)$$

The pulse transfer function after taking the zero order register into account is:

$$W_p(z)=\mathcal{Z}\{[(1-e^{-Ts})/S]\cdot[K_1e^{-NTs}/(\tau_1S+1)]\}$$
$$=K_1z^{-N-1}(1-e^{-T}/\tau_1)/(1-e^{-T/\tau_1}z^{-1}) \qquad (16)$$

By substituting equations (15) and (16) into equation (7), the pulse transfer function of the digital controller can be obtained:

$$D(z)=\frac{C(z)}{E(z)}=\frac{W_c(z)}{W_p(z)[1-W_c(z)]}$$
$$=\frac{(1-e^{-T/\tau})(1-e^{-T/\tau_1}z^{-1})}{K_1(1-e^{-T/\tau_1})[1-e^{-T/\tau}z^{-1}-(1-e^{-T/\tau})z^{-N-1}}$$
$$=\frac{(1-e^{-T/\tau})/K_1(1-e^{-T/\tau_1})-(1-e^{-T/\tau})e^{-T/\tau_1}z^{-1}/K_1(1-e^{-T/\tau_1})}{1-e^{-T/\tau}z^{-1}-(1-e^{-T/\tau})z^{-N-1}}$$
$$=\frac{b_0-b_1z^{-1}}{1-a_1z^{-1}-a_2z^{-N-1}} \qquad (17)$$

By cross-multiplying equation (17) with C(z)/E(z), we get

$$C(z)(1-a_1z^{-1}-a_2z^{-N-1})=(b_0-b_1z^{-1})E(z)$$

By doing a inverse z-transformation, the algorithm of the digital controller can be obtained.

$$c(k)=a_1c(k-1)+a_2c(k-N-1)+b_0e(k)-b_1e(k-1) \qquad (18)$$

where $a_1=e^{-T/\tau}$, $a_2=1-e^{-T/\tau}$, $b_0=(1-e^{-T/\tau})/K_1(1-e^{-T/\tau_1})$, $b_1=b_0e^{-T/\tau_1}$

(Based on equation (17).)

When this algorithm was used, some parameters were slightly modified; i.e. K_1=13, τ_1=48 sec, T=1 sec, 0=1 sec, N=0/T=1, $\tau=\tau_1/3$=16 sec. Based on equation (18), the specific control algorithm of the system can be obtained:

$$c(k)=0.9394c(k-1)+0.0606c(k-2)+0.2245e(k)-0.2199e(k-1) \qquad (19)$$

The result of this algorithm showed that no temperature overshoot at a given slope. The static temperature variation was less than ± 4°C. The transition time was under 45 seconds. The recovery time from an abrupt increase of 50°C was under 25 seconds. This method is not sensitive to slight changes in τ_1, K_1 and 0. The Dahlin method is a convenient way to design a digital controller.

5. Control Software and Its Operation

A comprehensive control program, including the control algorithm, switching parameters and alarms, was complied for a Z-80 microprocessor. There are 20 programs including the main program and subroutines. The program takes up approximately 4 k in memory and is loaded on an EPROM.

The operation of the system is shown in Figure 5. The flowchart controlling the epitaxial process is shown in Figure 6. The flowchart for the control program to realize the temperature pattern shown in Figure 3 is shown in Figure 7.

The system is easy to operate. For example, the power is turned on at the beginning of the day. The CPU and PIO are automatically initialized. The program and data are loaded in the RAM from the PROM. There are three user defined keys as well. By pressing the "set" key, in a man-machine dialogue mode, silicon wafer processing temperature, HCl etching time, transition layer growth time and epitaxial layer growth time are entered sequentially (in decimal numbers). They are displayed again to check for errors. If HCl etching or transition layer growth is not required, then just enter 00 minute. By pressing the "prepare" key, the lines are "purged." After pressing the "process" key, epitaxial process begins in furnace number 1. When similar process is done later, it is only necessary to press the "process" key besides loading and unloading the wafer. The entire epitaxial process will be done automatically.

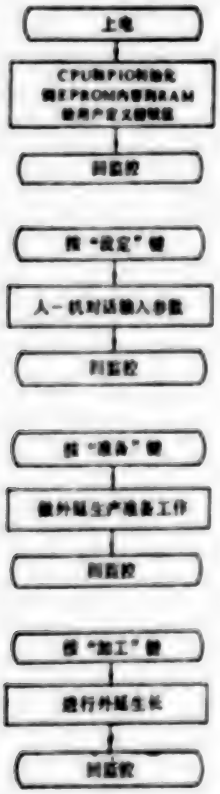

Turn power on
Initialize CPU and PIO
Load EPROM to RAM
Specify user defined keys
Return to monitor mode
Press "set" key
Enter parameters via man-computer dialogue
Return to monitor mode
Press "prepare" key
Prepare for epitaxial process
Return to monitor mode
Press "process" key
Proceed with epitaxial growth
Return to monitor mode

Figure 5. Operation of the System

Figure 6. Flowchart for Epitaxial Process

Key:

1. Press "process" key
2. Set parameters and clean lines?
3. no
4. Return to monitor mode
5. yes
6. clean reactor
7. raise temperature, PID control
8. HCl etching (or skip it)
9. H_2 treatment
10. grow transition layer (or skip it)
11. grow epitaxial layer
12. lower temperature
13. cool down
14. issue process finished signal
15. Return to monitor mode

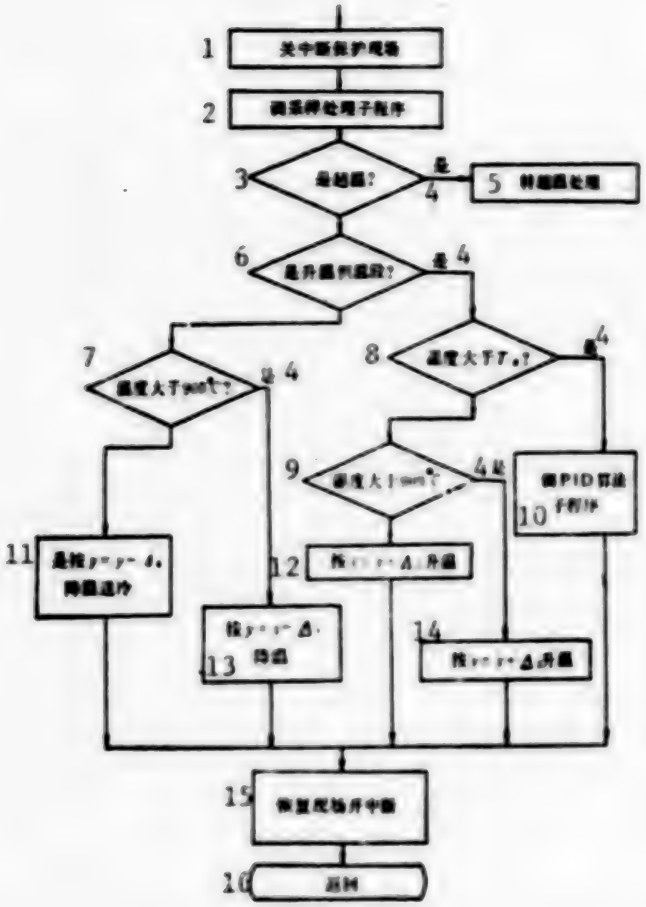

Figure 7. Flowchart of the Temperature Control Program

Key:

1. Activate interrupt to protect site
2. Call sampling subroutine
3. Temperature overshoot?
4. yes
5. Switch to overshoot treatment
6. rising constant temperature segment?
7. greater than 900°C
8. greater than T_R?
9. greater than 900°C?
10. Call PID subroutine
11. Cool down according to $y=y-\Delta 4$
12. raise temp. according to $y=\Delta 1$
13. cool down according to $y=y-\Delta 3$
14. raise temp. according to $y=y+\Delta 2$
15. Shut off interrupt to restore site
16. Return

6. Conclusions

Based on on-site testing and continuous on-line operation, the system performs well. It is reliable and meets all the original design requirements. After it was put in the production line at Beijing Electronic Tube Plant, the yield of epitaxial processes is greatly improved.

The authors wish to thank Beijing Electronic Tube Plant for its support in the development of this system. They also wish to express their gratitude to engineers such as Guo Ruichun [6753 3843 2504] and Tan Wengui [6223 2429 6311] as well as students of Qinghua University such as Guo Jianping [6753 1696 1627], Meng Jinyan [1322 6855 1750], Meng Benxian [1322 2609 0341], Yin Shuxin [1438 2885 2450] and Quan Yi [0356 1704] for their assistance.

FOOTNOTES

1. Edited by Fairchild Corporation: Semiconduction & Integrated Circuits Fabrication Techniques, Prentice-Hall Company, Reston, Virginia, USA, 1978.

2. Don Jackson: Solid State Technology, Vol. 15, No 11, pp 35-39, November, 1972.

3. Lu Daozheng [7120 6670 2398] and Ji Baoxin [1323 1405 2450]: Principle and Design of Automatic Control, Shanghai Science and Technology Publishing Co., 1978.

4. Liu Zhizhen [0491 2784 2823], Guo Muhe [6753 2606 3109] and He Kezong [0149 0344 1813]: Computer Control, Qinghua University Press, 1981.

5. Wang Yongchu [3679 3057 0443]: Engineering Design of Automatic Modulating Systems, Mechanical Industry Publishing Co., 1983.

6. E. B. Dahlin: Instruments and Control Systems, Vol. 41 No 6, pp 77-83, June, 1968.

7. Kuo-Chengchiu, Armando B. Corripio, Cell Smith: Instruments and Control Systems, Vol 46, No 10, pp 57-59, No 11, pp 55-58, No 12, pp 41-43, 1973.

12553/7358
CSO: 4008/1087

INTRODUCTION TO PROGRAM VECTORIZATION

Beijing DIANZI XUEBAO [ACTA ELECTRONICA SINICA] in Chinese Vol 14, No 3, May 86, pp 102-109, 113

[Article by Fan Zhihua [5400 2784 5478] of Changsha Institute of Technology: "An Introduction to Vectorization", manuscript received in February 1985]

[Text] Abstract: A systematic and comprehensive description of the basic concepts, principles, techniques and applications of the vectorization of serial arithmetic is given.

1. Main Frame Computer and Vector Computer

Since the 1970's, because of rapid advances in semiconductor and integrated circuit technology, a lot of high performance computers emerged. One type of computers continues to make breakthroughs in raising the computing speed. The average number of arithmetic operations per time unit (second) is increased astronomically toward the order of magnitude of billions. This is usually called "main frame" computers[1] (main frame for short). It is not characterized by speed alone.

Main frame computers are the best in terms of performance and size. They are the key equipment in solving major problems in scientific computation, engineering design and data processing. One way to attain super high speed is to increase its main frequency. The frequency of the CRAY-1 is 80 MHz.[2,3] However, the primary means is to drastically improve its capability in parallel processing.

The tremendous parallel processing capability of main frame computers is based on effective system structures such as pipeline technology, multifunction components, sample structure and multiprocessors.[1,3] To equip main frames with vector mechanisms is the current trend.[4] For example, the ILLIAC-IV, STAR-100, CYBER-203, CYBER-205, TI-ASC, CRAY-1, CRAY-1S, CRAY X-MP and CRAY-2S developed in the United States, the Model 757 computer[5] and galaxies computer developed in China, and the FACOM VP-100/200 super high speed computer in Japan[6] are vector computers. On the other hand, vector computers are at least one to two orders of magnitude higher in parallelism and they are main frame computers.

2. Vector Mechanism in Vector Computers

A vector computer is equipped with vector processors. For instance, the FACOM VP-100/200 computer developed by Fujitsu in Japan includes vector addition operators, vector logic operators, vector multipliers, vector dividers, masked registers, load storage and vector registers which are used to protect vector operation data (see figure 1).[6] Based on these hardware resources, a vector computer provides its users with vector mechanisms such as vector operation and vector chaining.

A vector is a non-empty ordered set of data of the same type. Vector operation deals with vectors. The vector length may be several hundreds, i.e. several hundred scalar operations are executed in parallel. From the programming point of view, CRAY-1 is equipped with eight vector registers. Each register is made of 64 64-bit elements (i.e. vector elements) and has 41 vector commands.[1-3] The FACOM VP computer equivalently has 16 times the vector registers as compared to the CRAY-1. It has 82 vector commands.[6]

Under the premise of vector operation, vector computers often use the vector chaining technique.[1,2] When the result of the previous command is the operand of the next command (which is frequently so in a program), in the same timing cycle, the vector register not only can receive the result from a functional component but also can deliver it to another functional component as the source for the next operation. Thus, two or more functional components are linked to resolve any contradictions related to the operand.

For example, we are looking for the product of a 5 column matrix X and a 5x125 matrix Y. The result is a 1x125 matrix Z:

$$Z_{1\times 125} = X_{1\times 5} Y_{5\times 125}$$

In scalar FORTRAN, two DO loops are used:

```
      DO 1 I = 1, 125
      Z(I) = 0
      DO 1 J = 1, 5
1     Z(I) = Z(I) + X(J) * Y(J, I)
```

Excluding overhead in modifying and decising the loop control variable, it has to execute 125+125x5=750 statements. In vector FORTRAN, it only employs a simple sequence of six statements:

```
Z(1:125) = 0
Z(1:125) = Z(1:125) + X(1) * Y(1, 1:125)
Z(1:125) = Z(1:125) + X(2) * Y(2, 1:125)
Z(1:125) = Z(1:125) + X(3) * Y(3, 1:125)
Z(1:125) = Z(1:125) + X(4) * Y(4, 1:125)
Z(1:125) = Z(1:125) + X(5) * Y(5, 1:125)
```

to be linked for execution. In addition, time overlap is utilized to further accelerate the computing speed.

Parallelism in computer system contains an abundance of contents[2,7,8]. In this paper only vector processing is discussed. Based on the classification introduced by M. J. Flynn in the United States, this parallel mechanism belongs to the single instruction multiple data stream system. This hardware based a parallel mechanism also requires that the data storage addresses be equally spaced.

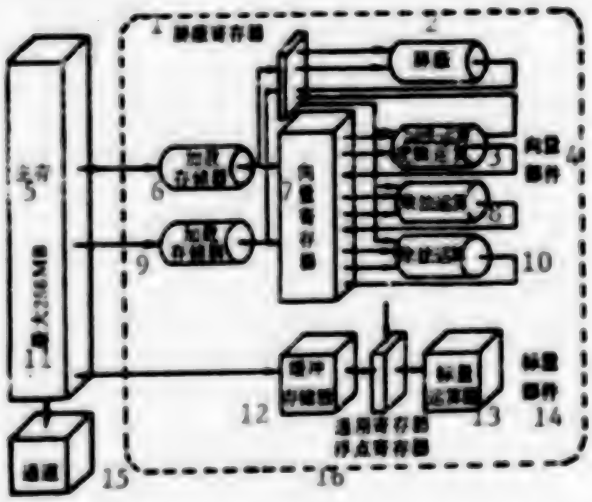

Figure 1. Block Diagram of Processor Part of FACOM VP-100/200

Key:
1. Mask register
2. Mask
3. Addition logic operation
4. Vector component
5. Main memory
6. Load storage
7. Vector storage
8. Multiplication
9. Load storage
10. Division
11. Maximum 256MB
12. Buffer register
13. Scalar operator
14. Scalar component
15. Channel
16. General register
    Floating point register

3. Embodiments of Programming Language

In order to use this hardware based vector mechanism, for the users, the concern is what descriptive means the programming language can offer.[9] Since the early 1970's, a great deal of studies had been done in vector languages. The mainstream is to add vector statements to high level serial languages.[10,11] For instance, the LRLTRAN on STAR-100, IVTRAN, CFD and GLPYNIR on ILLIAC-IV, STARAN on STARAN-IV, BSP FORTRAN on BSP, CRAY-FORTRAN on CRAY-1, vector FORTRAN on Model 757 and Glaxies, and vector ALGOL 60[12,13] are such high level vector languages.

Because data arrays are the data type used in high level languages, and one-dimensional array and its fragments as well as the fragment of a multi-dimensional array in a dimension are vectors, array operations are used in the expansion. The array processing capability of CRAY FORTRAN makes it possible to apply most of the operations defined for scalars in FORTRAN to arrays.[14] The four basic arithmetic operations and logic operations can be performed among arrays or between an array and a scalar. An array can be assigned. The array elements and its operations are conditionally selected. It is used as the input parameter of a function or as a process parameter.[15]

In the example in the last section, the statement

```
Z(1:125) = 0
```

is a vector assignment statement. "1:125" is an abbreviation of the three-dimensional selection symbol "1:125:1" in which the subscript is selected from 1 to 125 at an increment of 1. The statement also assigns 0 to Z(1), Z(2), and "randomly". Similarly, the statement:

```
Z(1:125) = Z(1:125) + X(1) * Y(1, 1:125)
```

is a vector statement which calculates the following 125 multiplications and additions and assigns Z(1), Z(2),..., Z(125) in parallel:

```
Z(1)   + X(1) * Y(1, 1)
Z(2)   + X(1) * Y(1, 2)
          :
Z(125) + X(1) * Y(1, 125)
```

The above vector operations are of the single instruction stream type. The individual processed data are stored in equally spaced intervals. This is ensured by the array compiler and storage distribution rule.

4. New Theories in Computer Science

It is known that one mind cannot be focused on two things. The traditional human thinking process is serial. Even in parallel events, things are being thought one by one. "Taking a walk in the park on Sunday and watching the flower show" can be considered as a parallel event. However, when people arrange this event, it is still a serial thinking process. The vector computer and high level vector language, nevertheless, ask us to describe serial thoughts with parallel statements. The following example show that simple substitutions will lead to mistakes.

Let us assume that there is an array A(0:101) in FORTRAN whose initial value is A(I)=I, I=0, 1, ..., 101. Therefore, the serial program

```
      DO 2 I = 1, 100
    2 A(I) = A(I + 1)
```

individually assigns A(2) to A(101) to be A(1) to A(100), respectively. The corresponding parallel program should be:

```
3     A(1:100) = A(2:101)
```

The serial program

```
      DO 4 I = 1, 100
4     A(I) = A(I - 1)
```

individually assigns A(0) to A(99) as A(1) to A(100). The corresponding parallel program should be

```
5     A(1:100) = A(0:99)
```

The results of these four programs are shown in Table 1.

From Table 1 we find out that the vectorization of a pair of similar serial programs may end up with totally different results. DO loop 2 and vector statement 3 end up with the same results. The results of DO loop 4 and vector statement 5 are quite different.

As another example, the double loop

```
      DO 6 I = 1, 100
      DO 6 J = 1, 100
6     B(I, J) = B(I, J - 1) * *2 - 4 * AC(I, J)
```

and

```
      DO 7 J = 1, 100
      DO 7 I = 1, 100
7     B(I, J) = B(I, J - 1) * *2 - 4 * AC(I, J)
```

are equivalent. However, the operation of the inner loop of the former program requires iterations everywhere. Its parallel algorithm tree is shown in Figure 2. The depth is 99. The inner loop of the latter program involves independent operations. Its parallel algorithm tree is shown in Figure 3. The depth is 1. Obviously, the intrinsic parallelism is quite different.

Table 1. Results of Four Programs

2 内容 / 1 下标 / 3 语句	0	1	2	3	4	5	6	7	...	95	96	97	98	99	100	101
4 初值	0	1	2	3	4	5	6	7	...	95	96	97	98	99	100	101
DO 2	0	2	3	4	5	6	7	8	...	96	97	98	99	100	101	101
3	0	2	3	4	5	6	7	8	...	96	97	98	99	100	101	101
DO 4	0	0	0	0	0	0	0	0	...	0	0	0	0	0	0	101
5	0	0	1	2	3	4	5	6	...	94	95	96	97	98	99	101

Key:
1. Subscript
2. Contents
3. Statement
4. Initial value

Figure 2. Algorithm Tree of Inner Loop of DO 6 Statement

Figure 3. Algorithm Tree of Inner Loop of DO 7 Statement

In summary, as vector computers and higher level vector languages become available, in order to offer algorithms with higher intrinsic parallelism, the development of parallel algorithms is booming. To automatically identify the parallelism hidden in serial programs, automatic identification in vector operation (vector identification or vectorization) has become a new subject in the domain of computer science.

Parallel algorithms and vector identification go hand in hand. In general, the better the parallel algorithm used in the program, the more vector operations produced by vector identification will be. An analog can be found in geology to describe their relationship. The coal layer was formed in the Permocarboniferous Period. Today, geological theories are used as weapon in geological surveys to search for coal. Parallel algorithm is equivalent to the earth environment in the Permocarboniferous Period and vectorization is more or less

equivalent to geological survey. The best theory cannot help us locate coal in a planet where coal does not exist. Similarly, the best vectorization theory cannot find vector operations from programs without any potential.

5. Basic Vectorization Theory

If a single instruction single data stream serial computer is considered as a dormitory with one seat for a person to dine in, then a vector computer is a restaurant with hundreds of seats to serve hundreds of people at the same time. The unit is "person * meal", i.e. meal per person. When we receive a reservation for 100 person * meals, we are not sure that there are 100 seats simultaneously available in the restaurant. We must first analyze a distribution plan. Let us consider the extremes. If there are 1 hundred people eating one meal, then we can arrange 100 seats for them to eat it at the same time. If one person is to eat 100 meals, then we have to serve one meal at a time even though there are empty seats available. It is not even possible to ask him to eat two meals together. The reason is obvious. In the former case, 100 meals are to be consumed by 100 people. They are independent. In the latter case, the same person will eat 100 meals. There are rigorous constraints. The meal served several hours after breakfast is lunch.

The vector mechanism in a vector computer his similar characteristics. The inner loop of DO 7 in the previous section is equivalent to 100 people eating one meal each. The inner loop of DO 6 is equivalent to one person eating 100 meals. The former can be vectorized while the latter cannot be.

Thus, the purpose of vectorization theory is to automatically identify parallelism in the source program based on an in depth analysis of the complex dependence of the data and to rewrite it in the vector form to obtain a vectorized target program. Obviously, the objective is to improve its efficiency. The equivalence of the source and the target program is a necessary premise. If vector identification is recognized as the identification work alone, then vectorization is more generalized, including the entire task of identification and rewriting.

Based on programming language theory,[16] a source program is statements in the source language and a target program is statements in the target language. The descriptive capabilities of the source language and target language determine the type and complexity of data dependence in the source and target programs; which also determine the ability of the vectorization theory to identify and to rewrite. To date, all vectorization methods are based on FORTRAN.[17-30] Most recent results[19-30] use FORTRAN77 as the source language[14] and use extended FORTRAN 77 with array processing capability such as that of the CRAY computer (VFORTRAN) as the target language.[15] (See Figure 4). The vectorization method thus derived is in general adaptable to various languages.

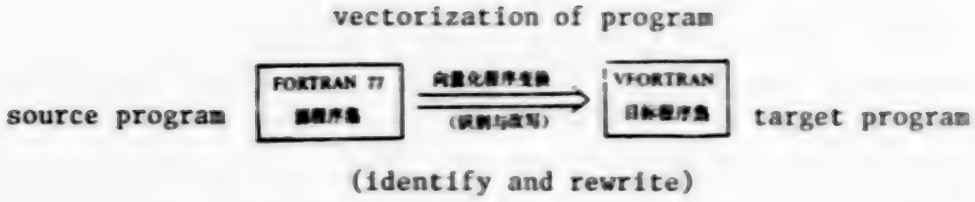

Figure 4. Program Transformation in Vectorization

A review of the history of the study on vectorization shows three areas of interest: explicit data dependence, implicit data dependence and identification instruction.

As mentioned before, the hardware based vector mechanism has two special features: single instruction multiple data stream and evenly spaced multiple data storage. Our programming design experience tells us that the statements in a DO loop can easily satisfy the requirements. Each statement in the DO loop gives an instruction (or a series of instructions) to be repeatedly applied to many data points, forming a single instruction multiple data stream. So long as the step remains unchanged, with the aid of the compiling system, the data storage happens to be equally spaced. On top of that, the loop concentrates the computing load of the program. Thus, all studies are focused on the vectorization of DO loops. Of course, it is also possible to form a loop with other statements (such as GOTO). However, based on the principle of programming structure design,[16,31,32] they can basically be transformed into DO loops by the source program itself.

The data dependence which is caused by the statements in the loop and covers a domain limited by the loop is an explicit dependence. Since the 1970's, there are many methods to identify explicit data dependence.[17-25, 28-30] They will be reviewed in the next section.

The data dependence which is caused by the statements in the loop and covers a domain beyond the loop is an implicit dependence.[28] To make sure that the source program is equivalent to the target program, vectorization theory must take implicit data dependence into consideration.

The current vectorization theories do not run the source program in the identification stage. Instead, they identify and rewrite in a "static mode." How to utilize dynamic information in static processing is an issue of great concern. Identification guidance instruction is an important way for the user to provide auxiliary information, particularly dynamic information which is lacking in static identification.

6. Review of Capability to Identify Explicit Data Dependence

The subscript tracking method,[19-25, 29,30] is established on the basis of using array elements as analytical nodes to solve the vectorization of all three basic modes (link, select and repeat)[16,31,32] in program structure design. Other methods such as coordinate method,[17] hyperplane method[18] and corelation analysis method[28] use the subscript as the analytical node.

To date, it is limited to the domain of the assigned statement loop. Through typical examples, their capabilities are reviewed in this section.

(1) For example, the following is a rigorous loop of assigned statements:

```
      DO 8 I = 1, N
      A(I) = B(I) * C(I)
      C(I) = B(I-1)
    8 B(I) = A(I+1) * D
```

All methods described above can be used to identify and rewrite it.

(2) A loop of assigned statements which can be vectorized along a slant line, such as the following[18]

```
      DO 9 I = 2, 10
      DO 9 J = 2, 20
    9 A(I, J) = (A(I+1, J) + A(I, J+1) + A(I-1, J) + A(I, J-1)) * .2
```

can be identified and rewritten by the hyperplane method.[18]

(3) A loop of assigned statements with a sequence change point,[19,21] such as the following

```
      DO 10 I = 1, N
      A(2 * I) = B(I)
   10 B(I) = A(I) + 1
```

can be identified and rewritten by the subscript tracking method[20-22] and corelation analysis method.[28]

(4) A loop of assigned statements whose absolute step is greater than 1 and the initial DO variable cannot be estimated,[22,23] such as the following

```
      M = -N * .2
      DO 11 I = M, 0, 2
      A(I) = 1
      A(2 * I) = 2
   11 A(3 * I) = 3
```

can be identified and rewritten by the subscript tracking method.[23]

(5) A loop of assigned statements with dynamic assigned step,[23] such as the following

```
      S = ABS(M - K)
      DO 12 I = 1, N, S
      A(2 * I) = B(I)
   12 B(I) = A(I) + 1
```

can be identified and rewritten by the subscript tracking method.[23]

(6) A loop of assigned statements with unestimable initial value, final value, step and subscript expression coefficient,[29] such as the following

```
      ⋮
      INTEGER M, N, L, S
      ⋮
      DO 13 I = M, N, S * *3
      A(L * I) = B(I - L) * C(3 * I + 1)
13    B(I - L) = C(I) * *3 - A(L * I)
```

can be identified for vectorization in the original form by the subscript tracking method.[29]

(7) A loop with logical IF statements or IF blocks,[24] such as the following

```
      DO 14 I = 1, 10
      A(I) = B(I) * C(I) + D(I) * *2
      IF (A(I).GT.4) THEN
      A(2 * I + 9) = E(I) * *2 + 3 * A(I) + 5
      A(2 * I + 10) = 2 * F(I) * *2 + A(I) + 1
      G(3 * I - 2) = B(2 * I - 1) * C(I) + A(2 * I + 9) - A(2 * I + 10)
      ELSE
      G(3 * I - 1) = A(I) * A(2 * I + 9)
      G(3 * I) = A(I) * A(2 * I + 10)
14    END IF
```

can be identified and rewritten by the subscript tracking method.[24]

(8) A loop with a triple control switch, such as the following

```
      DO 15 I = 1, 10
      A(I) = B(I) * C(I) + D(I) * *2
      IF(A(I) - 4)  18, 17, 16
16    A(2 * I + 9) = E(I) * *2 + 3 * A(I) + 5
      GOTO 20
17    A(2 * I + 10) = 2 * F(I) * *2 + A(I) + 1
      GOTO 19
18    G(3 * I - 2) = B(2 * I - 1) * C(I) + A(2 * I + 9) - A(2 * I + 10)
19    G(3 * I - 1) = A(I) * A(2 * I + 9)
20    G(3 * I) = A(I) * A(2 * I + 10)
15    CONTINUE
```

can be identified and rewritten by the subscript tracking method.[25]

(9) A loop with unestimable initial value, final value, step and subscript coefficient and with logic IF statements and IF blocks,[30] such as the following

```
      INTEGER M, N, L, S
      DO 21 I=-2*M, N+L, S**2
      IF ((B(I-L)+A(L*I)).EQ.C(2*I-1)) THEN
      A(L*I)=B(I-L)*A(L*I)+D(I+1)
      ELSE
      B(I-L)=C(I)**3-A(L*I)
      END IF
   21 D(I+1)=B(I-L)
```

can be identified and quasi-vectorized by the subscript tracking method.[30]

7. Applications of Vectorization Theory

To realize vectorization theory in engineering applications, the vector identifier is a key component to improve the operating efficiency of the vector computer. A vector identifier is a new software system of considerable size. On the vector computer developed by China, the earliest vector identifier is still in operation. It is being used in the following areas:

a. Transform Existing Serial Programs

Before vector computers became available, people already wrote a large number of serial programs which were successfully tested after investing an enormous amount of manpower and money. Now, we obviously would like to use these programs still "without making any changes." If we do that, since we did not include the vector mechanism when we wrote and tested these programs, the efficiency will in general be very low, leading to significant waste. Under the circumstance, vector identifier plays the role as a piece of "transplant software" to alter these serial programs so that they are automatically modified into new programs suitable for the operating environment of vector computers.

b. Modify Future Serial Programs

There are still a variety of computers in operation in parallel to vector computers. Because these computers can only execute serial programs, in order to fully utilize the results obtained on these computers, vector computers must have the capability to accept new serial programs and run these programs very efficiently. This capability comes primarily from the vector identifier. In addition, there will be considerable vector computer users who write and test their programs on other computers. The programs are run on vector computers only after they are compiled and debugged. These users will also introduce a lot of new serial programs. The vector identifier also plays the role of software transformation for these programs.

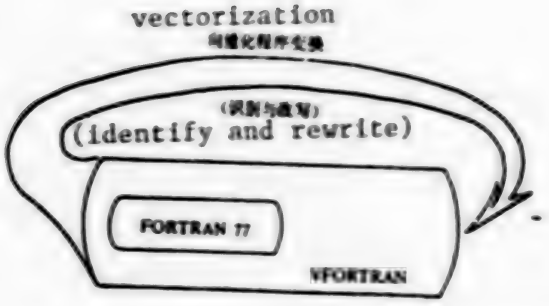

Figure 5. Program Vectorization by VFORTRAN

c. Modify Future Hybrid Programs

After vector computers are available, many users will write programs and run them directly on vector computers. They are not limited by serial FORTRAN. The system allows them to use direct vector statements.

However, as we mentioned before, our traditional way of thinking is serial. Unless in extremely simple cases, the most natural and dependable way for a programmer to express a parallel operation on a vector computer is still by using a serial program.

Thus, we will be facing a lot of hybrid programs with serial and parallel statements. In simple and obvious cases, vector operation will be used. In other areas, scalar operations are still being used. For this portion of the program, the vector identifier is again an optimization software. It can optimize the scalar operations which are masked by the complicated data dependencies into vector operations.

Because FORTRAN77 is a subset of VFORTRAN, the source program for the former must be that of the latter as well. From the viewpoint of program transformation, the function of the vector identifier is to extend the vectorization of FORTRAN77 to VFORTRAN (Figure 4) to the transformation of VFORTRAN itself (Figure 5).

d. Partially Modify Program Structure

As mentioned above, vector recognization is somewhat equivalent to a geological survey which basically identifies existing parallel components, instead of creating parallel components.

However, there are exceptions. For example, a vector identifier can alter the program structure within a small range to vectorize the program in Section 4 by changing DO loop 6 to 0 loop 7.

8. Conclusions

As vector computers become more popular, vectorization studies have both theoretical and practical significance. The essence of vectorization theory lies

in the static recognition of dynamic data dependencies. Its progress not only requires knowledge in mathematics and computer science but also relies on the vector identifier. It is expected to be widely used in computer science and mathematics such as in parallel algorithm, cyclic optimization and data stream analysis.

Vectorization is being perfected and will continue to be an important part of computer science.

FOOTNOTES

1. Ci Yungui [1964 7189 2710] and Hu Shouren [5170 1343 0088], Review of Main Frame Computer Systems, DIANZI XUEBAO [ACTA ELECTRONICA SINICA], Vol 11, No 3, 1983 p 91.

2. Jin Lan]6855 5695], Wang Dingxing [3769 7844 5281] and Shen Meiming [3476 5019 2494], Structure of Parallel Processing Computers, Defense Publishing Co., 1982.

3. Xu Zhengchun [1776 2973 2504], Introduction to CRAY-1 Computer System, Computer Status, No 4, 1978 p 9.

4. Chen Jingliang [7115 2529 5328], Parallel Numerical Method, Qinghua University Press, 1983.

5. Wu Jikang [0702 0415 1660], Zhao Renchang [6392 0088 2490] and Wang Zhenshan [3769 2182 1472], Introduction to the Model 757 Computer, Computer Research and Development, No 2, 1984.

6. Fujitsu, Super Computer FACOM VP-100/200, Japan Fujitsu 1P1035-827M, 1983.

7. Cao Dongqi [2580 2639 0796], Zhong Cuihao [0112 5488 6275], Zhang Youla [1728 1429 5248] and Jin Tinghu [6855 1656 3275], Computer Operating Systems, Science Publishing Co., 1979.

8. Wang Hongwu [3769 7703 2976], Operating Systems, Hunan Science and Technology Publishing Co., 1980.

9. Fan Zhihua, Structured Modular Program Design Methods, Chinese Journal of Computer, No 2, 1983 p 90.

10. Cheng Hu [4453 5706], Development of Computer Language, Computer Research and Development, No 3, 1983 p 11.

11. Lu Ruqian [7120 3067 6870], Development of High Level Language (II). Computer Research and Development, No 5, 1982 p 1.

12. Zhou Shaobo [6650 1421 2672] and Gao Qingshi [7559 1987 3740], Direct high level language Execution Computer, Chinese Journal of Computer, No 2, 1982 p 117.

13. Guo Jingeng [6753 6855 1649], Zhou Shaobo and Gao Qingshi, A Computer Capable of Direct Execution ALGOL60 Vector Language, Chinese Journal of Computer, No 4, 1983 p 272.

14. F. C. White et al.: American National Standard Programming Language FORTRAN, American National Standards Ins., 1978.

15. Charles Wetherell, Array Processing for FORTRAN, Cray Research Inc., 1980.

16. David Gries, Compiler Construction for Digital Computers, John Wiley & Sons, Inc., 1971.

17. L. Lamport: The Coordinate Method of the Parallel Execution of DO Loops, Proc. of the 1973 Sagamore Computer Conference on Parallel Processing, 1973.

18. L. Lamport: The Hyperplane Method for an Array Computer, Proc. of the 1974 Sagamore Computer Conference on Processing, 1974.

19. Fan Zhihua, Vectorization Research, Symposium of Chinese-American Software Engineering Discussion Meeting, 8-13 April 1982.

20. Fan Zhihua, A New Vectorization Method, Chinese Journal of Science, 27(1982), 16:1024.

21. Fan Zhihua, Subscript Tracking Method for Vectorization of Serial Operations, Chinese Sciences (Edition A), No 3, 1983 p 275.

22. Fan Zhihua, Engineering Use of Subscript Tracking for Vectorization, Chinese Sciences (Edition A), No 4, 1983 p 380.

23. Fan Zhihua, Strengthening Theory and Its Applications of Subscript Tracking in Vectorization, Chinese Sciences (Edition A), No 6, 1983 p 566.

24. Fan Zhihua, Vectorization of IF and GOTO Statements, Chinese Sciences (Edition A), No 8, 1983 p 756.

25. Fan Zhihua, Vectorization of Triple Control Switch, DIANZI XUEBAO [ACTA ELECTRONICA SINICA], No 5, 1984 p 27.

26. Fan Zhihua, Guo Qiang [6753 1730] and Liu Huimin [0491 2585 3046], Implicit Data Dependence in Vectorization, Chinese Journal of Computer, No 5, 1985 p 321.

27. Fan Zhihua, Wu Jianan [0702 0256 1344], Guo Qiang and Wei Kuaichao [7614 1145 6389], Identification of Commands in Vectorization, DIANZI XUEBAO [ACTA ELECTRONICA SINICA], No 3, 1985 p 1.

28. Guo Qiang and Chen Haibo [7115 3189 3134], Correlation Analysis in Vectorization of Serial Operations, Chinese Journal of Computer, No 5, 1985 p 342.

29. Fan Zhihua, Discretization Levels and Primary Form Vectorization, Chinese Journal of Science, 30(1985), 5:392.

30. Fan Zhihua, Discretization Levels and Quasi Primary Form Vectorization, Chinese Journal of Science, 30(1985), 7:551.

31. Tang Zhisong [0781 4460 2646], Program Structure Design and Program Structure Language, Institute of Computer Technology, Chinese Academy of Sciences, 1978.

32. Zhong Cuihao and Feng Yulin [7458 3768 3829], Methodology of Program Design, Computer Research and Development, No 3, 1983 p 1.

12553/7358
CSO: 4008/1087

CLONING OF THE $P_{7.5}$ PROMOTER FROM VACCINIA VIRUS

Shanghai SHENGWUHUAXUE YU SHENGWUWULI XUIBAO [ACTA BIOCHIMICA ET BIOPHYSICA SINICA] in Chinese Vol 18, No 1, Jan 86 pp 74-79

[Article by Feng Zongming [7458 1350 6900], Wu Xiangfu [0702 4382 3940], Wang Yuan [3076 0997], Chu Meijin [0328 5019 3866], and Li Zaiping [2621 6528 1627], Shanghai Institute of Biochemistry, Chinese Academy of Science]

[Text] Abstract: This article reports on the gene segment and cloning of 7.5K early protein $P_{7.5}$ promoter from vaccinia virus isolated from the genomic DNA of vaccinia virus, strain WR, collected in China. Use of restrictive endonuclease mapping, Southern hybridization, and DNA sequence analysis has confirmed that the $P_{7.5}$ promoter has been obtained. Comparison with data on the WR strain as reported in foreign literature shows its DNA sequence varies by a difference in one nucleotide. As one of the stronger promoters found in vaccinia virus, the $P_{7.5}$ promoter can be very useful for activating foreign gene expression.

The host environment for vaccinia virus used in genetic engineering studies is extensive and safe, and the capacity of the vaccinia virus genome to carry foreign genes is also great, thereby permitting insertion of many foreign genes. Hopefully, the vaccinia virus can be used this way to produce multivalent vaccine. For this reason, research during the past 2 years on the use of vaccinia virus to study the expression of foreign genes has been on the increase.[1-6] In this approach, expression of the inserted foreign genes need to be controlled by the vaccinia virus genome's own promoter gene, and not by any foreign promoter.

The basic purpose of developing such studies is to obtain a strong promoter from the vaccinia virus and to allow the expression of foreign genes which is controlled by this promoter in the vaccinia virological system to produce needed products. This article reports primarily on the cloning and assay of a comparatively strong $P_{7.5}$ promoter fragment from vaccinia virus, WR strain, collected in China. It also reports on its nucleotide sequence and its difference from known WR strain $P_{7.5}$ promoter.

Materials and Methodology

1. Vaccinia virus, WR strain. Provided by colleague Yan Zilin [0917 1311 2651] of the Bureau of Pharmaceuticals and Biologicals Assay and Certification, Ministry of Health.

2. Restrictive Endonucleases and T_4DNA ligase. Supplied by the Enzyme Tooling Section of our laboratory and from Biolabs.

3. Alpha-^{32}P-dATP (3000 Ci/mmol). From Amersham.

4. DNA isolation. Isolation of vaccinia virus DNA based on method used by Esposito et al.[7] Isolation and purification of DNA particles, their in vitro recombination and transformation, and selection of recombinants etc., are based on previous work done in this laboratory.[8]

5. DNA probe labeling. Reference made to Rigby's method.[9]

6. DNA gel transfer and hybridization. Reference made to Southern's method.[10]

7. DNA sequence analysis. Based on Maxam-Gilbert's method.[11]

Results

1. Cloning

We have completed the cloning of HindIII fragment of the genome of vaccinia virus, WR strain (yet to be published report). However, cloning was difficult, because the HindIII-A fragment was too large. Moreover, the linear double linear strands at the terminal end of the vaccinia virus' DNA molecule were joined to each other by a covalent bond to form a closed ring. Therefore, the HindIII-B and HindIII-C fragments at both ends of the DNA molecule were not able to be cloned. Coincidentally, the $P_{7.5}$ promoter we needed was located on the HindIII-C fragment of the left terminal of the vaccinia virus genome. If the HindIII-C fragment were to be cleaved with SalI enzyme, the $P_{7.5}$ promoter would be found in the SalI-C_1 fragment.[12] Toward this end, the recombinant plasmid containing the SalI-C_1 fragment must first be obtained, after which the $P_{7.5}$ promoter could be isolated from it.

In this experiment, we started by using a BglI-C fragment to replace the HindIII-C fragment, because the map positions of these two fragments are quite similar. Also, HindIII enzyme cleavage of vaccinia virus, WR strain, yields 15 segments, whereas cleavage with BglI yields only four segments A, B, C, and D,[13] the distance between C and B, D segments being rather larger and more easily isolated. We first isolated the BglI-C segment. Then the BglI-C segment and pBR322 were each cleaved with SalI, after which they were placed together for recombination and transformation. LB plates containing ampicillin and tetracycline were used to screen-select the Ap^rTc^s recombinants. DNA extracted from these recombinant plasmids then underwent enzyme cleavage analysis to select out the required cloning strain (Fig. 1).

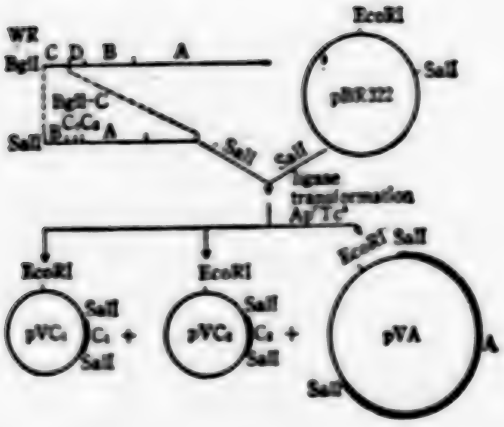

Figure 1. Diagram showing the cloning of DNA fragment containing the $P_{7.5}$ promoter

2. Analysis and Selection of Restrictive Enzyme Cleavage

Results of enzyme cleavage analysis of the WR strain's genome shows four SalI cleavage points on the BglI-C fragment, which yields five segments when cut with SalI. At the end of the left segment is the single-stranded ring formed by covalent bonding of the double-stranded DNA. At one end of the right segment is the SalI cleavage point; at the other, the BglI cleavage point. The DNA in these two segments cannot recombine with pBR322 cleaved by SalI. Using an antibiotic-treated LB plate to screen and select Ap^rTc^s colonies yields only SalI-A, Sal-C_1 and SalI-C_2 cloned strains[12] (Fig. 1), of which the A segment is 9 kb in length, while C_1 and C_2 segments measure only about 0.9 kb. Only analysis of recombinants in the 0.9-kb segments is needed to select out the required SalI-C_1 segment. Colonies are cultured in small quantities for quick extraction of the DNA. The recombinant plasmids of 0.9-kb length are first selected out. After this, enzyme cleavage analysis, selection, and determination are made of the inserted fragment, from which the cloned strain containing the $P_{7.5}$ promoter, that is, the SalI-C_1 segment, is selected out.

The results of work by Venkatesan at al[12] show that the SalI-C_2 segment contains three HpaII cleavage points, which are distributed fairly evenly and cut the C_2 segment of 0.9-kb length into very small fragments. However, the SalI-C_1 segment only has one cleavage point which is displaced toward one end of the 0.9 kb long C_1 segment (Fig. 2A), which may be used for selection purposes to distinguish between the two. As shown in Figure 2B, after the 0.9 kb long recombinant DNA has been enzyme cleaved by SalI, and the two recombinant plasmids are found to definitely contain insertion segments about 0.9 kb long (Fig. 2B, a and c), adding HpaII will show a segment of about 0.8 kb in the DNA of one recombinant (Fig. 2B, b), while the other strand is cut into numerous small fragments (Fig. 2 B, d). Quite possibly, recombinant a in Figure 2B may be the cloned strain containing the SalI-C_1 segment now called pVC_1, pVC_2 being the strain containing the C_2 segment. After the DNA of pVC_1 has been digested by enzymes SphI, PvuI, and HincII, the resulting segments (Fig. 2B, e~g) and sites are similar to those reported by Puckett et al,[14] in both the number of cleavage points and sites.

Figure 2. Enzyme cleavage electropherogram of pVC_1
a. pVC_1-SalI; b. pVC_1-SalI-HpaII
c. PVC_2-SalI; d. pVC_2-SalI-HpaII
e-g. Addition to pvC_1 of SphI, PvuI, and HincII.

As for the RsaI cleavage point, according to the restrictive enzyme cleavage electropherogram as described by Venkatesan et al,[12] the C_1 segment only indicates one RsaI cleavage point, which is also one of the points used by Smith et al[2] to isolate the 275-bp long $P_{7.5}$ (P_2) promoter. We have found three RsaI cleavage points on the SalI-C_1 segment. Figure 3 shows how the SalI-C_1 fragment (a), separated from pVC_1 is being digsted by HpaII(b) and RsaI(c); that there is a HpaII cleavage point on the SalI-C_2 fragment that shears out a small fragment of about 100 bp (Fig. 3,b); that shearing by RsaI results in four fragments, of which one measures 280 bp. What is interesting is the synergistic effect of using enzymes RsaI and HpaII together that eliminates the approximately 280-bp fragment in the digestion process. These results explain that this fragment is very likely to be the SalI-C_2 fragment that contains the $P_{7.5}$ promoter.

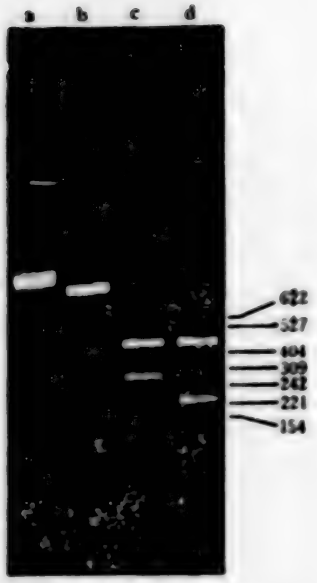

Figure 3. Enzyme cleavage electropherogram of SalI-C_1 fragment showing

a. SalI-C_1 fragment; b. SalI-C_1 + HpaII;

c. SalI-C_1 + RsaI; d. SalI-C_1 +RsaI + HpaII

3. DNA Transfer and Hybridization

After we had obtained the DNA fragment that very likely contained the $P_{7.5}$ promoter, we obtained from Dr. Moss a vector plasmid pGS20 that contained the promoter $P_{7.5}$ from the 7.5K early protein gene of vaccinia virus. Then ^{32}P was used to label the approximately 280-bp fragment isolated from SalI-C_1 in a probe to be hybridized with pGS20. The results are noted in Figure 4 where the $P_{7.5}$ promoter in pGS20 was partially sheared out by EcoRI (Fig. 4A, a), confirming the fact that the ^{32}P-labeled probe can hybridize with it, while the other parts of pGS20 do not respond to hybridization (Fig. 4A-B, a and a'). Because a small fragment of polymerized connectors is located behind the $P_{7.5}$ promoter in pGS20, it shows up as being larger than the approximately 280-bp fragment we had obtained (Fig. 4, c and c'). This definitely proves the fact that we had found the DNA fragment containing the $P_{7.5}$ promoter.

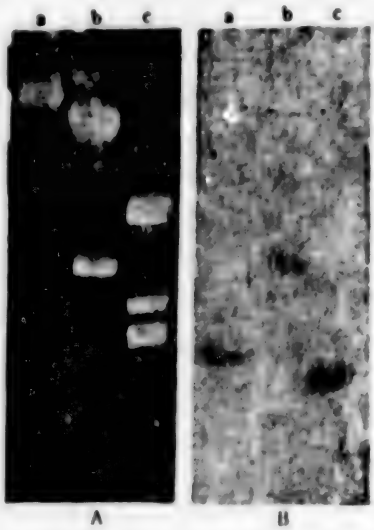

Figure 4. Hybridization of $P_{7.5}$ promoter by Southern's method.

A. a. pGS20 + EcoRI; b. pVC_1 + SalI; c. pVC_1 + SalI + RsaI.

B. Respective autoradiographs (a, b, c) of a, b, and c in A.

4. DNA Sequence Analysis

Mapping analysis of the restrictive endonucleases described above, and the results of DNA gel transfer and hybridization according to Southern's method, have confirmed the fact that we had obtained the $P_{7.5}$ promoter. Requirements for the promoter we need must have the distinguishing sequence of RNA polymerase, its synthesis sites and transcription initiation codon, and not contain the translation initiation codon ATG from the original code of the protein gene. This way, it will help the foreign protein gene inserted behind it to directly utilize its own translation initiation codon ATG to begin translation and avoid formation of a mixed peptide chain. For this reason, when the promoter is being isolated, the site for accurately excising the promoter must be accurately placed between the transcription initiation codon and the translation initiation codon ATG of its adjacent protein gene.

Toward this end, we conducted partial DNA sequence analysis of the $P_{7.5}$ promoter. Beginning near the translation initiation codon ATG of the 7.5K protein and going toward the transcription initiation codon, we analyzed a total of 142 nucleotides as shown in Figure 5. When the results are compared with those published by Venkatesan et al,[15] the only difference was found in the 48th nucleotide located upstream along the translation initiation codon ATG5' of the 7.5K protein. In their results, this site is occupied by C; in the fragment we obtained, this is occupied by T. No other differences were noted. This experiment to isolate the $P_{7.5}$ promoter has given us reliable data which indicates we need only shear off this DNA fragment and insert it into the appropriate site on the vaccinia virus, and the foreign gene spliced downstream on its 3' side will be expressed.[16]

a. AGTTTTTCAC CCATAAATAA TAAATACAAT A/ .TAATTTC
b. AGTTTTTCAC CCATAAATAA TAAATACAAT AATTAATTTC

TCGTAAAAGT AGAAAATATA TTCTAATTTA TTGCACGGTA
TCGTAAAAGT AGAAAATATA TTCTAATTTA TTGCATGGTA

AGGAAGTAGA ATCATAAAGA ACAGTACTCA ATCAATAGCA
AGGAAGTAGA ATCATAAAGA ACAGTAGTCA ATCAATAGCA
RsaI

ATCATGAAAC AATATATCGT CC
ATCATGAAAC AATATATCGT CC

Figure 5. Partial DNA sequence analysis of $P_{7.5}$ promoter.
a. Venkatesan's results; b. Authors' results.

Discussion

Due to the unique characteristics of the vaccinia virus, the use of vaccinia virus DNA as vector units to construct recombinant viruses for studying the expression of foreign genes has received wide attention. At present, expression of such foreign genes as herpesvirus thymidine kinase,[1] hepatitis B surface antigen,[2,4] influenza virus hemagglutinin,[3] herpes simplex virus glycoprotein,[4] chloroamphenicol acetyltransferase (CAT),[5] and plasmodium sporozoite

antigen[6] in vaccinia virus has become realities. To study these modes of expression, a vector plasmid which contains a fragment of vaccinia virus DNA into which the foreign gene can be inserted must first be constructed. To achieve a more pronounced expression of the foreign gene, a stronger promoter from a vaccinia virus fragment is inserted ahead of the foreign gene. Among several known vaccinia virus promoters, in vitro experiments have found promoter $P_{7.5}$ in the 7.5K early protein gene to be stronger.[14] Smith et al[2] have used it to successfully express hepatitis B surface antigen.

Consequently, we have isolated and purified viral DNA from vaccinia virus, WR strain, collected in China, conducted endonuclease mapping analysis, and established a gene bank. Following this, we have also cloned a DNA fragment containing the 7.5K early protein gene, and have analyzed and assayed its promoter. Using enzyme cleavage mapping, Southern hybridization, and partial DNA sequence analysis, we have determined the site of the $P_{7.5}$ promoter. When, the fragment is cut at the RsaI point, an approximately 280-bp fragment is obtained between the RsaI and SalI points. As the RsaI cleavage point is located 18 bp on the 5' side of the 7.5K protein gene's translation initiation codon, it does not contain the 7.5K protein's ATG codon, but contains rather, the RNA's polymerase synthesis locus and its transcription initiation codon. We can very conveniently excise this promoter, and insert it into the expression plasmid's vaccinia virus tk gene, and construct a transcribed expression vector that is controlled by the $P_{7.5}$ promoter. We have used it to successfully study expression of the hepatitis B virus surface antigen gene.[16] As for our DNA sequence analysis studies where the $P_{7.5}$ promoter discovered by us show a T and C difference with already published results by others, the effect of this difference on the strength of the promoter can pose an interesting problem.

Experiments using in vitro systems show the $P_{7.5}$ promoter to be more effective than other promoters.[14] However, the strength of these promoters within the genome has not been determined. For this reason, after the location and structure of the promoters concerned have been clarified, foreign genes can be constructed behind different promoters, undergo in vivo recombination and be placed in vaccinia virus genome for comparing the strength of the various promoters. Such an approach can be quite significant.

Using the vaccinia virus promoter to study the regulation and control mechanism of gene expression is quite meaningful. Recently, Weir et al[17] took a 366-bp fragment of the P_{LT} promoter from a 28K late protein gene and inserted it into an early protein--thymidine kinase (tk) gene, to study its effect on the expression of the CAT gene inserted behind it, and found CAT activity surfacing late, appearing only after DNA replication had begun. This explains the fact that this promoter only begins activity at this time. If a DNA inhibitor were present, this P_{LT} would remain inactive, completely unaffected by the early gene environment. On such a short DNA fragment are the on and off transcription signals, RNA polymerase recognition signals and synthesis loci and the transcription initiation site. Not only does selection of a simpler and quicker method to screen and select promoters have practical application value, it is also significant, through comparative analysis, in understanding the regulation and control pattern of true gene expression.

Acknowledgments

We thank colleague Yan Zilin [0917 1311 2651] for providing the virus strain; our laboratory's Enzyme Tooling Section for the enzymes; colleagues Zhong Wuwei [6945 2976 1218] and Kong Yuying [1313 3768 5391] for assistance with the virus cultures; colleague Qian Bin [6929 1430] for preparing some of the DNA particles; and colleague Gan Keda for processing and enlarging the photographs.

FOOTNOTES

1. Mackett, M. et al. Vaccinia virus: A selectable eukaryotic cloning and expression vector. Proc. Nat. Acad. Sci. U.S.A., 1982, 79, 7415.

2. Smith, G.L. et al. Infectious vaccinia virus recombinants that express hepatitis B virus surface antigen. Nature, 1983, 302, 490.

3. Smith, G.L., et al. Construction and characterization of an infectious vaccinia virus recombinant that expresses the influenza hemagglutinin gene and induces resistance to influenza virus infection in hamsters. Proc. Nat. Acad. Sci. U.S.A., 1983, 80, 7155.

4. Paoletti, E. et al. Construction of live vaccines using genetically engineered poxviruses: Biological activity of vaccinia virus recombinants expressing the hepatitis B virus antigen and the herpes simplex virus glycoprotein D. Proc. Nat. Acad. Sci. U.S.A., 1984, 81, 193.

5. Mackett, M. et al. General method production and selection of infectious vaccina vector. J. Virol., 1984, 49, 857.

6. Nussenzweig, R.S. et al. Plasmodium knowlesi sporozoite antigen: Expression by infectious vaccina virus. Science, 1984, 224, 397.

7. Esposito, J. et al. The preparation of orthopoxvirus DNA. J. Virol. Method, 1981, 2, 175.

8. Wu Xiangfu [0702 4382 3940] et al. Cloning of human hepatitis B virus--HBVadr subgenome and restrictive enzyme mapping. ZHONGGUO KEXUE [CHINESE SCIENCE], Vol. B, 1983, 2, 162.

9. Rigby, P.W.J. et al. Labeling deoxyribonucleic acid to high specific activity by nick translation with DNA polymerase I.J. Mol. Biol., 1977, 113, 237.

10. Southern, E. Detection of specific sequences among DNA fragments separated by gel electrophoresis. J. Mol. Biol., 1975, 98, 503.

11. Maxam, A.M. et al. A new method for sequencing DNA. Proc. Nat. Acad. Sci. U.S.A., 1977, 74, 560.

12. Venkatesan, S. et al. In vitro transcription of inverted terminal repetition of the vaccinia virus genome: Correspondence of initiation and cap sites. J. Virol., 1981, 37, 738.

13. Defilippes, F.M. Restriction enzyme mapping of vaccinia virus DNA. J. Virol., 1982, 43, 136.

14. Puckett, C. et al. Selective transcription of vaccinia virus genes in template dependent soluble extracts of infected cells. Cell, 1983, 35, 441.

15. Venkatesan, S. et al. Distinctive nucleotide sequences adjacent to multiple initiation and termination sites of an early vaccinia virus gene. Cell, 1981, 25, 805.

16. Wang Yuan [3076 0997] et al. Recombinant vaccinia virus expressing hepatitis B virus surface antigen--a possible live vaccine for hepatitis B. To be published report.

17. Weir, J.P. et al. Regulation of expression and nucleotide sequence of a late vaccinia virus gene. J. VIROL., 1984, 51, 662.

5292/7358
CSO: 4008/1112

FINITE ELEMENT ANALYSIS FOR TEMPERATURE FIELD PRODUCED BY MOVING HEAT SOURCE

Chongqing YINGYONG SHUXUE HE LIXUE [APPLIED MATHEMATICS AND MECHANICS] in Chinese Vol 7 No 5, May 86 pp 383-400

[English abstract of article by S. N. Atluri of Georgia Institute of Technology; and Kuang Zhenbang [0562 7201 6721] of Xi'an Jiaotong University]

[Text] Using the moving mesh finite element method, the authors discuss the temperature field produced by a moving heat source with variable thermal conductivity and with radioactive and convective boundary conditions in a wide velocity range. The temperature-time relationships at various velocities in the static and moving coordinate systems are studied. The steady-state temperature distributions at various velocities in the moving coordinate systems are given. The temperature field produced by the plastic deformation at the process region (a region very near the crack tip) is also studied, and the results show that the highest temperature at the process region is lower than 1000°C or 1832°F. (Paper received 9 May 1985.)

REFERENCES

[1] Schönert, K. and R. Weichert, *Chem. Ing. Technik*, 41 (1969), 295.
[2] Weichert, R. and K. Schönert, *J. Mech. Phys. Solids*, 22 (1974), 127.
[3] Weichert, R. and K. Schönert, *Q. Jl. Mech. Appl. Math.*, XXXI, pt.3, (1978), 363.
[4] Weichert, R. and K. Schönert, *J. Mech. Phys. Solids*, 26 (1978), 151.
[5] Döll, W., *Int. J. Fra.* 12 (1976), 595.
[6] Rice, J. R., *Proc. 1st Int. Congr. Fract.*, Editors: T. Yokobori, et al., Japanese Soc. for Strength and Fract., Tokyo, 1 309.
[7] Eckert, E. R. G. and R. M. Drake, *Analysis of Heat and Mass Transfer*, McGraw-Hill (1972).
[8] Mathe, K. J. and R. Koshgoftar, *Nuclear Eng. and Design*, 51 (1979), 389.
[9] Atluri, S. N., T. Nishioka and M. Nakagaki, *Nonlinear and Dynamic Fracture Mechanics*, Edited by N. Perrone and S. N. Atluri, *ASME AMD*-Vol. 35, p37.
[10] Nishioka, T. and S. N. Atluri, *J. Appl. Mech.* 47 (1980), 570.
[11] Brickstad, B., *J. Mech. Phys. Solids*, 31 (1983), 307.

MORE GENERALIZED HYBRID VARIATIONAL PRINCIPLE AND CORRESPONDING FINITE ELEMENT MODEL

Chongqing YINGYONG SHUXUE HE LIXUE [APPLIED MATHEMATICS AND MECHANICS] in Chinese Vol 7 No 5, May 86 pp 443-449

[English abstract of article by Chen Wanji [7115 8001 0679] of Dalian Institute of Technology]

[Text] According to recent studies of the generalized variational principle by Professor Qian Weizhang [6929 0251 7022], a more generalized hybrid variational principle for the finite element method is given. Thus, a new kind of generalized hybrid element model is established. Using the thin plate bending element with varying thickness as an example, various hybrid elements based on different generalized variational principles are compared. (Paper received 9 April 1985.)

REFERENCES

[1] 钱伟长. 高阶Hu氏乘子法和弹性理论中更一般的广义变分原理.应用数学与力学, 4, 2 (1983).

[2] Liang Guo-ping(梁国平)and Fu Zi-zhi(付子智), A New method for the construction element, *Proceedings of the International Conference On Finite Element Methods*, Shanghai, 2—6, August (1982), 593—599.

[3] Michael., L. Day and T. Y. Yang, A mixed variatianal principle for finite element analysis, *Int. J. Num. Methods Engng.*, 8 (1982), 1212—1230.

[4] Oden, J. T., The classical variational principles of mechanics, *Energy Methods in Finite Element Analysis*, Edited by R. Glowinsk, E. Y. Rodin., O. C. Zienkiewicz (1979), 1—31.

[5] 陈万吉. 杂交广义变分原理及杂交模型. 大连工学学报. 4 (1983).

[6] 陈万吉. 变厚度薄板、壳广义杂交元. 力学学报 (待发表).

[5] 钱伟长. 《变分法和有限元》, 科学出版社 (1980).

[8] 龙驭球. 弹性力学中的分区广义变分原理. 上海力学, 2 (1981).

9717
CSO: 4009/1013

NEW LADDER-TYPE ACTIVE BANDPASS FILTER BY USE OF FDNR EMBEDDING, NIC

Beijing DIANZI KEXUE XUEKAN [JOURNAL OF ELECTRONICS] in Chinese Vol 7, No 6, Nov 85 pp 401-410

[English abstract of article by Li Wenzhe [2621 2429 0772], and Hu Yun [5170 4596] of Beijing Institute of Posts and Telecommunications]

[Text] A new method of realizing elliptic ladder-type active bandpass filters is proposed. Comparing with the methods of the same category, it has the advantage of using fewer operational amplifiers, so the power consumption can be reduced. It also has the advantage of ease in adjustment. The low sensitivity property of ladder networks is maintained. The stability and the error of the fundamental circuits are analysed in detail. A sixth-order bandpass circuit is realized with this method and it shows that the experimental results agree pretty well with the theoretical design. (Paper received 3 May 84, finalized 10 Aug 84.)

REFERENCES

[1] R. Schaumann, M. A. Soderstrand, K. R. Laker, Modern Active Filter Design, IEEE Press, Inc. New York, 1981.
[2] H. J. Orchard, *Electron. Lett.*, **2**(1966), 224.
[3] H. J.Orchard, *IEEE Trans. on CAS*, CAS-**26** (1979), 293.
[4] M. S. Ghausi and K. R. Laker, Modern Filter Design: Active RC and Switched Capacitor, Prentice-Hall, Inc., Englewood Cliffs, NJ, 1981.
[5] Raj Senani, *Electron. Lett.*, **14** (1978), 828.
[6] L. Q. The and T. Yanagisawa, *Proc. IEEE*, **65**(1977), 1071.
[7] M. A. Reddy, *IEEE Trans. on CAS*, CAS-**23** (1976), 171.
[8] D. Patranabis, M. P. Tripathi and S. B. Roy, ibid, CAS-**26** (1979), 892.
[9] L. T. Bruton, *IEEE. Trans. on CT*, CT-**16** (1969), 406.
[10] A. S. Sedra and P. O. Brakett, Filter Theory and Design: Active and Passive, Matrix Publishers, Inc., Portland, 1978, Sec. 11-4.
[11] K. Martin and A. S. Sedra, *IEEE Trans on CAS*, CAS-**24** (1977), 495.
[12] L. T. Bruton, RC-Active Circuits Theory and Design, Prentice-Hall, Inc., Englewood Cliffs, New Jersey, 1980. 427, 448, 415, 147, 158.
[13] 石橋幸男，電子通信学会論文誌 **J60-A**(1977), 1089.
[14] Esturo Havahara, Active RC Filter Design Using Impedance Transformation, Proc. of ISCAS' 79, pp. 34—35.
[15] J. D. Brownlie, *IEEE Trans. on CT*, CT-**13** (1966), 98.
[16] A. C. Davis, ibid, **CT-15** (1968), 80.
[17] Y. W. Li, F. Lin, Y. Hu and Y. Lou, A Novel Investigation on NIC, IEEE ISCAS' 84, Montreal, p. 642.
[18] H. J. Orchard and A. N. Willson, Jr., *Electron. Lett.*, **10**(1974), 261.

THEORETICAL ANALYSIS OF NEW TYPE OF RF SENSOR ON SATELLITE

Beijing DIANZI KEXUE XUEKAN [JOURNAL OF ELECTRONICS] in Chinese Vol 7, No 6, Nov 85 pp 411-420

[English abstract of article by Zhang Jinbiao [1728 6855 2871] of Tianjin Institute of Technology]

[Text] A theoretical analysis of the performances of RF sensor proposed by B.K. Watson et al. (1981) on the large Satellite is carried out in this paper. By use of the method given here for dealing with the error signals, it makes the RF sensing system be indeed a big performance system. Except the case of $b=1$, $\gamma=0$ or $\pi/2$, the RF sensor is insensitive to depolarization of the coming waves, and because the horizontal channel does not couple with the vertical one, so it is obvious that the precision of dynamic tracking of the RF sensor on satellite is high and in ground station this RF sensing system will be a good one for tracking high-speed vehicles. (Paper received 25 Mar 85, finalized 16 Jul 85.)

REFERENCES

[1] B. K. Watson, N. D. Dang and S. Ghosh, A mode Extraction Network for RF Sensing in Satellite Reflector Antenna, Second Int. Conference on Atennas and Propagation, part 1, Antennas, 1981, pp. 323—327.
[2] 章日荣等，卫星地面站天线新技术研究，国防工业出版社，1982.
[3] M. L. Kales, *Proc. IRE* 39 (1951), 544.
[4] D. R. Rhodes, Introduction to Monopulse, McGraw-Hill, New York, 1959.
[5] J. S. Cook and R. Lowell, *Bell Syt. Tech. J*. 42(1963), 1283.
[6] 张金标，电子科学学刊，6(1984)，495.

IMPEDANCE MATCHING ELEMENT OF DIELECTRIC IMAGE LINE

Beijing DIANZI KEXUE XUEKAN [JOURNAL OF ELECTRONICS] in Chinese Vol 7, No 6, Nov 85 pp 421-427

[English abstract of article by Shi Meiqi [0670 5019 3825] of Department of Radio Electronics, Beijing University]

[Text] In this paper the wave impedance of dielectric image line as a function of geometry dimensions and frequency is analyzed. Both the necessity and the possibility of impedance matching are studied. An optimal matching element is put forward. Its bandwidth with VSWR≤1.10 can be as wide as 10.5 GHz, when it is connected between two dielectric image lines with an impedance ratio of 4.7. Its properties are obviously better than those of classical type. (Paper received 16 May 84, finalized 21 May 85.)

REFERENCES

[1] J. A. Paul and Y. W. Chang, *IEEE Trans. on MTT*, **MTT-26** (1978), 751.

[2] 北京大学数学系试验设计组编,正交试验法,科学普及出版社, 1979.

[3] R. M. Knox and P. P. Toulios, Integrated circuits for Millimeter-Optical Waveguide, Proc. Symp. Submillimeter Wave, N. Y., Edited by Jerome Fox, Mar. 1970, pp. 497—516.

[4] 史美琪,郭定华,通信学报, 1985 年,第 2 期,第 1 页.

[5] R. E. Collin and J. Brown, *Proc. IEE Pt. C*, **103** (1956), 153.

[6] 上海科大 CAD 组,微波阶梯阻抗均衡器的最优设计初探,全国电子线路 CAD 学术讨论会文集, 1980 年 10 月.

[7] 陈开周,赵希明等,西北电讯工程学院学报, 1982 年第 2 期,第 22 页.

NEW FORMULAS FOR DESIGNING FREQUENCY DEVIATION OF CRYSTAL FM OSCILLATOR

Beijing DIANZI KEXUE XUEKAN [JOURNAL OF ELECTRONICS] in Chinese Vol 7, No 6, Nov 85 pp 443-449

[English abstract of article by Ji Jian [0679 0256] of Nanjing Jinling Zhiye University]

[Text] On the basis of analyzing the oscillatory frequency of crystal oscillator, the general expression of the frequency deviation of crystal frequency-modulation oscillator is derived. The design formulas of the frequency deviation under optimum load condition and under condition of the modulating stage with series negative current feedback are also given. (Paper received 23 Apr 84, finalized 20 May 85.)

REFERENCES

[1] P. W. Wood, *Electronics*, 32(1959) 3, 64.
[2] R. E. Sentz and R. A. Barthowiak, Feedback Amplifiers and Oscillators, Holt, Rinehart and Wilson, Inc., New York, 1968, pp. 137—139.
[3] 清华大学通信教研组，高频电路，人民邮电出版社，1983，p. 508.
[4] M. E. Frerking, Crystal Oscillator Design and Temperature Compensation, Litton Educational Publishing Inc. New York, 1978, pp. 20—48.
[5] 谢嘉奎，电子线路(非线性部分)，高等教育出版社，1984，pp. 229—246.

I-V CHARACTERISTIC ANALYSIS OF SCHOTTKY AMORPHOUS SILICON SOLAR CELLS

Beijing DIANZI KEXUE XUEKAN [JOURNAL OF ELECTRONICS] in Chinese Vol 7, No 6, Nov 85 pp 458-465

[English abstract of article by Xu Le [1776 2867] of Department of Physics, Nankai University]

[Text] The present paper introduces an experimental method for measuring the width of illuminated and short-circuited Ni/a-Si:H Schottky barriers. The current-voltage curves for the Schottky barrier solar cells under AM1, 100 mW/cm^2 illumination are calculated by using the parameters determined by experiments. The diffusion length of holes in a-Si:H obtained from the illuminated I-V curve is consistent with the results measured by the author with the surface photovoltage method in 1983. The factors affecting the fill factor are analysed on the basis of the calculated results. A comparison of the calculated results to the experiment's reveals that the very low fill factor of the solar cells measured is due to series and shunt resistances rather than the low diffusion length of the holes. (Paper received 16 Apr 84, finalized 20 May 85.)

REFERENCES

[1] M. H. Brodsky, Amorphous Semiconductors, Springer-Verlag, Berlin, 1979, Chap. 10.
[2] Y. Kuwano, S. Tsuda and M. Ohnishi, *Jpn. J. Appl. Phys.* 21 (1982), 235.
[3] M. Konagai, H. Miyamoto and K. Takahashi, ibid, 19 (1980), 1923.
[4] 徐乐, 刘铁一, 电子科学学刊 6(1984), 247.
[5] A. Catalano et al. 16th IEEE Photovoltaic Specialists Conf. San Diego, (1982).
[6] A. R. Moore, *J. Appl. Phys.* 54(1983), 222.
[7] Xu Le, D. K. Reinhard and M. G. Thompson, *IEEE Trans. on ED*, ED-29 (1982), 1004.
[8] R. C. Neville, Solar Energy Conversion: The Solar Cell, Elsevier Scientific Publishing Co. New York, 1978, p. 37.
[9] F. S. Sinencio and R. Williams, *J. Appl. Phys.* 54(1983), 2757.
[10] R. S. Crandall, R. Williams and B. E. Tompkins, ibid, 50 (1979), 5506.
[11] J. Beichler, W. Fuhs, H. Mell and H. M. Welsch, *J. Non-Cryst. Solids*, 35/36 (1980), 587.

CIRCULARLY POLARIZED BACKFIRE ANTENNA WITH HIGH GAIN

Beijing DIANZI KEXUE XUEKAN [JOURNAL OF ELECTRONICS] in Chinese Vol 7, No 6, Nov 85 pp 473-476

[English abstract of article by Song Ximing [1345 6932 2494] of The Huanghe Machine-Building Factory]

[Text] In this paper, a new type of high-gain circular polarized backfire antenna is presented. It is developed on the basis of equivalent reflector method proposed by the author (1979, 1981). A circular polarized wave is obtained by use of two orthogonal dipoles. The lengths of the two dipoles are so chosen that the real parts of their input admittances differ in 90°. The transverse dimension of the antenna is 2.24λ, the axial dimension is 2λ, the weight of the complete antenna assembly is only 1.2 kg. The gain measured is 17.5 dB, the axial ratio is 0.5 dB, VSWR is 1.18 at centre frequency. (Paper received 23 Apr 84, finalized 8 May 85.)

REFERENCES

[1] H. W. Ehrenspeck, *Proc. IRE*, 48(1960), 109.
[2] H. W. Ehrenspeck, *Proc. IEEE*, 53(1965), 639.
[3] E. D. Nielsen, *IEEE Trans. on AP*, AP-18(1970), 367.
[4] AD-730616.
[5] 马文明, 宋锡明, 电讯工程, 1978年, 第4期, 第20页.
[6] 宋锡明, 林昌禄, 成都电讯工程学院学报, 1981年, 第1期第75页.
[7] 林昌禄, 同上, 1979年, 第1期, 第97页.
[8] 林昌禄, 宋锡明, 电子学通讯, 4(1982), 331.
[9] Lin Changlu and Song Ximing, Short Backfire Antenna Research, 1983 IEEE-APS Symposium and URSI Meeting Symposium Digest, pp. 138—141.

/7358
CSO: 4009/1021

FORMATION OF (γ+γ') EUTECTIC AND CONTROL OF σ-PHASE IN HIGH Al-Ti CAST Ni-BASE SUPERALLOY

Beijing JINSHU XUEBAO [ACTA METALLURGICA SINICA] in Chinese Vol 22 No 2, 18 Apr 86 pp A93-A100

[English abstract of article by Zhu Yaoxiao [2612 5069 1366], et al., of the Institute of Metal Research, Chinese Academy of Sciences, Shenyang]

[Text] An investigation has been made of the various phases formed in order and composed under different temperatures during the process of solidification and segregation of alloying elements in a high Al-Ti cast Ni-base superalloy. The formation of (γ+γ') eutectic and the control of σ-phase precipitation are discussed. During solidification of the alloy, the dendritic segregation of Al and V is almost unespied, and that of Ti, Cr and Mo is positive, with that of Ti being the most serious. This may impel the formation of a segregation zone at the eutectic reaction and the enrichment with the σ-phase forming elements, e.g., Cr, Mo and Co, in the remaining liquid. Therefore, the increasing of the σ-phase transformation may be tended. However, the σ-phase may be avoided either by adjusting the ratio Al/Ti, taking advantage of the difference of the segregation behavior of Al and Ti, or by controlling the cooling rate after casting. (Paper received 21 November 1983; finalized 15 May 1985.)

REFERENCES

1 金柱，马实忠，金属学报，10 (1974)，12.
2 Mihalisin, J.R.; Bieber, C.G.; Grant, R.T., *Trans. Metall. Soc. AIME*, 242 (1968), 2399.
3 Barrett, C.S., *J. Inst. Met.*, 100 (1972), 65.
4 Sims, C.T., *J. Met.*, 18 (1966), 1119.
5 Woodyatt, L.R.; Sims, C.T.; Beattie, H.J., *Trans. Metall. Soc. AIME*, 236 (1966), 519.
6 朱耀宵，张颖南，徐乐英，佟来杰，宁秀珍，刘泽洲，侯翠萍，毕敬，金属学报，21 (1985)，A1.

RELATIONSHIP BETWEEN $\gamma \rightarrow \varepsilon$ TRANSFORMATION TEMPERATURE $M_{\varepsilon s}$ AND COMPOSITION OF METASTABLE AUSTENITE REGION IN Fe-Mn-Al-Cr SYSTEM

Beijing JINSHU XUEBAO [ACTA METALLURGICA SINICA] in Chinese Vol 22 No 2, 18 Apr 86 pp A101-A108

[English abstract of article by Tian Xing [3944 5281], et al., of the Institute of Metal Research, Chinese Academy of Sciences, Shenyang]

[Text] The $\gamma \rightarrow \varepsilon$ martensite transformation temperature $M_{\varepsilon s}$ of 40 metastable austenitic alloys in an Fe-Mn-Al-Cr system was determined by dilatometry. As a result of the multicomponent linear regression, a formula for a linear relationship between $M_{\varepsilon s}$ and the alloy composition has been developed in that each wt-percent of Al, C and Cr decreases 51, 339 and 8°C of $M_{\varepsilon s}$ of the Fe-Mn alloy respectively. This is in agreement with the results of previous allied works and Ishida's calculation of the influence of alloying elements on the driving force of the $\gamma \rightarrow \varepsilon$ transformation in Fe-Mn alloys. A brief discussion on the effects of Al, C and Cr on $M_{\varepsilon s}$ is also made which refers to the mechanism of stacking fault for the $\gamma \rightarrow \varepsilon$ martensite transformation. (Paper received 18 October 1984; finalized 4 January 1985.)

REFERENCES

1 Eichelman, G.H.; Hull, F.C., *Trans. ASM*, 45 (1953), 77.
2 Monkman, F.C.; Cuff, F.B.; Grant, N.J., *Met. Progr.*, 7 (1957), 94.
3 Pickering, F.B., *Physical Metallurgy and the Design of Steels*, Appl. Sci. Publ., London, 1978, p. 228.
4 张彦生，中国金属学会1979—1980年优秀论文选集，第三分册，p. 221，中国金属学会编，冶金工业出版社，1984.
5 张彦生，师昌绪，金属学报，7 (1964), 285.
6 金属研究所编，未公开发表资料.
7 张彦生，苏丽娟，金属学报，19 (1983), A253.
8 张彦生，金属学报，19 (1983), A262.
9 Troiano, A.R.; Mcguire, F.T., *Trans. ASM*, 31 (1943), 340.
10 Holden, A.; Bolton, J.D.; Petty, E.R., *J. Iron Steel Inst.*, 209 (1971), 721.
11 贾文北，未公开发表资料.
12 *Handbook on Materials for Superconducting Machinery*, Metal and Ceramic Information Center, Publ. 1974, p. 5. 1. 1.
13 Cina, B., *Acta Metall.*, 6 (1958), 748.
14 Ishida, K.; Nishizawa, T., *Trans. Jpn Inst., Met.*, 15 (1974), 225.
15 Andrews, K.W., *J. Iron Steel Inst.*, 203 (1965), 721.
16 Kato, T.; Fukui, S.; Fujikura, M.; Ishida, K., *Trans. Iron Steel Inst. Jpn.*, 16 (1976), 673.
17 Yoshimura, H.; Yamada, N.; Yada, H.; Honma, H.; Ito, T., *Trans. Iron Steel Inst. Jpn.*, 16 (1976), 98.
18 White, C.H.; Honeycombe, R.W.K., *J. Iron Steel Inst.*, 200 (1962), 457.
19 冯端，王业宁，丘第荣，金属物理，上册，科学出版社，1964, p. 241.
20 Breedis, J.F., *Trans. Metall. Soc. AIME*, 230 (1964), 1583.
21 Breedis, J.F.; Kaufman, L., *Metall. Trans.*, 2 (1971), 2359.
22 Ishida, K., *Scr. Metall.*, 11 (1977), 237.

EFFECT OF HYDROGEN ON CREEP IN AUSTENITIC STAINLESS STEEL

Beijing JINSHU XUEBAO [ACTA METALLURGICA SINICA] in Chinese Vol 22 No 2, 18 Apr 86 pp A115-A118

[English abstract of article by Chu Wuyang [5969 2976 2254], et al., of Beijing University of Iron and Steel Technology]

[Text] Dynamic charging does not influence the creep rate of type 321 austenitic stainless steel if the initial strain is less than 2 percent in which the amounts of evolving hydrogen after the test were below 1.5 ppm (by wt). However, the creep rate increased markedly when the initial strain was larger than 8 percent or when the specimen was precharged for a long time. In this case, the corresponding amount of evolving hydrogen was 5 to 12 ppm (by wt). (Paper received 1 February 1985.)

REFERENCES

1 Shin, K. S.; Park, C. G.; Nagakawa, J.; Meshii, M., *Scr. Metall.*, **14** (1980), 279
2 Oriani, R. A.; Josephic, P. H., *Acta Metall.*, **27** (1979), 997; **29** (1981), 669
3 Chu, W. Y. (褚武扬), Yao, J. ([illegible]), Hsiao, C. M. (肖纪美), *Metall. Trans.*, **15A** (1984), 729
4 [illegible], 褚武扬, 肖纪美, 金属学报, **20** (1984), A124
5 Chu, W. Y. (褚武扬), Wang, H. L. ([illegible]), Hsiao, C. M. (肖纪美), *Corrosion*, **40** (1984), 487
6 [illegible], 褚武扬, 肖纪美, [illegible], 1984, [illegible]
7 [illegible], 褚武扬, 肖纪美, 金属学报, **18** (1982), 673
8 褚武扬, 肖纪美, [illegible], 金属学报, **17** (1981), 10

BEHAVIOR OF Hf IN SOLIDIFICATION OF CAST Ni-BASE SUPERALLOYS

Beijing JINSHU XUEBAO [ACTA METALLURGICA SINICA] in Chinese Vol 22 No 2, 18 Apr 86 pp A119-A124

[English abstract of article by Zheng Yunrong [6774 6663 2837] of the Institute of Aeronautical Materials, Beijing]

[Text] Results of quantitative metallography, SEM, EDAX and EMPA studies of Hf on the solidification of cast Ni-base superalloys are presented. The Hf is found to lower the liquid temperature of the superalloys, with the final solidification temperature even dropping to 1130°C. The Hf may narrow down the range between the temperature lost during the interdendritic capillary feeding action and that of the solid, as well as decreasing the liquid content necessary for linking the interdendritic pools in the late solidification. The Hf-rich melts have superior fluidity, wettability and skin effects. These are the factors in increasing the castability of Hf-containing superalloys. The Hf is not found in the dendritic arms of the superalloys, but is exceedingly concentrated in the narrow interdendritic zones, usually in the form of Hf-rich phases. The Hf content in primary Hf-rich phases may be arranged in decreasing order of $MC_{(2)}$, $(Hf, Ti)_2$ SC, Ni_5Hf, $MC_{(1)}$ and eutectic γ'. The Hf may depress the formation temperature of primary phases. The solidification temperatures of all Hf-rich phases are lower than 1250°C. These phases may precipitate from the molten pools with Hf concentration over 13 wt-percent at late solidification and may have an intergrowth feature.
(Paper received 21 September 1984; finalized 27 March 1985.)

REFERENCES

1 郑运荣，蔡玉林，中国航空科技文献 HJB 830117(1983).
2 郑运荣，蔡玉林，金属学报，16 (1980), A151.
3 郑运荣，蔡玉林，王罗宝，金属学报，19 (1983), A190.
4 Burton, C. J., *Superalloys: Metallurgy and Manufacture*, Proc. 3rd Int. Symp. on Su[illegible] Eds. Kear, B. H.; Muzyka, D.R.; Tien, J. K., *et al*, Claitor's Publ., Baton Rouge, Louis[illegible] p. 147.
5 Bachelet, E.; Lesoult, G., *High Temperature Alloy for Gas Turbines*, Eds. Coutsou[illegible] Felix, P.; Fischmeister, H., *et al*., Appl. Sci. Publ., London 1978, p. 665.
6 Ouichou, L.; Lavaud, F.; Lesoult, G., *Superalloys 1980*, Proc. 4th Int. Symp. on Su[illegible] Eds. Tien, J. K., *et al*, ASM, Metal Park, Ohio, 1980, p. 235.

ON RAPIDLY SOLIDIFIED Cu-Zn-Al SHAPE MEMORY ALLOY

Beijing JINSHU XUEBAO [ACTA METALLURGICA SINICA] in Chinese Vol 22 No 2, 18 Apr 86 pp A125-A129

[English abstract of article by Jin Jialing [6855 0857 7117], et al., of Shanghai Institute of Iron and Steel Research]

[Text] The shape memory properties, microstructure and influence of heat treatment on them of Cu-24.9 wt-percent Zn-4.5 wt-percent Al alloy ribbon of different sizes prepared by the rapid solidification technique have been investigated by means of σ-ε and R-T curves, optical metallography, X-ray diffraction, SEM and TEM. The results show that the alloy ribbon is of a fine-grained β structure, about 20 μm originally, and grows to about 100 μm after water quenching from 720°C for 10 min. As for the alloy with a β+M structure at room temperature, its optimum shape memory properties may be obtained and the embrittlement by grain coarsening may be avoided. The complete memory recovery may be realized with strain of no more than 8 percent. The formation of granular relief and martensite on the specimen surface seems to be reversible during deformation under loading. (Paper received 6 October 1984; finalized 12 March 1985.)

REFERENCES

1 Perkins, J., *Metall. Trans.*, 13A (1982), 1367.
2 Wood, J.V., Shingu, P.H., *Metall. Trans.*, 15A (1984), 471.
3 [illegible], [illegible], [illegible], (1983), № 2, 49.

EQUILIBRIA OF Ce-Al-O AND Nd-Al-O IN MOLTEN IRON

Beijing JINSHU XUEBAO [ACTA METALLURGICA SINICA] in Chinese Vol 22 No 2, 18 Apr 86 pp A139-A148

[English abstract of article by Diao Shusheng [0431 3219 3932], et al., of Beijing University of Iron and Steel Technology]

[Text] The equilibrium of the Ce-Al-O or Nd-Al-O systems in molten iron was studied by separately smelting the radioactive isotope of ^{141}Ce or ^{147}Nd in an Al_2O_4 crucible filled with pure iron to form $^{141}CeAlO_3$ or $^{147}NdAlO_3$ around its inner wall. The content of dissolved Ce or Nd in iron was determined by means of radioassay and electrolysis in an organic electrolyte. The analysis of the dissolved Al in iron was obtained by colorimetry, followed by calculations. The activity of oxygen in a dissolved state in liquid iron was directly measured by solid electrolyte sensors made of $ZrO_2(MgO)$ tube. By extrapolation of the data obtained, the temperature dependence of the equilibrium constant of RE-Al-O in molten iron, K_{REAlO_3}, or of the interaction coefficient, e_{RE}^{Al}, may be described as:

For the reaction $CeAlO_{3(s)} = [Ce] + [Al] + 3[O]$

$$\lg K_{CeAlO_3} = -37900/T + 5.84$$

$$\Delta G^{\circ}_{CeAlO} = 173400 - 26.7T \text{ cal/mol}$$

$$e_{Ce}^{Al} = 20500/T - 13.53$$

For reaction $NdAlO_{3(s)} = [Nd] + [Al] + 3[O]$

$$\lg K_{NdAlO_3} = -24700/T + 0.69$$

$$\Delta G^{\circ}_{NdAlO_3} = 113030 - 3.16T \text{ cal/mol}$$

$$e_{Nd}^{Al} = 13500/T - 9.33$$

(Paper received 14 July 1984; finalized 20 January 1985.)

REFERENCES

1 [illegible], 中国钢铁学术会议, 第一届钢铁学术会议报告, 中国金属学会, 北京, 1981年 p. 25; 钢铁, 17 (1982), № 2, 1.
2 [illegible], 金属学报, 18 (1982), 176.
3 [illegible], 日本, 中国钢铁学术会议第二届钢铁学术会议报告, 东京, 1983, p. 10.
4 [illegible], 金属学报, 20 (1984), 204.
5 [illegible], 北京钢铁学院学报, (1982), № 2, 157.
6 [illegible], 北京钢铁学院研究生论文, 1979.
7 Sigworth, G.K.; Elliott, J.F., *Met. Sci.*, **8** (1974), 298.
8 [illegible], 北京钢铁学院学报, (1982), № 2, 157.
9 Тюрин, А.Т.; Михайлов, Т.Т., Шишков, В.И., *Изв. АНСССР Металлы*, (1982), № 6, 48.
10 Кинис, Г.; Виникарев, А.Ф.; Яковлев, В.И., *Изв. вуз. Черная металлургия*, (1963), № 5, 65.

PRECIPITATION DIAGRAM OF [Ce]-[O]-[S] IN LIQUID IRON AND ITS APPLICATION

Beijing JINSHU XUEBAO [ACTA METALLURGICA SINICA] in Chinese Vol 22 No 2, 18 Apr 86 pp A149-A155

[English abstract of article by Dong Yuanchi [5516 0337 4654], et al., of Beijing University of Iron and Steel Technology]

[Text] A space precipitation diagram of [Ce]-[O]-[S] in pure liquid iron has been constructed by the proper selection of recent and correct experimental thermodynamic data collected from allied equilibrium systems of RE-O, RE-S and RE-O-S. The quantitative correlation between the activity of oxygen or sulphur and the constitution of RE inclusions formed has been evaluated theoretically by thermodynamic calculations. This was verified well by the experimental results from which the correlation between the initial activities of oxygen and sulphur in liquid iron and the constitution of RE inclusions formed was also determined. (Paper received 17 April 1984; finalized 13 January 1985.)

REFERENCES

1 Langenberg, F.C.; Chipman, J., *Trans. AIME*, **212** (1955), 290.
2 Ejima, A.; Suzuki, K.; Harada, N.; Sanbong, K., *Trans. Iron Steel Inst. Jpn.*, **17** (1977), 349
3 Buzek, Z.; Schinderova, V.; Sbornik, V.S.B., *Ostrava*, (1965), № 3, 149.
4 Mclean, A.; Lu, S.K., *Met. Mater.*, **8** (1974), 542.
5 Janke, D.; Fischer, W.A., *Arch. Eisenhuttenwes.*, **49** (1978), 425.
6 王常珍，王福华，杜丰敏，张小平，金属学报，**16** (1980), 1, 83.
7 韩其勇，董元篪，丰耀安，冯长祥，杨萌，金属学报，**20** (1984), A 204.
8 韩其勇，刘士伟，牛红兵，雷言伟，金属学报，**18** (1982), 176.
9 韩其勇，冯长祥，董元篪，杨萌，日本、中国[illegible]金属学会第二届[illegible]学术会议论文集，1983, 11 东京，p. 30.
10 丰耀安，北京钢铁学院研究生论文，1982.
11 Vahed, A., Kay, D.A.R., *Metall. Trans.*, **7B** (1976), 375.
12 王纪霖，未公开发表，(1982).
13 陈冬，韩其勇，冯长祥，王海，金属学报，22 (1986), A156
14 Fruehan, R.J., *Metall. Trans.*, **10B** (1979), 143.
15 董元篪，北京钢铁学院研究生论文，1981.

EQUILIBRIUM OF Fe-La-O-S SYSTEM

Beijing JINSHU XUEBAO [ACTA METALLURGICA SINICA] in Chinese Vol 22 No 2, 18 Apr 86 pp A156-A162

[English abstract of article by Chen Dong [7115 0392], et al., of Beijing University of Iron and Steel Technology]

[Text] A study was made of the equilibrium of the Fe-La-O-S system. The oxygen activity was directly measured by the solid electrolyte sensors made of a $ZrO_2(MgO)$ tube. The stability of La_2O_2S in the electrolytic separation and the content of La as a dissolved state in liquid iron were examined by means of radioassay and electrolytic isolation of inclusions in organic electrolytes under low temperatures. By extrapolation of the data obtained, the equilibrium constant of La_2O_2S may be described as:

$$1550°C \quad K_{La_2O_2S} = 3.81 \times 10^{-19} \quad e_S^{La} = -4.1$$

$$1600°C \quad K_{La_2O_2S} = 6.45 \times 10^{-19} \quad e_S^{La} = -4.8$$

$$1650°C \quad K_{La_2O_2S} = 7.41 \times 10^{-19} \quad e_S^{La} = -4.2$$

$$La_{(l)} = [La]$$

$$\Delta G^0_{sol.} = -136700 + 59.82T, \quad \gamma^0_{La} = 0.33 \ (1873 \ K)$$

It seems that the deoxysulphurizing effect of La is more intense than that of Ce, Nd and Y. (Paper received 18 June 1984; finalized 15 December 1984.)

REFERENCES

1 Vahed, A.; Kay, D.R., *Metall. Trans. B*, 7B (1976), 375.
2 王常珍，王福珍，杜丕植，张小平，金属学报，16 (1980), 83.
3 董元箎，北京钢铁学院研究生毕业论文，1981.
4 周长行，北京钢铁学院研究生毕业论文，1981.
5 钟新璧，北京钢铁学院研究生毕业论文，1982.
6 韩其勇等，*Proc. of Sino-Jpn. Symp. on Steelmaking*. Beijing, 1981, p. 25.
7 江岛等，铁と钢，63 (1977), 943.
8 Worrell, W.L.; Chipman, J., *Trans. Metall. Soc. AIME*, 230 (1964), 1682.
9 Кинне, Г.; Вишкарев, А. Ф.; Явойский, В. И., *Изв. Вуз. Черная металлургия*, (1963), №5, 65.
10 杜挺，中国金属学会冶金过程物理化学学术会议论文，1980.
11 Fischer, W.A., *Arch. Eisenhuttenwes.*, 49 (1978), 425.
12 韩其勇，球铁，1980, №2, 31.
13 韩其勇，刘士伟，牛红兵，唐志伟，*Proc. of First China-USA Bilateral Metallurgical Conf.*, Beijing, 1981, p. 192.
14 李静宏，北京钢铁学院研究生毕业论文，1982.
15 Wilson, W.G., *et al*', *J. Met.*, 26 (1974), №5, 14.
16 Schindlerva, V.; Buzek, Z., *Hutn. Listy*, 25 (1970), №5, 316.
17 Buzek, Z., *Chemical Metallurgy of Iron Steel*, *ISI*, London, 1973, p. 174.; Buzek, Z., *Hutn. Listy*, 29 (1974), 784.
18 Ejima, A., *et al.*, *Trans. Iron Steel Inst. Jpn.*, 17 (1977), 349.
19 Vahed, A.; *et al.*, *Metall. Trans.*, 7B (1976), 375.
20 Elliott, J.F., *et al.*, *Thermochemistry for Steelmaking*, Addison-Wesley, 1963, p. 410.
21 Sigworth, G.K.; Elliott, J.F., *Met. Sci.*, 8 (1974), 298.

ESTIMATE OF FRACTURE TOUGHNESS FOR POLYCOMPONENT COMPOSITE MATERIALS

Beijing JINSHU XUEBAO [ACTA METALLURGICA SINICA] in Chinese Vol 22 No 2, 18 Apr 86 pp A175-A180

[English abstract of article by Li Zhonghua [2621 0022 5478] of Xi'an Jiaotong University]

[Text] The expressions for estimating fracture toughness of the polycomponent composite materials have been derived in terms of the fracture toughnesses and volume fractions of each individual component included. The expression, conforming to the mixed rule, of the upper ($n \to \infty$) or lower ($n=1$) bound value is also derived based on limit analysis. (Paper received 18 June 1984; finalized 8 November 1984.)

REFERENCES

1 Kameswararao, C. V. S., *Eng. Fract. Mech.*, **18** (1983), 35
2 Parton, V. Z.; Morozov, E. M., *Elastic Plastic Frature Mechanics*, 1978, p. 74.
3 Фихренгольц, Г. М. ([illegible]), [illegible], p. 59
4 Hagiwara, Y.; Knott, J. F., *5th Int. Conf. on Fracture*, Vol. 2, 1981, 707.
5 Kunio, T.; Shimizu, M.; Yamada, K., *Fracture Mechanics of Ductile and Tough Materials Applications to Energy Related Structure*, Eds. Liu, H.W.; Kunio, T., Martinus Nijhoff Publ., The Hague Boston/London, 1980, p. 221
6 Harris, B.; Cawthorne, D., *Plast. and Polym.* **42** (1974), № 161, 209.
7 Cawthorne, D.; Harris, B., *Composites*, **6** (1975), p. 115
8 Kaplan, M. F.; *ACI J. Proc.*, **58** (1961), 591
9 Swamy, R. N., *Fracture Mechanics Applied to Concrete, In Developments in Concrete Technology*, Vol. 1, Ed. Lydon, F.D., Applied Science Publ., London, 1978, p. 221.

KINETICS OF COMBUSTION OF PULVERIZED COAL IN RACEWAY BEFORE TUYERE OF BLAST FURNACE

Beijing JINSHU XUEBAO [ACTA METALLURGICA SINICA] in Chinese Vol 22 No 2, 18 Apr 86 pp B49-B62

[English abstract of article by Yang Yongyi [2799 3057 1355], et al., of Beijing University of Iron and Steel Technology]

[Text] A combustion efficiency study was made of partially burned pulverized coal, sampled from the raceway before the tuyere of two blast furnaces. Results show that the injected coal started to volatilize and burn just as it entered the blowpipe, which seems to be an important preheating and precombustion space before the raceway; however, it could not be burned completely in front of the tuyere. In order to replace more coke by injecting more coal, the laboratory simulation test on the combustion kinetics of the pulverized coal used by the two blast furnaces under conditions prior to tuyeres indicated it was technically possible by: pulverizing the coal down to 40 μm; enriching the blast with oxygen up to 30-40 percent; further raising the blast temperature; improving the injected coal distribution early in the blowpipe; consistently injecting the coal at all tuyeres and selecting a variety of coal which would be more combustible, e.g., bituminous coal is superior to anthracite. Petrographic observations of coal samples prior to injection and after being partially burned revealed that the bituminous coal burned violently and simultaneously, not only on the surface but also in the interior of its particles, while the anthracite burned mostly on the surface. Based on the theory of heat-transfer and mass-transfer, a set of mathematical models for the combustion of pulverized coal has been derived. By substituting the combustion conditions of both blast furnaces and the laboratory test furnace into the model and with the aid of a computer, a close approximation to what happens in actual practice has been obtained. (Paper received 25 February 1985; finalized 27 June 1985.)

REFERENCES

1 Gao Bocong; Wei Shengming; Qi Zongda, *The Technique of Coal Powder Injection on BF of SISC*, p. 8, Preprint of Conf. on Direct Use of Coal in Iron and Steelmaking, The Metals Society, Oct. 1982, London.
2 [illegible], 北京钢铁学院研究生论文, 1984, 5月.
3 日本钢管, 私人通信.
4 [illegible], 高炉喷吹煤粉的几个基本问题, 北京钢铁学院, 未公开发表资料, 1984.
5 Van Heek, K.H.; Muehlen, H.-J., *Brennstoff-Waerme-Kraft*, 37 (1985), №1—2, 20—27.
6 Yang Naifu; Yang Yong Yi, *Revue de Metallurgie*, Nov. 1984, p. 120E, Presentation at annual conference of French Met. Association [ATS], Dec. 1984, Paris.
7 [illegible], 冶金过程动力学, 冶金工业出版社, 1983, p. 157.
8 Smoot, L.D.; Pratt, D.T., *Pulverized-Coal Combustion and Gasification*, Plenum Press, 1979, p. 149—164, 198—200.
9 Smith, I.W., *Combustion and Flame*, 17 (1971), 421.
10 Bortz, S.; Flament, G., *Experiment on Pulverized Coal Combustion under Conditions Simulating a Blast Furnace Environment*, Preprint at the same Conference as [1].

LIQUIDUS AND INTERMETALLIC COMPOUND IN Al-RICH REGION OF Al-Mg-Ce SYSTEM

Beijing JINSHU XUEBAO [ACTA METALLURGICA SINICA] in Chinese Vol 22 No 2, 18 Apr 86 pp B63-B67

[English abstract of article by Zheng Chaogui [6774 2600 6311], et al., of the Department of Chemistry, Beijing University]

[Text] The liquidus of the Al-rich corner in the Al-Mg-Ce phase diagram and the intermetallic compound, if any, formed in this region have been studied by thermal, EMPA, chemical analysis, metallography and X-ray examination. An intermetallic compound in the solid phase was observed to form a solid solution of a rather extensive range. The pseudo-ternary system Al-Mg_5Al_8-$CeAl_4$ is of the ternary eutectic type. Three surfaces corresponding to the primary crystallization of α-Al, Mg_5Al_8 and $CeAl_4$ respectively, three univariant curves associated with secondary crystallization and a ternary eutectic with a composition of about 12.6 wt-percent Ce and 26.0 wt-percent Mg at 446°C were detected. (Paper received 20 August 1984; finalized 1 February 1985.)

REFERENCES

1 Заречняк, О.С.; Крипякевич, П.И., *Изв. АНСССР Металлы*, (1967), №4, 188.
2 Hansen, M., *Constitution of Binary Alloys*, McGraw-Hill, New York, 1958, p. 105; 78.
3 Mondolfo, L.F., *Aluminium Alloys: Structure and Properties*, Butterworth, London, 1976, p. 242; 311.
4 [illegible], 19 (1983), A515.

COMPUTERIZED SIMULATION OF STRUCTURE OF CRYOLITE MELT

Beijing JINSHU XUEBAO [ACTA METALLURGICA SINICA] in Chinese Vol 22 No 2, 18 Apr 86 pp B68-B74

[English abstract of article by Xu Chi [1776 7459], et al., of Shanghai Institute of Metallurgy, Chinese Academy of Sciences; Li Qingzhi [2621 1987 5347], et al., of Shanghai Institute of Computational Technology; Shen Shiying [3088 2514 5391] of Northeast Institute of Technology, Shenyang]

[Text] The structure of molten cryolite has been investigated by computerized simulation using the Monte Carlo method. The radial distribution functions and some parameters describing the local structure of $3NaF \cdot AlF_3$ melt at 1283 K have been calculated. It is concluded that a part of the F^- ions in AlF_6^{3-} moves away from Al^{3+} ions after the melting of cryolite, forming $xNa^+ \cdot yF^-$ clusters with the Na^+ ions. The removal of a part of the F^- from AlF_6^{3-} makes it disintegrate into some local structures, such as AlF_4^- or AlF_5^{2-}. Some Al^{3+} ions are connected to each other by Al-F-Al bridges, forming ionic clusters, e.g. $Al_2F_7^-$, etc. It is also concluded that the distribution of the free space in molten cryolite is not uniform. There are more fissures and holes in $xNa^+ \cdot yF^-$ clusters and between AlF_4^- and $xNa^+ \cdot yF^-$ clusters. (Paper received 7 November 1984.)

REFERENCES

1 Grjotheim, K., *Contribution to the Theory of the Aluminium Electrolysis*. Kgl. Norske Videnskabers Selskabs Skrifter, nr. 5. 1956. F. Bruns Bokhandel. Trondheim. 1956.
2 Piontelli, R., Chim. Ind. (Milan). 22 (1940). 501.
3 Holm, J.L., *Inorg. Chem.*, 12 (1973). 2062.
4 Антипин, Л.Н. *Электрохимия расплавленных солей*. Металлургиздат. Москва. 1964.
5 Dewing, E.W., *Metall. Trans.*, 3 (1972). 495.
6 Inman, D., *et al. Ionic Liquids*. Plenum Press. New York. 1981. p. 27.
7 Metropolis, N., *et al. J. Chem. Phys.*, 21 (1953). 1087.
8 Solomons, C., *et al. J. Chem. Phys.*, 49 (1968). 445.

ON THE CRYSTALLIZATION OF AMORPHOUS Ni-BASE ALLOY

Beijing JINSHU XUEBAO [ACTA METALLURGICA SINICA] in Chinese Vol 22 No 2, 18 Apr 86 pp B75-B79

[English abstract of article by Wang Yuming [3769 3558 2494], et al., of Jilin University, Changchun]

[Text] The crystallization of amorphous $Ni_{83}Cr_7Fe_3Si_4B_3$ alloy was investigated under dynamic heating and isothermal annealing conditions. Identical crystallization and unaltered phases were revealed under both treatments. However, the initial crystallization was mainly due to the nucleation of crystals under dynamic heating, while crystal growth played a major role under isothermal annealing. It was also found that the microhardness approached its highest value just before the specimen was totally crystallized. (Paper received 5 July 1984; finalized 19 January 1985.)

REFERENCES

1 Tiwari, R.S.; Ranganathan, S.; Heimendahl, M. V., *Z. Metall.*, 72 (1981), 563.
2 Scott, M.G., *J. Mater. Sci.*, 13 (1978), 291.
3 Von Heimendahl, M.; Haussner, G., *J. Mater. Sci.*, 14 (1979), 1238.
4 Chang, H.; Sastri, S., *Metall. Trans.*, 8 (1977), 1063.
5 Waseda, Y.; Okazaki, H.; Masumoto, *T.J. Mater. Sci.*, 12 (1977), 1927.

CORRELATION BETWEEN STRUCTURE OF ELECTROCHEMICALLY DEPOSITED (Fe, Co, Ni)-P LAYERS AND PROCESS CONDITIONS

Beijing JINSHU XUEBAO [ACTA METALLURGICA SINICA] in Chinese Vol 22 No 2, 18 Apr 86 pp B80-B89

[English abstract of article by Jiang Xiaoxia [1203 2556 7209], et al., of the Institute of Metal Research, Chinese Academy of Sciences, Shenyang]

[Text] A study has been made of the structure of electrochemically deposited amorphous (Fe, Co, Ni)-P layers in relation to the process conditions, e.g., pH value, current density, metallic salt concentration, etc., by means of X-ray analysis, SEM and EPMA. Results show that the effect of the process on the structure is realized by changing the P content of the layer. When the P contained is over 8 percent, below 3 percent or between 3 and 8 percent, a layer may be constructed as an amorphous alloy, supersaturated solution or mixed structure respectively. The major factors affecting the structure of the deposited layer are found to be the concentration of NaH_2PO_2 and pH value of the bath. The structure of the layer may also be influenced by the potential of electro-deposition. The Fe-P, Co-P or Ni-P system is similar in amorphous structure when the highest thickness of the atomic face stack is 2.0, 2.5 or 6.5 nm respectively. (Paper received 6 January 1984; finalized 15 October 1984.)

REFERENCES

1 石桥知，渡野忠，青木公二，金属表面技術，21 (1970), 541; 31 (1980), 28.
2 Brenner, A., *J. Res. Nat. Bur. Stand.*, 44 (1950), 109.
3 增井宽二，日本金属学会誌，41 (1977), 1130.
4 Абербух, М. Е., Вахидов, Р. С., *Электрохимия*, 12 (1976), 397.
5 Бондарь, В. В., *Электрохимия*, 5 (1969), 1242.
6 云南省交通科学研究所，镀铁电沉积研究，1970.
7 武汉锅炉厂403车间，[illegible]，1979.
8 [illegible]，金属表面技術，32 (1981), 601.
9 吉岡正三，金属表面技術，20 (1961), 172.
10 林树智，[illegible]，物理学报，33 (1984), 302.
11 Dixmier, J.; Guinier, A., *Rev. Metall.*, (Paris), 64 (1967), 53.

9717
CSO: 4009/1011

NEUTRON EMISSION BEHAVIOR IN LIGHT-CHARGED-PARTICLE ACCOMPANIED FISSION OF ^{252}Cf

Beijing YUANZIHE WULI [CHINESE JOURNAL OF NUCLEAR PHYSICS] in Chinese Vol 7 No 4, Nov 85 pp 289-296

[English abstract of article by Han Hongyin [7281 3163 6892], et al., of the Institute of Atomic Energy, Beijing]

[Text] The neutron emission probabilities for long range alpha (LRA), helium-3, triton and proton accompanied fission of ^{252}Cf are measured in a three-parameter experiment in which a liquid scintillation detector and a telescope are used to record the number of prompt neutrons and the energy of light charged particles. The average number of neutrons per fission for various particle accompanied fission events mentioned above are 3.13 ± 0.02, 3.09 ± 0.09, 2.95 ± 0.05 and 3.24 ± 0.07 respectively. The differentials of the average number of neutrons with respect to the energy of LRA particles and tritons are -0.037 ± 0.003 and -0.039 ± 0.008 neutron/MeV, respectively. The dependence of the width of neutron emission probability on LRA energy, described by Diven's empirical formula, and the correlations between the neutron number and triton energy have not yet been reported in the literature.

^{58,60,62}Ni(α,p) THREE-NUCLEON TRANSFER REACTIONS AND α OPTICAL POTENTIAL AMBIGUITIES

Beijing YUANZIHE WULI [CHINESE JOURNAL OF NUCLEAR PHYSICS] in Chinese Vol 7 No 4, Nov 85 pp 297-306

[English abstract of article by Wang Yuanda [3769 6678 1129] and Bao Xiumin [7637 4423 2404], et al., of the Institute of Atomic Energy, Beijing]

[Text] The differential cross sections are measured using a 26.0 MeV α particle for ^{58,62}Ni(α,α) ^{58,62}Ni and ^{58,62}Ni(α,p) ^{61,65}Cu reactions as well as a 25.4 MeV α particle for ^{60}Ni(α,α)^{60}Ni and ^{60}Ni(α,p)^{63}Cu reactions. Consistent calculations with the optical model and ZR DWBA are made for (α,α) and (α,p) reactions by using single, two, three and four nucleon optical potential parameters. For elastic scattering due to the α optical potential ambiguities, all the above optical potentials can reproduce the experimental angular distributions. However, the single, two and three nucleon potential, including Baird's mass systematics and Chang's energy systematics of α potentials, obviously cannot provide a reasonable fitting with the (α,p) reaction experimental data. Only the results from the four nucleon potential are in good agreement with the (α,p) reaction experimental data. This reveals that in the α-particle induced transfer reactions, the real depth of the α-nucleus optical potential should be rather deep.

CERIUM CROSS SECTION BETWEEN 12 AND 18 MeV

Beijing YUANZIHE WULI [CHINESE JOURNAL OF NUCLEAR PHYSICS] in Chinese Vol 7 No 4, Nov 85 pp 307-312

[English abstract of article by Teng Dan [3326 0030], et al., of the Institute of Atomic Energy, Beijing]

[Text] The cross sections for $^{142}Ce(n,2n)^{141}Ce$ and $^{140}Ce(n,2n)^{139}Ce$ from 12 to 18 MeV, $^{136}Ce(n,2n)^{135}Ce$ and $^{140}Ce(n,p)^{140}La$ from 13 to 15 MeV, and $^{138}Ce(n,2n)^{137m}Ce$ at 14.07 MeV are measured by the activation method. The neutron fluence is determined by the associated particle counting at 14.59 MeV for the $^{142,140}Ce(n,1n)$ reactions. The $^{138,136}Ce(n,2n)$ and $^{140}Ce(n,p)$ reactions are determined relative to the cross sections of the $^{142,140}Ce(n,2n)$ reactions at 14.07 MeV. The measured values are 1981, 1766, 925, 1244 and 6.70 mb for the $^{142,140,138,136}Ce(n,2n)$ and $^{140}Ce(n,p)$ reactions respectively.

MICROSCOPIC ANALYSIS OF (p,n) AND (p,p) SCATTERING ON TIN ISOTOPES

Beijing YUANZIHE WULI [CHINESE JOURNAL OF NUCLEAR PHYSICS] in Chinese Vol 7 No 4, Nov 85 pp 313-319

[English abstract of article by Ning Pingzhi [1337 1627 3112] of Nankai University, Tianjin]

[Text] Microscopic calculations are performed for the (p,n) charge exchange reaction and (p,p) elastic scattering on ^{116}Sn and ^{124}Sn at a proton energy of 24.5 MeV. The optical potentials and the isospin-coupling potential are generated from a density-dependent complex effective nucleon-nucleon interaction and the nucleon density distributions of the target nucleus. The (p,n) and (p,p) differential cross sections are calculated simultaneously by solving the coupled Lane equations exactly. The results of these microscopic calculations yield reasonable agreement with the measured values, even though they contain no adjustable parameters.

VALIDITY OF M-3Y FORCE EQUIVALENT G-MATRIX ELEMENT FOR CALCULATIONS OF NUCLEAR STRUCTURE IN s-d SHELL

Beijing YUANZIHE WULI [CHINESE JOURNAL OF NUCLEAR PHYSICS] in Chinese Vol 7 No 4, Nov 85 pp 320-324

[English abstract of article by Song Hongqiu [1345 1347 4428], et al., of Shanghai Institute of Nuclear Research, Chinese Academy of Sciences]

[Text] The matrix elements of the M-3Y force are adopted as the equivalent G-matrix elements and the Folded Diagram Method is used to calcuiate the spectra of ^{18}O and ^{18}F. The results show that the matrix elements of the M-3Y force as the equivalent G-matrix elements are suitable for microscopic calculations of the nuclei in the s-d shell.

TRANSITION POTENTIAL OF QUARK-ANTIQUARK PAIR (MESON) EXCHANGE IN CONSTITUENT QUARK MODEL

Beijing YUANZIHE WULI [CHINESE JOURNAL OF NUCLEAR PHYSICS] in Chinese Vol 7 No 4, Nov 85 pp 325-331

[English abstract of article by He Hanxin [0149 3352 2450] of the Institute of Atomic Energy, Beijing]

[Text] The amplitude to the lowest order for the exchange of quark-antiquark pairs ($q-\bar{q}$) between two three-quark clusters (nucleons) are obtained by QCD perturbation theory when the two nucleons overlap, and thus the transition potential for the exchange of the color-singlet ($q-\bar{q}$) pairs (mesons) between the two nucleons is defined. The non-relativistic approximation of this transition potential is also discussed and the expression of the potential is consistent with the one-boson exchange one. The nucleon-meson vertex structure is consistently included in this potential due to the quark structure of the hadron.

SHELL MODEL CALCULATIONS OF ^{90}Zr WITH WOODS-SAXON POTENTIAL

Beijing YUANZIHE WULI [CHINESE JOURNAL OF NUCLEAR PHYSICS] in Chinese Vol 7 No 4, Nov 85 pp 332-337

[English abstract of article by Yuan Haiji [5913 3189 7535] of Hangzhou University; and Shen Qingbiao [3947 1987 1753] of The Institute of Atomic Energy, Beijing]

[Text] In this paper a set of local Woods-Saxon potential parameters for the asymmetric nucleus ^{90}Zr are adjusted to perform the single-particle shell model calculations. The calculated results of the single-particle energies and the root mean square radius of the charge distribution are in good agreement with the experimental data. Based on previous studies, the nucleon densities, kinetic energy densities and spin densities of the asymmetric nucleus ^{90}Zr are calculated. Their shape and values are presented in this paper.

DEFORMED HF STATES OF EVEN TITANIUM AND CHROMIUM

Beijing YUANZIHE WULI [CHINESE JOURNAL OF NUCLEAR PHYSICS] in Chinese Vol 7 No 4, Nov 85 pp 338-343

[English abstract of article by Liao Jizhi [1675 4949 1807] of Sichuan University]

[Text] Using KB matrix elements, the deformed Hartree-Fock calculations for ^{44,46,48,50}Ti and ^{48,50}Cr nuclei are performed. The oblate, prolate and triaxial deformed solutions, as well as the solutions of some particle-hole excited configurations, are obtained. The results show that there is a form transition from mass number 48 to 50, and that the single-particle energy spectra are different not only for different mass numbers of the nuclei, but also for different configurations.

GLOBAL ANALYSIS OF NEUTRON DIFFERENTIAL ELASTIC CROSS SECTION CALCULATIONS WITH MICROSCOPIC OPTICAL POTENTIAL

Beijing YUANZIHE WULI [CHINESE JOURNAL OF NUCLEAR PHYSICS] in Chinese Vol 7 No 4, Nov 85 pp 344-351

[English abstract of article by Tian Ye [3944 6851], et al., of the Institute of Atomic Energy, Beijing; and Liu Wei [0491 3555], et al., of Northwest University, Xi'an]

[Text] Neutron differential elastic cross sections are calculated by the microscopic optical potential (S-MOP) and compared with available and independent experimental data as well as those calculated with Greenlee's phenomenological potential. The global analysis shows that for the original Skyrme forces, such as GS2 and SKa, without adjusting any parameters, S-MOP can reproduce the tendency of angular distributions, positions and absolute values of peaks and valleys of experimental data in the neutron energy region of 1-26 MeV for nuclei ranging from ^{12}C to ^{240}Pu. Thus, it is shown that S-MOP has a capability for predicting neutron differential elastic cross sections in optical model calculations for a nucleon even-even nucleus in a rather wide range of energies and nuclei.

FIFTH-ORDER ANGULAR ABERRATIONS OF INHOMOGENEOUS MAGNETIC FIELD WITH AXIAL SYMMETRY AND THEIR CORRECTION

Beijing YUANZIHE WULI [CHINESE JOURNAL OF NUCLEAR PHYSICS] in Chinese Vol 7 No 4, Nov 85 pp 352-360

[English abstract of article by Lu Hongyou [0712 3163 3731], et al., of the Institute of Atomic Energy, Beijing]

[Text] The fifth-order approximate solution is derived from the equation of motion for a charged particle in inhomogeneous magnetic field with axial symmetry by the method of successive approximation. The angular aberrations of different orders and the coefficients of the magnetic field to correct these angular aberrations are given.

TRANSPORT OF BEAM PHASE SPACES WITH NONCENTROSYMMETRIC CONFIGURATION THROUGH LINEAR FIELD

Beijing YUANZIHE WULI [CHINESE JOURNAL OF NUCLEAR PHYSICS] in Chinese Vol 7 No 4, Nov 85 pp 361-368

[English abstract of article by Fu Shinian [0265 0013 1628], et al., of the Institute of Atomic Energy, Beijing]

[Text] The transport theory of the beam phase spaces with noncentrosymmetric polygonal configuration $x + b_i x' - a_i = 0$ $(i = 1, 2, \ldots, n)$ as well as noncentrosymmetric smooth convex close curve configuration $f(x, x') = 0$ through the linear field is developed. The formulas of the beam envelope of such beam phase spaces through the linear field are derived. Detailed calculations are worked out for typical examples to show the practical application of the theory.

SCHEME FOR RAISING BEAM BLOW-UP (BBU) THRESHOLD CURRENT OF CONSTANT IMPEDANCE STRUCTURE

Beijing YUANZIHE WULI [CHINESE JOURNAL OF NUCLEAR PHYSICS] in Chinese Vol 7 No 4, Nov 85 pp 369-378

[English abstract of article by Yao Chongguo [1202 0339 0948] of Nanjing University]

[Text] This paper presents a design scheme for a constant impedance structure that raises the BBU threshold current but does not degrade the performance of the structure. Two holes opened on disks in certain positions on the structure can stop the EH_{11} wave that brings about BBU, but they have little effect on the TM_{01} wave that accelerates electrons. Their function is equivalent to dividing the whole structure into n segments (n is usually two to four, depending on the length of the structure), so that the BBU threshold current roughly increases by the same factor of n.

9717
CSO: 4009/4

SYNERGISTIC EXTRACTION OF U, Th, Nd, Y BY BINARY SYSTEM OF AB SPECIES COMPOSED OF PMBP-TOPO--A STUDY USING TITRATION CALORIMETRY, KARL FISCHER TITRATION AND SOLVENT EXTRACTION

Beijing HE HUAXUE YU FANGSHE HUAXUE [JOURNAL OF NUCLEAR AND RADIOCHEMISTRY] in Chinese Vol 8 No 1, Feb 86 pp 1-7

[English abstract of article by Wang Wenqing [3769 2429 3237], et al., of the Department of Technical Physics, Beijing University; Li Xingfu [2621 6821 1133], et al., of the Institute of High Energy Physics, Chinese Academy of Sciences, Beijing; and Sun Pengnian [1327 7720 1628] of the University of Science and Technology of China, Hefei]

[Text] The present study is a detailed investigation of the synergistic extraction of uranium, thorium, neodymium and yttrium with a binary system of 1-phenyl-3-methyl-4-benzoyl-pyrazolone-5(PMBP) and trioctyl-phosphine oxide (TOPO) using a direct calorimetric titration method together with Karl Fischer titration and solvent extraction.

Calorimetric titration and temperature dependence studies of the extraction method allow calculation of the enthalpy and entropy changes associated with the synergic reaction. From the magnitude and signs of the ΔS values, it is possible to determine whether synergism is associated with the replacement of solvate water by the adduct molecule TOPO with no change in the coordination number, or with an expansion of the coordination sphere upon addition of the adduct molecule but no replacement of water. Uranium, thorium, neodymium and yttrium have been shown to form $UO_2(PMBP)_2(TOPO)$, $Th(PMBP)_4(TOPO)$, $Nd(PMBP)_3(TOPO)$ and $Y(PMBP)_3(TOPO)$ respectively. Water analysis is made by Karl Fischer titration. The equilibrium constants, enthalpy, entropy and free energy changes for the addition reaction are determined. The data indicate that the main driving force of the synergistic effect is the substitution of the coordinated water molecule by TOPO.

STUDY OF PREPARATION OF URANIUM (III) BY ELECTROLYSIS AND KINETICS OF REACTION OF U^{3+} WITH H^+

Beijing HE HUAXUE YU FANGSHE HUAXUE [JOURNAL OF NUCLEAR AND RADIOCHEMISTRY] in Chinese Vol 8 No 1, Feb 86 pp 26-31

[English abstract of article by Wu Jizong [0702 4949 1350] and Luo Wenzong [5012 2429 1350] of the Institute of Atomic Energy, Beijing]

[Text] In studying the factors affecting the percentage and rate of reduction of tetravalent uranium to the trivalent state by controlled potential electrolysis, it is found that the main factor is the cell constant β, which depends on the design of the cell system. The bigger the β, the higher the percentage and rate of the reduction. The kinetics of the redox reaction of U^{3+} ions with H^+ ions in hydrochloric acid determined by controlled potential electrolysis follows a second order reaction and can be represented as:

$$-d[U^{3+}]/dt = k[U^{3+}][H^+].$$

INVESTIGATION OF STABILITY OF U_3O_8

Beijing HE HUAXUE YU FANGSHE HUAXUE [JOURNAL OF NUCLEAR AND RADIOCHEMISTRY] in Chinese Vol 8 No 1, Feb 86 pp 53-55, 7

[English abstract of article by Feng Guoning [1409 0948 1337], et al., of the Uranium Mining Research Institute, Hengyang]

[Text] The source of the weight increase of U_3O_8 during storage is investigated. The main source comes from the absorption of water in the atmosphere. Probably $U_3O_8 \cdot H_2O$, $U_3O_8 \cdot 2H_2O$ and $U_3O_8 \cdot 3H_2O$ are formed. The increase in weight is related to methods of preparation, storage period and conditions during storage. It is shown that the process of water absorption is irreversible. Therefore, it is advisable to store the U_3O_8 in an ampoule, or to ignite the U_3O_8 at 850°C in a muffle furnace for two hours vefore use.

9717
CSO: 4009/5

COMPARATIVE STUDY OF PHOTODYNAMIC EFFECT, PHOTOSENSITIVE SIDE ACTION AND TOXICITY OF SEVERAL CHINESE PHOTOSENSITIZERS

Beijing YAOXUE XUEBAO [ACTA PHARMACEUTICA SINICA] in Chinese Vol 21 No 1, 29 Jan 86 pp 7-11

[English abstract of article by Wang Naiqin [3769 5082 0530], et al., of Beijing Institute for Cancer Research, Beijing; and Ye Ailian [0673 1947 5571], et al., of Beijing Pharmaceutical Industrial Institute, Beijing]

[Text] In this paper, the photodynamic effect, photosensitive side action and acute toxicity of three new Chinese hematoporphyrin derivatives, HPS, LF-019 and Y-HPD, are compared with those of America-made photofrin II. The experimental method included: (1) the killing effect of the photosensitizer plus exposure to light on the MGC-803 cells; (2) the survival time of mice after receiving L_{615} cells pretreated with the photosensitizer and light; (3) the inhibitory effect on ^{3}H-TdR and ^{3}H-UR incorporated into DNA and RNA; (4) the uptake and storage of photosensitizers in L_{1210} cells; (5) the ear and skin indexes showing skin photosensitive side action and (6) the LD_{50} in mice.

The results show that the photodynamic effect of the three Chinese photosensitizers was more potent than that of photofrin II. In the three Chinese photosensitizers, except for the skin photosensitive side action, Y-HPD was more potent than HPS or LF-019 in the killing effect of MGC-803 cells, the survival time of L_{615} mice, the inhibitory effect of nucleic acid biosynthesis and the content of photosensitizers in L_{1210} cells. The acute toxicity of Y-HPD was lower than that of other photosensitizers. (Paper received 4 May 1985.)

REFERENCES

1. 王耐勤等. 血卟啉新分离物-HPS 光敏效应的实验研究. 肿瘤 1985; 5:49.
2. 程雨时等. 一种简便的比较光敏副作用的方法及其在寻找光敏副作用防治药的作用. 药学学报 1985; 20:395.
3. 王凯华. 人体胃低分化粘液腺癌系 MGC-803 的建立及其生物学特性初步观察. 实验生物学报 1983; 16:257.
4. Dougherty TJ et al. Photoradiation therapy 2. Cure of animal with hematoporphyrin and light. *J Nat Cancer Instit* 1975; 55:115.
5. Dougherty TJ, et al. Photoradiation therapy for the treatment of malignant tumor. *Cancer Res* 1978; 33:2628.
6. Nicoline AC, et al. Inhibition of DNA synthesis and lateral mobility in hematoporphyrin treated cells. *Proc Am Assoc Cancer Res* 1981; 22:1114.
7. 李古荣等. 血卟啉衍生物-光辐射对 L_{1210} 白血病细胞核酸生物合成的影响. 药学学报 1985; 20:17.
8. 卢志达等. 血卟啉衍生物 (HPD)-激光对动物移植性癌杀伤作用的实验研究. 中华医学杂志 1983; 63:326.

STUDIES OF SYNTHESIS AND STRUCTURE-ACTIVITY RELATIONSHIPS OF N-(α,β-DISUBSTITUTED-4-CHLOROCINNAMYL)-SEC-BUTYLAMINES

Beijing YAOXUE XUEBAO [ACTA PHARMACEUTICA SINICA] in Chinese Vol 21 No 1, 29 Jan 86 pp 20-28

[English abstract of article by Peng Shiqi [1756 1597 1142], et al., of the College of Pharmaceutical Sciences, Beijing Medical University, Beijing; and Chen Suming [7115 4790 2494], et al., of the Institute of Chemistry, Chinese Academy of Sciences, Beijing]

[Text] In this paper the synthesis of 13 N(α, β-disubstituted-4-chlorocinnamyl)-sec-butylamine derivatives (4Ea, 4Eb~e, 4Zb~e, 6Ea~b, 6Za~b) are reported. The configuration of pairs of geometrical isomers has been assigned by NMR. Four compounds have been configurationally confirmed by X-ray diffraction. The θ_1 (the twist angle between the phenyl ring and the carbon-carbon double bond) and θ_2 (the twist angle between the carbonyl group and the carbon-carbon double bond) of stable conformations of the compounds have been calculated by the EHMO method. The values of θ_1, θ_2, and anticonvulsant activity (ED_{50}) of 18 compounds are given here. The relationships of θ_1 and θ_2 and the anticonvulsant activities of these compounds are discussed. The pattern in which these compounds bind with the receptor in order to produce the anticonvulsant effect is tentatively proposed. (Paper received 12 February 1985.)

REFERENCES

1. 裘印权等.抗痫灵的药理研究.中华医学杂志 1978;58:216.
2. 张晓晖等.桂皮酰胺类及其类似物的化学结构与生理活性的关系 I. 北京医学院学报 1980;12:83.
3. Balsamo A, et al. Structure-activity relationships of cinnamides. *J Med Chem* 1975;18:842.
4. 刘维勤等.β-取代桂皮酰胺类化合物的化学结构与抗惊活性的关系.药学学报 1983;18:912.
5. 刘维勤等.桂皮酰胺类化合物脂水分配系数的测定.北京医学院学报 1983(增刊);1:75(七十周年校庆专辑(三)).
6. Cope C. et al. Condensation reactions: Alkylidene cyanoacetic and malonic esters. *J Am Chem Soc* 1941; 63:3452.
7. Cragoe EJ, et al. The synthesis of *α, α*-disubstituted succinic acid from ethyl alkylidenecyanoacetates. *J Org Chem* 1951;15:381.
8. Hayashi T. Studies on geometric isomerism by NMR. III. Stereochemistry of *α*-cyanocinnamic ester *Ibid* 1966;31:3253.
9. 彭师奇等.N-(*α, β*-双烷基-4-氯桂皮酰基)另丁胺类化合物的合成.高等学校化学学报 待发表
10. Doyle FP, et al. Furyl-and thienylpenicillins. US 3,470, 151. 30 sep 1969.
11. 陈素明等.N-(*α,β*-双取代-4-氯桂皮酰基)另丁胺类化合物的核磁共振及构型研究.波谱学报 1985;2:19.

9717
CSO: 4009/3004

END

END OF FICHE DATE FILMED

DEC. 10, 1986